# Establishing Isokinetic Flow for a Plasma Torch Exhaust Gas Diagnostic for a Plasma Hearth Furnace

by

Brian R. Pollack

B.S., Mechanical Engineering
Manhattan College, 1994

Submitted to the Department of Nuclear Engineering and the Department of Mechanical Engineering
in Partial Fulfillment of the Requirements for the Degrees of

Master of Science in Nuclear Engineering

and

Master of Science in Mechanical Engineering

at the
Massachusetts Institute of Technology
May 1996



Signature of Author. .....
Department of Nuclear Engineering, May 10, 1996

Certified by..... .....
Paul P. Woskov, Senior Research Engineer, Plasma Fusion Center, Plasma Systems Division, Thesis Supervisor

Certified by. .....
Kevin W. Wenzel, Professor of Nuclear Engineering, Department of Nuclear Engineering, Thesis Advisor

Certified by.... .....
Neil E. Todreas, Professor of Nuclear Engineering, Professor of Mechanical Engineering, Department of Mechanical Engineering, Thesis Advisor

Accepted by..... .....
Jeffrey P. Freidberg, Chairman, Committee on Graduate Students

**Establishing Isokinetic Flow for a Plasma Torch Exhaust Gas Diagnostic for a Plasma Hearth Furnace**

by
Brian R. Pollack

Submitted to the Department of Nuclear Engineering
on May 10, 1996

in Partial Fulfillment of the Requirements for The Degrees of Master of Science in Nuclear Engineering and Master of Science in Mechanical Engineering.

## Abstract

Real time monitoring of toxic metallic effluents in confined gas streams can be accomplished through use of Microwave Induced Plasmas to perform atomic emission spectroscopy.

For this diagnostic to be viable it is necessary that it sample from the flowstream of interest in an isokinetic manner. A method of isokinetic sampling was established for this device for use in the exhaust system of a plasma hearth vitrification furnace.

The flow and entrained particulate environment were simulated in the laboratory setting using a variable flow duct of the same dimensions (8-inch diameter, schedule 40) as that in the field and was loaded with similar particulate (less than 10 μm in diameter) of lake bed soil typically used in the vitrification process. The flow from the furnace was assumed to be straight flow. To reproduce this effect a flow straightener was installed in the device.

An isokinetic sampling train was designed to include the plasma torch, with microwave power input operating at 2.45 GHz, to match local freestream velocities between 800 and 2400 ft/sec.

The isokinetic sampling system worked as planned and the plasma torch had no difficulty operating at the required flowrates. Simulation of the particulate suspension was also successful. Steady particle feeds were maintained over long periods of time and the plasma diagnostic responded as expected.

Thesis Supervisor: Dr. Paul P. Woskov

Title: Senior Research Scientist, Plasma Systems & Technology Division, MIT Plasma Fusion Center

## Nomenclature

$E$ = Energy associated with spectroscopic transition;[Energy]
$h$ = Planck's Constant; [6.6261 $10^{-34}$ Js]
$\nu$ = Emitted photon frequency; [1/t]
$\lambda_s$ = Spectroscopic wavelength; [L]
$V$ = Fluid velocity; [L/t]
$Q_n$ = Volume flowrate through duct sub-region; [$L^3$/t]
$V_n$ = Air velocity at geometric center of sub-region; [L/t]
$A_n$ = Cross-sectional area of sub-region; [$L^2$]
$Q_{tot}$ = Approximated duct volume flowrate; [$L^3$/t]
$a_n$ = Area of sampling probe; [$L^2$]
$E_m$ = Approximate total duct emissions; [M/t]
$A$ = Total duct cross-sectional area; [$L^2$]
$m_n$ = mass flow rate through sub-region per unit area;[$M/L^2t$]
$t_n$ = Sample collection time; [t]
$Z_o$ = Total head of fluid; [L]
$p_s$ = local flow static pressure; [$F/L^2$]
$g$ = local acceleration due to gravity; [$L/t^2$]
$H_v$ = velocity head; [L]
$\rho$ = Density of fluid; [M/L3]
$\sigma$ = Density of particle; [$M/L^3$]
$\upsilon$ = Stokes velocity of particle; [L/t]
$\lambda_{ent}$ = Particle entrainment distance; [L]
$\mu$ = Absolute viscosity of fluid; [M/Lt]
$d$ = Stokes diameter of particle; [L]
$\lambda_a$ = Mean free path of air molecule; [L]
$\nu$ = Kinematic viscosity of fluid; [$L^2$/t]
$k$ = Boltzmann's Constant; [1.3807 $10^{-23}$ J/K]
$T$ = Absolute temperature; [T]
$m$ = Molecular mass; [M]
$E_q$ = Energy of plasma ion/electron; [Energy]
$P_{pl}$ = Plasma pressure; [$F/L^2$]
$n$ = Plasma number density; [#atoms/$L^3$]
$v_d$ = Particle transport velocity; [L/t]
$p$ = gas pressure; [$F/L^2$]
$k_t$ = gas thermal conductivity; [energy/LTt]
$v_s$ = Slip velocity; [L/t]
$\sigma`$ = Slip velocity coefficient; [dimensionless]
$Re_D$ = Reynold's number of flow; [dimensionless]
$A_{st}$ = Sample probe cross-sectional area; [$L^2$]
$F_s$ = Applied suction force; [F] (=[$ML/t^2$])
$P_s$ = Suction pressure; [$F/L^2$]
$\alpha$ = Accomodation coefficient; [dimensionless]
$f$ = Friction factor; [dimensionless]
$L_e$ = Equivalent pipe length; [L]
$D$ = Sample tube diameter; [L]

**Acknowledgments:**

In any research project, one person gets the least amount of sleep. That would be the person writing the thesis when the smoke clears. However, that person would not sleep at all if it were not for the help of others.

I would therefore like to convey my deepest gratitude to all those who made this project (and the resulting thesis) possible.

I would like to thank Dr. Paul P. Woskov, my advisor, for the opportunity to undertake this exciting research and for his endless patience in teaching a engineer how to be a physicist. Not to mention tolerating all the time I devoted to the courses I had to take to satisfy the dual degree requirement, particularly in my first year!

I would like to thank Dr. Daniel R. Cohn for his financial support during my first year at MIT. I also offer thanks to the Magnetic Fusion Energy Technology (MFET) fellowship for their support during my second year at MIT and beyond.

Special thanks goes out to Paul Thomas, for his good advice in setting up experiments and swiping parts. I would also like to thank Bill Keating for squeezing my parts into his tight machining schedule.

I would also like to thank Prof. Neil Todreas, for his priceless advice early on in my studies which really gave me the direction necessary to design, build, and carry out this experiment in the first place. I would also like to thank him for reading my thesis on behalf of the Mechanical Engineering Department.

I also wish to convey my gratitude to Prof. Kevin Wenzel, for reading my thesis on behalf of the Nuclear Engineering Department. I would also like to thank Kevin for all his advice in scholastic matters during my shaky first semester at MIT, not to mention the first class barbecue he had to celebrate the end of Plasma Lab in 1995.

Last but certainly not least, special thanks goes to Dr. David Rhee, Paul Falkos and Karyn M. Green, who all worked on the plasma torch but have since moved on to bigger things. I wish them the best of luck.

Well, it's time to take a little break from academia. No, I am not leaving MIT. I am just being temporarily paroled. I shall be spending this summer in jolly old England to satisfy my fellowship practicum requirement. For this opportunity I would once again like to thank Paul Woskov for helping set it all up and for the support of MFET to make it all possible.

When this fall comes around, I'll be back at MIT, breaking rocks again. It's been great.

## Table of Contents


**Table of Figures**.....p.9

**1.0) Introduction**.....p.10

**2.0) Background**.....p.12

**2.1** Use of Low and High Temperature Plasmas.....p.12

**2.2** Motivation for Plasma Diagnostic Development.p.12

**2.3** Basic MIP Setup.....p.14

**2.4** Plasma Torch Detection Limits.....p.15

**2.5** Current Challenge.....p.15

**3.0) Theory**.....p.16

**3.0.1** Relevant Plasma Physics.....p.16

**3.1** Plasma Diagnostic Operational Issues.....p.17
**3.1.1** Addition of Helical Flow.....p.17
**3.1.2** Reln. Between Flow & Power Consumption.p.17
**3.1.3** Volatilization of Entrained Particulate.....p.18
**3.1.4** Spectroscopy Theory.....p.18
**3.1.5** Torch Calibration Theory.....p.19

**3.2** Isokinetic Flow Sampling.....p.21
**3.2.1** Basic Concepts.....p.21
3.2.1.1 Determination of Duct Volume Flowrate.....p.21
3.2.1.2 Determination of Particulate Mass Flowrate.....p.22

**3.3** Different Sampling Schemes.....p.23
**3.3.1** Method 1.....p.23
**3.3.2** Method 2 (EPA Method 29).....p.24
**3.3.3** Method 3 (Static Pressure Taps).....p.25

**3.4** Entrained Particulate Behavior.....p.27
**3.4.1** Dust Introduction System.....p.27
**3.4.2** Particulate Carrying Characteristics of Duct Flow.....p.28
**3.4.3** Sampling Train.....p.29
3.4.3.1 Inertial Deposition.....p.29
3.4.3.2 Turbulent Deposition.....p.30
**3.4.4** Plasma-Dust Interactions.....p.30

3.4.4.1 Thermophoresis.....p.30

**3.5** Temperature Effects on Isokinetic Sampling...p.33

**4.0) Experimental Approach**.....p.35

**4.1** Conditions at SAIC.....p.35
**4.1.1** Exhaust Gas.....p.35
**4.1.2** Particle Characteristics.....p.35

**4.2** Experimental Apparatus.....p.36
**4.2.1** Main Duct.....p.36
**4.2.2** Flow Straightener.....p.37
**4.2.3** Isokinetic Method.....p.38
**4.2.4** Sampling Train.....p.38
4.2.4.1 Sizing of Sampling Head and Choice of Manometer.....p.38
4.2.4.2 Plasma Torch.....p.39
4.2.4.3 Starting Mechanism.....p.39
4.2.4.4 Primary Exhaust.....p.40
4.2.4.5 Heat Exchanger.....p.40
4.2.4.6 Suction Pump and Adjustment.....p.41

**4.3** Particulate Introduction System.....p.42

**4.4** Plasma Torch Operation.....p.43

**5.0) Results**.....p.45

**5.1** Accuracy of Sampling Scheme.....p.45
**5.1.1** Temperature Effects.....p.49
**5.1.2** Device Sensitivity.....p.49
**5.1.3** Effect of Plasma Torch Operation on Manometer.....p.49

**5.2** Results of Particulate Studies.....p.50
**5.2.1** Particle Characteristics.....p.50
**5.2.2** Flow Characteristics.....p.50
5.2.2.1 Flow Straightener Performance.....p.51
**5.2.3** Entrained Solids Distribution.....p.51
5.2.3.1 Sampling Concerns.....p.52
**5.2.4** Calibration of Particle Feeder.....p.52
**5.2.5** Plasma Torch Studies.....p.52

**5.3** Summary.....p.54

**6.0) Conclusions & Future Work**.....p.55

**6.1** Research to Date.....p.55

**6.2** Future Work.....p.55
**6.2.1** Future Plasma Torch Studies.....p.55

**6.2.2** Future Applications of the Diagnositc..p.56
**6.2.3** Commercialization of the Diagnostic....p.57
**6.2.4** Future Nozzle Design.....p.57

**6.3** Overall Perspective of Plasma Torch Diagnostic.....p.58

**7.0) References**.....p.59

**7.1** Cited.....p.59

**7.2** Non-Cited.....p.60

**8.0) Appendix**.....p.61

**8.1** Appendix A Tables:
Table 1, Torch Detection Limits.....p.62
Table 2, Lake Bed Soil Analysis.....p.63
Table 3, Analysis of Manometer Discrepancy...p.64
Table 4, Variable Flow Data for Main Duct....p.65
Table 5, Flow Study Data.....p.66
Table 6, Particulate Collection Data.....p.68
Table 7, Dust Feed Mechanism Performance.....p.69

**8.2** Appendix B Figures:
Diagrams.....p.71
Charts.....p.93

## Table of Figures


**8.2.1 Diagrams:**

Figure 1, Basic MIP Setup.....p.71
Figure 2, Isokinetic Sampling.....p.72
Figure 3, Duct Sampling Points.....p.73
Figure 4, Sampling Method No.1.....p.74
Figure 5, EPA Method No. 29.....p.75
Figure 6, Sampling Method No.3.....p.76
Figure 7, Sampling Head, Cutaway View.....p.77
Figure 8, Experimental Apparatus.....p.78
Figure 9, Flow Straightener.....p.79
Figure 10, Sampling Method for SAIC.....p.80
Figure 11, Plasma Torch Setup.....p.81
Figure 12, Heat Exchanger.....p.82
Figure 13, Cross Sectional View of Feeder.....p.83
Figure 14, Conical Funneling Chamber.....p.84
Figure 15, Outside View of Feeder.....p.85
Figure 16, Complete Feed Apparatus.....p.86
Figure 17, Dust Collector Assembly.....p.87
Figure 18, Sampling Calibration.....p.88
Figure 19, Flow Behavior Over Sampling Nozzle.....p.89
Figure 20, Flow Sampling Geometry.....p.90
Figure 21, Sample Calibration Gun.....p.91
Figure 22, Basic In-Situ Arrangement.....p.92

**8.2.2 Charts:**

Figure 23, Duct Centerline Velocity Profiles at Sampling Location.....p.93
Figure 24, Calibration Curve for Sampling Nozzle..p.94
Figure 25, Simulant Particulate Size Distribution.p.95
Figure 26, Duct Velocity Profile Development along 0-Degree Plane.....p.96
Figure 27, Duct Velocity Profile Development along 45-Degree Plane.....p.97
Figure 28, Duct Velocity Profile Development along 90-Degree Plane.....p.98
Figure 29, Duct Velocity Profile Development along 135-Degree Plane.....p.99
Figure 30, Duct Solids Flux Distribution.....p.100
Figure 31, Feeder Mechanism Performance.....p.101
Figure 32, Observed Iron Spectrum.....p.102
Figure 33, Intensity vs. Time, Run 1.....p.103
Figure 34, Intensity vs. Time, Run 2.....p.104
Figure 35, Intensity vs. Time, Run 3.....p.105
Figure 36, Intensity vs. Time, Run 4.....p.106
Figure 37, Intensity vs. Time, Run 5.....p.107

## 1.0 Introduction

The plasma torch continuous metal emissions monitor was invented by Dr. Paul Woskov, a research scientist at the MIT Plasma Fusion Center. It can detect metallic effluent in gas streams with sensitivities as low as several parts per billion for most elements.

### 1.1 Thesis Motivation:

The purpose of this thesis is to create a sealed version of this device to continuously monitor effluents in the exhaust duct of the SAIC Plasma Hearth Furnace at Idaho Falls National Laboratory. This will involve the construction of a test-bed to carry out the necessary studies to answer the fundamental questions of plasma torch behavior and effluent sampling. The specific issues are addressed at a later point.

Test-bed design will entail detailed analysis of the field conditions to be simulated in the lab. These factors will be incorporated into an operable scheme. This mechanism will then be constructed and operated. The plasma torch has certain operational characteristics that make a workable and reliable design challenging to create.

### 1.2 Information to Follow:

Chapter 2 deals with the basic motivation for the development of this device, and the competing technologies also currently under development.

The third chapter deals with the relevant theoretical aspects of plasma torch operation, particulate collection concerns, and isokinetic sampling theory including concerns of temperature effects. Several systems for isokinetic sampling are considered.

The fourth chapter discusses the experimental approach. The equipment used in the experiments is explained in

detail, relating the various design concerns to the relevant theory discussed in the third chapter.

The fifth chapter deals with analysis of the data that was taken in the various experiments. Conclusions of device effectiveness and operability are covered in detail.

The sixth and final chapter summarizes the important results and discusses relevant future work that may be undertaken in the area.

## 2.0 Background

### 2.1 Use of Low Temperature Plasmas:

In both research and industry, low temperature plasmas are used for a wide variety of applications. Perhaps the most familiar use of cold plasmas is in fluorescent bulbs or in the etching of microchips in the semiconductor industry. Other uses include applications of thin films of metal for corrosion protection, and in waste treatment.

Plasmas can also be used as a high temperature heat source for vitrification furnaces used to process soils contaminated with radionuclides.

In the fabrication of weapons grade plutonium, the separation processes involved the use of toxic chemicals. After the separation processes were complete, these chemicals were placed in storage facilities combined with whatever radionuclides were separated from the plutonium. This is sometimes called mixed waste.

A plasma hearth can serve two purposes in processing this type of waste. In addition to vitrifying the radionuclides, the toxic molecules that become airborne in the hearth are broken apart in the high temperature plasma environment.

### 2.2 Motivation For Plasma Diagnostic Development:

The EPA is in the process of implementing strict new laws pertaining to the emissions of toxic metallic effluents in exhaust streams. Twelve metals are targeted in this legislation (Ag, As, Ba, Be, Cd, Cr, Hg, Ni, Pb, Sb, Se,

Tl). This legislation, (40 CFR Part 60) also requires that these metals be monitored continuously [1].

Equipment capable of this type of monitoring is not available commercially. Currently, samples must be drawn from the flowstream through a cyclone probe/impinger train. The collected sample is sent for laboratory analysis. This hardly constitutes real-time monitoring.

Plasma based atomic emission spectroscopy measurements provide a promising basis for real time monitoring. The basic concept is to ionize a portion of the gas passing through the flowstream of interest, and observing the spectroscopic transitions that result. This can be accomplished in several ways.

Much work has been pursued in the study of Inductively Coupled Plasmas (ICPs) and Laser Spark Discharges.

ICPs have long been used in a laboratory setting to conduct sensitive measurements [1]. They are very sensitive to flow transients and the composition of the purge gas that flows through it. ICP plasma stability is a major issue. ICP plasmas can generally only operate over a narrow range of flowrates.

Units have been adapted recently for use in real-time monitoring purposes in the field [1], but their sensitivity for stable plasma operation greatly limits the environment that they can be placed in. The units are large and bulky making in-situ placement (i.e. placement directly in a flowstream) impossible.

As a result of this, when using an ICP, one must use a complicated isokinetic sampling system. The sample must follow a long sampling train including bends, restrictions, and flow separators to treat the flow and alter its composition to make it more digestible for the plasma. This dilution of the sample and complex flow geometry can lead to errors in measured quantities.

Laser-Spark Discharges can be used for in-situ measurement, but the area of the flow that is monitored is

very small due to the narrow cross-section of the beam [1]. This can lead to results that may not be meaningful. These systems also have trouble detecting vapors.

Microwave Induced Plasmas (MIPs) don't suffer from these shortcomings. With thoughtful design of the unit it is possible to place it directly inside the duct in a straight-through orientation that minimizes loss of the sample due to deposition. MIPs are less sensitive to flow transients and can operate over a wider range of flowrates. Most important of all, MIP units are much less expensive than ICPs.

## 2.3 Basic MIP Setup:

The present setup of the in-lab MIP diagnostic (See Fig.1,p.71) consists of a waveguide attached to a magnetron microwave source. Microwave power is transmitted by the rectangular waveguide to its shorted end in a transverse electric field (TE) mode.

A hole is drilled through the end of the waveguide along the direction of the electric field 1/4 wavelength from the end of the waveguide where the E field is at a maximum. An axial flow is established by purging a carrier gas through this hole. Below the waveguide is a swirl-jet assembly that injects additional gas into the flowpath with tangentially mounted jets. This adds vorticity to the flow, effectively causing the streamlines to twist into a helical pattern.

With the flow established, 2.45 GHz microwaves are launched down the waveguide into a standing wave pattern. To start the plasma, free electrons are released into the flow near the waveguide with an antenna or spark discharge.

These electrons interact with the electric field causing an electron cascade resulting in breakdown of the carrier gas. This causes the formation of a plasma.

Fused quartz fiber optic lines view the atomic emission that occurs in the plasma and transmit this light to a high-

resolution grating spectrometer with a maximum resolution of $10^{-11}$ meters where the spectrum is dispersed, and a detector array transmits this data to a computer.

The end result is the capability to monitor the atomic emission from the plasma in real time. If metallic particles become entrained in the carrier gas, they are similarly excited in the plasma and their transitions may also be monitored. This is the basis of monitoring metallic effluents in real time.

## 2.4 Plasma Torch Detection Limits:

Most of the research to date has been in determining the absolute detection limits of the torch. The detection limits for some of the metals targeted by EPA legislation are less than one part per billion (See Table 1, p.62). It varies from element to element due to the fact that the atomic transitions of some elements are stronger than those of other elements.

In the establishment of these absolute limits, direct insertion of sample powders on probes were used in addition to the introduction of aqueous solutions with a nebulizer (a small atomizer for liquids), and direct vapor introduction.

## 2.5 Current Challenge:

One thing that this device has not yet done is sample from a flowstream in an isokinetic manner. Isokinetic sampling, simply stated, is matching the suction velocity of a sampling probe to the local freestream velocity where the sampling is taking place. It is required by the EPA that any diagnostic of this nature to be able to sample in this fashion [1]. This is the principal issue that this thesis shall deal with. Once this requirement has been satisfied, the diagnostic will be considered valid for EPA compliance monitoring.

## 3.0 Theory:

### 3.0.1 Relevant Plasma Physics:

The plasma physics involved in an MIP can be very complicated. Such a plasma is not in local thermal equilibrium. There are different temperatures for electrons (excitation and rotational), and the neutral gas temperature. However, for the purposes of this work, only the neutral gas properties (temperature, pressure) will be discussed.

#### Concept of Temperature:

The neutral gas temperature in an MIP is defined in the following manner:

$$T = E_q/k \qquad (1)$$

$E_q$ is the average energy of the gas molecules. k is the Boltzmann Constant ($1.3807\ 10^{-23}$ J/K) and T is the absolute temperature of the gas. The temperature of the plasma is some 5800 K [1]. This means that on the average, each molecule in the plasma has an energy of $8\ 10^{-20}$ J or about .5 eV.

#### Concept of Pressure:

The pressure in the plasma $P_{pl}$, is the number density, n, of atoms in the plasma multiplied by the average energy, or:

$$P_{pl} = nkT \qquad (2)$$

It is clear that as the temperature of the plasma increases, so does the kinetic energy of its molecules. As their speed increases, so do the number of collisions in the plasma. This collisional phenomenon is how pressure arises in a plasma, or any other gas.

## 3.1 Plasma Diagnostic Operational Issues

Even though this MIP diagnostic is very robust, there are certain operational parameters and device characteristics that must be observed in order to ensure reliable operation.

### 3.1.1 Addition of Helical Flow:

In the early stages of research with the microwave torch, only axial flow was sent through the torch to create the plasma. Helical flow injectors have been added only recently to the design. The idea of adding helical flow to the plasma is an idea that came out of ICP research.

The symmetric flow vorticity added by the injectors gives the plasma enhanced stability and better protects the side walls of the flow tube through the waveguide. Also, the plasma can sustain itself on the flow provided by the tangential injectors alone. This is of added benefit during operation in the case where the axial flow alone could not be enough to sustain the plasma. One would encounter this situation in a very low-speed flowstream.

### 3.1.2 Relationship Between Flow and Power Consumption:

The plasma torch has an axial flow operating range of approximately 0-1.5 cfm for nitrogen at standard conditions with the helical injectors operating. As mass flow rate is increased through the torch, it is necessary to increase power input to maintain plasma integrity. This is due to the fact that as the number of atoms of gas per unit time increases, there are less ionizations per unit volume of gas, and the plasma self-extinguishes. One simply must increase the average ionization by increasing the microwave power input.

### 3.1.3 Volatilization of Entrained Particulate:

The amount of time that a particle resides in the plasma needs to be maximized because some effluents (particularly refractory materials such as U-238) are very hard to volatilize and cause to undergo transitions in the plasma. The residence time of an effluent particle in the plasma is between 15 and 30 milliseconds (approximately). Since the temperature of the neutral gas is some 5800 K, a substantial amount of energy may be transferred to the particle. However, if the melting temperature of the material is too high, it will not volatilize while in the plasma.

Unfortunately, the plasma temperature is not greatly affected by changes in power input or purge flowrate. However, by increasing the microwave power input to the torch, more of the passing atoms in the flowstream per unit volume of gas may be ionized. This results in an increase in the population of high energy free electrons that can collide with the particle. If there are more collisions with the particle, clearly more energy is transferred and the particle may be excited.

Another possibility is to reduce the purge flowrate so that the available microwave power is being absorbed by less atoms per unit time. This will also increase the residence time of the particle in the plasma giving it that much more of a chance to interact and absorb energy.

### 3.1.4 Spectroscopy Theory:

When an electron loses its energy and jumps back to its ground state, it emits a photon with an energy unique to that quantum transition for that element. This energy can be expressed as [2]:

$$E = h\nu \qquad (3)$$

Where $\nu$ is the frequency of the photon and h is Planck's Constant ($6.6261\ 10^{-34}$ Js). Then, the transmitted wavelength, $\lambda_s$, can be determined by:

$$\lambda_s = c/\nu \qquad (4)$$

A given element may have many different wavelengths at which it may emit light throughout the entire spectrum.

Virtually all of the emission lines that have been observed have been from excited neutrals, where no electrons have been stripped from the metal atom. Ionization of atoms would require a great deal of energy and in any event, all that is necessary to identify the presence of an element uniquely is to just excite it. An exception was observation of the singly ionized nitrogen molecules in the background gas.

### 3.1.5 Torch Calibration Theory:

Device calibration has been quite challenging. Most of the earlier research raised more challenging questions rather than good answers. The calibration of this device is not exact. The light intensity from spectroscopic transitions for a particular element do not necessarily increase linearly for an increase in mass in ionized particulate.

As the particles get larger, atoms at the center of the particle will most likely not become excited for a given microwave power input. At higher microwave power levels, more energy is available which results in an increase of the population of free high-energy electrons. With more of these electrons available to collide with the metal particles two things may occur.

Primarily, the atoms on the exterior of the particle will have more collisions per unit time. The corresponding light signature that the spectrometer intercepts will therefore increase.

Second, this higher effective energy flux bombarding the surface of the particle will cause increased conduction of heat toward its center. This can result in vaporization of the exterior atoms which will expose the inner atoms to the plasma as well. When these inner atoms then become excited by the free electrons in the plasma, they too will radiate. This cumulative effect will serve to increase the signal to the spectrometer.

If one considers variation of flow, residence time is affected which will have similar unpredictable effects on the recorded spectroscopic transitions at a given wavelength.

It has become clear that the issue of calibration is unique to each application and should be handled on a case by case basis. This is due to the wide variation of parameters that can exist between applications. It involves a great deal of work, but it also has the largest chance for success.

The calibration of light level to known mass of effluent should ideally be performed for several flowrates through the torch, each corresponding to expected flowrates necessary to create an isokinetic sampling condition at different flowstream conditions. At these flowrates, it must be determined how variations of input power affect the light signature detected for a given size range of particles. In this manner, regardless of particle size distribution, it should be possible to predict particle emissions for certain operational conditions.

For the purposes of the present experiments however, it will merely be attempted to obtain a steady spectrometer signal over time for particular conditions. The determination of the quantity of trace metal constituents in a flowstream remains a task for the future.

## 3.2 Isokinetic Flow Sampling:

### 3.2.1 Basic Concepts:

Isokinetic sampling is a fairly straight-forward condition that has to be satisfied. The local unperturbed flow velocity at the point of sampling must be matched exactly by the suction inflow of the torch. This is important from the standpoint of extracting a "representative" sample from the flowstream [3].

In a situation where there are entrained particles in the flowstream, upsetting the flow by either super or sub-isokinetic sampling [4] can cause the local solids distribution to change, causing either too much or too little of the particulate to be drawn in (See Fig. 2, p.72).

As can be seen in this diagram, Isokinetic sampling can only be achieved when the critical streamline (i.e. the streamline that defines the edge of the sample stream) is perpendicular to the plane of the sampling nozzle.

#### 3.2.1.1 Determination of Duct Volume Flowrate:

It is important to determine the duct volume flowrate at a given operating condition. This may be closely approximated by direct measurement with a technique provided in [3]. In this technique, the duct is broken up into a number of imaginary sub-areas, $A_n$. Different schemes are displayed in Fig.3, p.73.

The volume flow throughout the region can then be found in the following manner:

$$Q_n = V_n A_n \qquad (5)$$

and the total duct flowrate can be found from:

$$Q_{tot} = (Q_1 + Q_2 + Q_3 + \ldots + Q_n) \qquad (6)$$

This technique, and the one in the next section will be important in the field measurements that are performed by SAIC out in Idaho.

### 3.2.1.2 Determination of Particulate Mass Flowrate:

One can closely approximate the particulate mass flowrate in the duct by techniques related to those discussed in the previous section.

Using the same area scheme as above, a close approximation to the emissions, $E_m$ [mass/time], can be found from:

$$E_m = A(m_1A_1/A + m_2A_2/A + \ldots + m_nA_n/A) \qquad (7)$$

where A is the total cross-sectional area of the duct and $m_n$ is the local mass flowrate per unit area given by:

$$m_n = w_n/a_nt_n \qquad (8)$$

Here, $a_n$ is the area of the sampling probe, and $w_n$ is the sample mass collected in time $t_n$.

Referring back to Figure 3, one can obtain progressively better and better accuracy by sampling from more and more points. This can be important if the solids distribution is unusual in character.

In these different schemes, the magnitudes of the areas with respect to one another is essentially arbitrary. The determining factor is the selection of the sampling point location with respect to that area. The sampling point in the sub-area should correspond to a location that experiences the average mass flowrate of entrained particulate.

Clearly, this cannot be known beforehand. One has to make a careful study of the profile. If the profile is sharply peaked toward the center or to one side, it may be wisest to choose many sampling points to obtain an accurate picture of the profile during operation. However, if the mass flux profile is fairly steady, fewer sections will do.

In either of these cases, for a round duct, the areas may be selected to be equal in magnitude for convenience. The sampling point is typically selected to lie half-way between the inner and outer radii of the sub-area. The key

is to match the appropriate scheme to the nature of the profile.

That is a brief look at how the data obtained from isokinetic sampling can be used to construct useful estimates of duct flow and solids transport when taking data in the field. Now is an appropriate time to consider different ways of satisfying the requirements to establish isokinetic sampling.

### 3.3 Different Sampling Schemes:

In selecting a sampling setup, several options were considered. They are discussed in the following sections.

#### 3.3.1 Method 1:

This method was originally drawn from [3]. This reference dealt with the measurement of solids in high-temperature flue gases from coal combustion using isokinetic means. The approach used was one of direct measurement of the velocity profile in the region of interest.

Although the magnitude of the velocity profile changes with a change in volumetric flow rate, the characteristic shape of the profile usually does not [3]. The flowrates at all points in the duct's cross-section should all increase or decrease in the same relative ratio [3]. No mention was made by [3] as to how this was known. It is therefore to be taken as fact.

Therefore, a detailed study can be made of the velocity profile and a relationship can be established between the specific sampling point and a "control" point near the wall of the duct (See Fig.4, p.74). A pitot tube and a thermocouple can be inserted into the flow to continuously monitor flow speed and temperature at the control point. One can take this continuously measured velocity value at the side of the duct and multiply it by an appropriate ratio that gives the corresponding velocity at the sampling point.

**Advantages:**

This method is fundamental. It is clean and the sampling probe can have an extremely low profile minimizing condensation on it.

**Disadvantages:**

The method of obtaining the profile is very time consuming. In the event that one wanted to sample in a different portion of the duct, or wanted to sample in another device altogether (i.e. to have a "portable" unit), the profile would have to be re-established, which would not be practical.

With this method, one has to be very concerned with temperature changes in the flow. If there is an appreciable change in density in the gas, then the suction rate must be modified to pull in the correct mass flow rate. This concern is addressed in Section 3.5.

### 3.3.2 Method 2 (EPA Method 29):

This method is one outlined by the EPA [5] as a viable method to perform isokinetic sampling(See Fig.5 ,p.75). In this method, a probe is designed that has a pitot tube and thermocouple to measure flow and temperature right next to the inlet nozzle.

The flow velocity measured by the pitot tube is assumed to be the same as that near the inlet nozzle. The temperature read by the thermocouple is assumed to be equal to the local gas temperature at the sampling location. With this information, and the suction inlet area, one can calculate the mass flow rate necessary to pull through the sample line in order to perform isokinetic sampling. The mass flow rate for suction is then adjusted to this value.

**Advantages:**

The major advantage that this system has over the one previously mentioned is that one does not have to determine the velocity profile. This method is therefore versatile enough to use at different points of the same duct or in an entirely different environment.

**Disadvantages:**

If the stream happens to be heavily ash laden, one has to filter out the particulate before it goes through the mass flow-meter. This technique works well when particulate are collected (i.e. with a cyclone probe), but the plasma torch is a passive diagnostic and adds a great deal of heat energy to the sampled gas. This would therefore require the installation of a heat exchanger to avoid damaging the mass flowmeter.

### 3.3.3 Method 3, Static Pressure Taps:

This method was found in [6] for isokinetic sampling in a dense gas-solids stream. In this method, a thermocouple is not utilized (see Fig.6, p.76). Instead, static pressure taps are located at the inside and the outside of a low-profile stainless steel nozzle. Both taps are connected to a differential manometer. The difference in manometer head is the difference in dynamic pressure head in inches of fluid. In theory, if the manometer reading is "zero", then the pressure head at the inside and outside must be equal, hence the velocities must be the same.

This pressure difference, $\Delta P$, is given by:

$$\Delta P = \rho V_i^2/2 - \rho V_o^2/2 \qquad (9)$$

Here, $\rho$ is the fluid density, and $V_i$ and $V_o$ are the flow velocities at the inner and outer pressure taps.

The sampling nozzle has a very sharp tip to minimize collection (See Fig.7, p.77). The pressure taps

are hooked up to a high pressure purging system where the leads to the manometers can be shut off via valves, and a path can be opened between the taps and a high-pressure nitrogen source. This is of great benefit in case the pressure taps become clogged by particulate deposition.

**Advantages:**

This device measures the local velocity closer than any of the other methods described. It is simple, and temperature effects do not have to be considered. It is especially appropriate for use with the plasma torch, because a mass flowmeter is not required. This is due to the fact that the whole "business-end" of the device is located in the flowstream. This consequently eliminates the need for a heat exchanger (as long as the suction pump can handle the heat).

**Disadvantages:**

Although this device looks great on paper, the manometer reading at flow balance may not be zero for all encountered flowrates. So it is necessary to calibrate this device by establishing "true" isokinetic sampling via exterior means. This is discussed in the next chapter.

**Other Comments:**

To properly size the differential manometer for this application, one must calculate the maximum velocity head that can be encountered, and double it. That is the approximate manometer range that can be expected in operation.

This extreme condition can arise in the case that there is no suction with full duct flow or full suction with no duct flow. In either of these cases, the manometer head difference will be due to the maximum expected velocity. The velocity head, $H_v$, can be calculated from:

$$H_v = V^2/2g \quad (10)$$

This will provide the velocity head in length dimensions of air. The manometer has water in it so this head value must be converted to length dimensions of water:

$$(\rho g H)_{air} = (\rho g H)_{water} \quad (11)$$

This will provide the necessary head value for sizing the manometer.

### 3.4 Entrained Particulate Behavior:

There are several issues concerning particulate behavior for the use of the plasma torch diagnostic. These areas are in the feed introduction system, the sampling train, and the effect of the plasma on the particulate.

The prevailing loss of particles from the flowstream will be due to turbulent transport and Brownian motion.

#### 3.4.1 Dust Introduction System:

A way must be devised to entrain particulate in the flow in order to perform measurements. This system should be capable of introducing feed at a steady mass flow rate.

A critical figure of merit that must be calculated is the minimum distance required, $\lambda_{ent}$, for particulate to become entrained in the flowstream [3]. This can be calculated with the following relation:

$$\lambda_{ent} = \upsilon V/g \quad (12)$$

Here, V is the velocity of the flowstream that is accelerating the particle, g is the local acceleration due to gravity, and $\upsilon$ is the Stokes velocity that can be found from [3]:

$$\upsilon = (\sigma-\rho)gd^2/18\mu \quad (13)$$

Here, $\sigma$ is the particle density, d is the Stokes diameter of the particle, and $\rho$ and $\mu$ are the carrier gas density and viscosity respectively.

The Stokes velocity is sometimes called the "settling velocity" of the particle in a gravitational field. It is important because if it is too large, the particle may settle out of the flow before it becomes entrained. This therefore sets a lower limit on the velocity of the airstream if one wishes the particulate to become airborne.

The Stokes diameter is the diameter of a sphere having the same Stokes velocity as the particle. However, for the sake of convenience, let us consider the particles to be spherical. An exact value is not necessary for the purposes at hand, an approximate one will be sufficient.

This entrainment length is important because the particulate must be fully entrained in the flow by the time the sampling plane is reached, otherwise the experimental results will be invalid.

### 3.4.2 Particulate Carrying Characteristics of Duct Flow:

Typically, the shape of the solids profile mimics that of the velocity profile across the duct to a certain degree. This depends on the size of the particles and the speed of the airstream [3]. It is tied to the concept of entrainment as discussed above. If there is a change in flow direction and the momentum of the particulate keeps them from reacting quickly enough, the carrier gas velocity and solids velocity profiles will diverge. This will be more significant for larger particulate due to their higher momentum.

Another important concept is the Reynold's number, $Re_D$. It is the ratio of inertial to viscous forces in the fluid:

$$Re_D = \rho VD/\mu \qquad (14)$$

Here, $\rho$ is the fluid density and $\mu$ is its absolute viscosity. V is the freestream velocity and D is the duct or tube diameter. If the Reynolds number ventures far above 2300, the flow will become turbulent. This is important

because it may change the dominant mechanisms of particulate transport that results in deposition. For the main duct, the Reynold's number is in the neighborhood of 120,000. This is clearly turbulent. The flow will also be turbulent going through the plasma torch.

In the process of simulating an environment, geometric factors have a tremendous effect on the distribution of entrained particulate across a duct [3].

An example of this effect is that of a particulate laden airflow through an elbow in a duct. In the fluid itself, the elbow will cause a secondary flow rotation, resulting in the addition of a helical component to the flow. Viscous interactions will eventually even the profile out as the gas travels down the duct in 5-8 duct diameters [3].

The particulate are also affected by the elbow. Their tendency will be to migrate toward the outer side of the elbow, primarily as a result of "centrifugal force" [3]. After passing through the elbow, the mass profile will return to its original shape approximately 5-8 duct diameters downstream[3].

### 3.4.3 Sampling Train:

#### 3.4.3.1 Inertial Deposition:

The design of the isokinetic sampling head and the rest of the sampling train, particularly the portions leading up to the plasma, must be performed very carefully.

A major concern is the deposition of particulate on the insides of the sampling train before the plasma, called inertial deposition [7]. Particulate tends to collect in areas where a rapid change in momentum occurs (i.e. an elbow). Elbows and bends must therefore be kept to a minimum.

Inertial deposition is adequately described by mechanics. For high speed flows, such as encountered in

this situation, when a particle strikes a surface, it will rebound with a certain force. If that force is sufficient to overcome the attractive forces that tend to make the particle stick to the surface(commonly referred to as Van Der Wall forces), the particle will not deposit [7]. However if the particle is flowing at a lower speed, its rebounding force may not be enough to overcome the attractive force, causing the particle to deposit.

#### 3.4.3.2 Turbulent Deposition:

Deposition on the walls of the main duct is a result of turbulent deposition [7]. In turbulent deposition, the entrained particulate flowing parallel to the surface is deposited as a result of the fluctuating flow velocity component normal to the wall. This is significant for particles larger than 1μm in diameter [7].

### 3.4.4 Plasma-Dust Interactions:

The temperature at the centerline of the plasma is approximately 5800 K [1]. If the particulate resides long enough in this region for significant heat transfer to occur from the plasma to the particulate, there will be a certain degree of vaporization of the particulate. The degree of vaporization will depend on the size of the particulate and its composition. These heating interactions result in thermophoresis [7], where small particles in the presence of a temperature gradient will diffuse from hot to cooler regions.

#### 3.4.4.1 Thermophoresis:

In the case at hand, the temperature at the center of the plasma and exhaust stream is the highest. The cool region is the wall of the tube. The particles will tend to diffuse toward the wall of the tube, and condense. The

reasons for this transport for large and small particulate are subtlely different.

The defining factor in determining what type of transport phenomena is occurring is the mean free path of the carrier gas, in this case, air. The mean free path is the average distance that a molecule will travel before it undergoes a collision with another molecule:

$$\lambda_a = \nu(\frac{\pi m}{2kT})^{1/2} \tag{15}$$

For air at standard conditions, the mean free path is about .065 μm.

**Small Particles:**

In the case where the mean free path of the molecules of the carrier gas is considerably larger than the particle diameter (such as in a metal that vaporizes in the plasma), molecule-particle collisions dominate. From a single particle point of view, the air molecules at the center of the tube are hotter and are moving faster than the ones toward the edge. Hence, a particle will have more collisions and acquire more energy from the molecules on the inside, resulting in transport to the outside. So, for this case ($d_p << \lambda_a$), the velocity at which they diffuse to the wall can be found from:

$$v_d = \frac{-3\nu\nabla T}{4(1+\frac{\pi}{8}\alpha)T} \tag{16}$$

Here, $\nu$ is the kinematic viscosity of the carrier gas (in this case air) and $\alpha$ is the accommodation coefficient which must be found experimentally, but is usually near 0.9 for momentum transfer [7]. Note that velocity is in the negative direction of the temperature gradient, as in heat transfer.

**Large Particles:**

For the larger particles that do not ablate in the plasma ($d_p >> \lambda_a$), the deposition arises through a different mechanism. A pressure develops on the hot side of the particle due to a creeping flow along the particle's surface from the cold side to the hot side as described below.

Gas molecules striking the sides of the particle obliquely from the higher temperature direction will lose more tangential momentum to the particle than those striking from the cold direction. The net effect on the gas is that the high temperature molecules will lose more momentum in the gas layer near the particle's surface than the colder molecules. As a result of this local momentum imbalance at the surface, the colder molecules flow over the surface toward the hotter side. Hence creeping flow.

The free flow of these creeping molecules are affected adversely by the surrounding gas. Due to viscous interactions, they will slow down a short distance after reaching the hot side of the particle. As a result of the creeping gas piling up on the high temperature side, the particle is propelled in the low-temperature direction [7]. The transport velocity is given by:

$$v_d = \frac{-2k_t\sigma'}{2k_t + K}\left(\frac{k_t}{p}\right)\nabla T \qquad (17)$$

Here, p is the pressure of the gas, $k_t$ is the thermal conductivity of the gas and K is the thermal conductivity of the particle. $\sigma'$ is a coefficient that relates the slip velocity generated at the surface due to the viscous interaction to the temperature gradient:

$$v_s = \frac{\sigma' k_t \nabla T}{p} \qquad (18)$$

$\sigma'$ is usually taken to be 1/5 (no dimensions)[7].

Thermophoresis is important because it will eventually be necessary to transfer the heat energy of the plasma to a

low-temperature sink via a heat exchanger. If the thermophoresis is significant in the heat exchanger, it will result in fouling of the tubes thereby reducing heat transfer. This phenomena was also noted when a version of the torch was placed in-situ in MARK-II. There was a uniform buildup of material on all surfaces after the plasma, particularly in the suction pump demonstrating that thermophoresis can indeed occur as a result of the plasma.

### 3.5 Temperature Effects on Isokinetic Sampling:

Elevated temperatures have an effect on isokinetic sampling, depending on the situation. If one looks at a simple situation such as that outlined in 3.2.1, if the duct temperature increases significantly above room temperature, the gas that is being drawn into the sample tube will be of a lower density than air at room temperature. What this means is that if the isokinetic system is calibrated to pull air at room temperature, it will be pulling harder on the higher temperature gas than it should be. This can be seen if one looks at the conservation of linear momentum:

$$\rho V^2 A_{st} = F_s = P_s A_{st} \qquad (19)$$

Here, $\rho$ is the density of the fluid, V is the suction velocity, $A_{st}$ is the cross sectional area of the sample tube and $P_s$ is the suction pressure supplied by the pump. This is the simplest representation regarding pulling a sample through a line (neglecting viscous effects).

If the system is calibrated at room temperature, a relationship will be established relating suction pressure, $P_s$, to flowrate, V. As the sampled gas temperature increases, its density must decrease. This reduces the magnitude of the inertial term, $\rho V^2 A_{st}$ at a given velocity, V. The suction pressure is applied externally. If that remains constant, in order for momentum balance to exist more gas will be pulled in until the magnitude of $\rho V^2 A_{st}$

equals that of $P_s A_{st}$. For this compensation to occur, the only thing that can increase is the velocity.

To summarize, the increase in temperature caused a decrease in fluid density resulting in a decrease in the momentum of the flow passing through the tube. To compensate for the momentum imbalance, more gas was drawn in which resulted in a higher gas flow velocity than before. This velocity is higher than the local freestream velocity of the flow, hence the isokinetic sampling criterion is violated. The amount by which the velocity will be off can be estimated by [9]:

$$(\rho V^2)_{hot} = (\rho V^2)_{cold} \tag{20}$$

Since the area, $A_{st}$, does not change. This becomes:

$$V_{hot} = (\rho_{cold}/\rho_{hot})^{1/2} V_{cold} \tag{21}$$

So the suction velocity will scale like the square root of the density difference. The viscosity will result in a head loss term due to friction with the walls of the tube. An expression in terms of pressure including this term is:

$$P_s = \rho V^2 + (f/2)(\rho V^2)(L_e/D) \tag{22}$$

Here, f is the friction factor, $L_e$ is the equivalent length of the tube between the sampling point and the pump (including entrance losses, bends, etc.), and D is the diameter of the tube. Re-arranging by equating the right hand side to itself for two different temperatures:

$$V_{hot}=V_{cold}\{[1+(f_{cold}-f_{hot}/2)(L_e/D)](\rho_{cold}/\rho_{hot})\}^{1/2} \tag{23}$$

The friction factor depends on the Reynold's number which depends on density and viscosity.

For a temperature change from room temperature (25 C) to 200 C, using (21), $V_{hot} = 1.27\ V_{cold}$. This is not acceptable. However, if one accounts for viscous effects using (23), $V_{hot} = 1.09\ V_{cold}$ for $L_e/D = 75$ and D = 1.0 cm. This is a practical high-temperature limit below which temperature effects may be neglected.

## 4.0 Experimental Approach

To ensure the success of the plasma torch diagnostic out at SAIC, it is clear that the most conservative design and testing approach should include simulating the expected operating conditions in the laboratory. The following section summarizes characteristics that will be important in this simulation.

It is required to sample isokinetically from the flowstream and characterize the torch performance to attempt to obtain a steady spectrometer signature over time. This spectrometer signature must be repeatable.

### 4.1 Conditions at SAIC:

#### 4.1.1 Exhaust Gas:

At SAIC, the furnace is purged with pure nitrogen as an operating medium for the plasma, but the hot exiting exhaust gas is cooled by mixing it with compressed air. The point of sampling in the exhaust stream for the plasma torch occurs far downstream after this mixture has had a chance to equilibrate and go through the primary components of a filtration system [8].

The exhaust gas temperature is between 200 and 300 degrees Fahrenheit at the point of interest. Flowrates vary between 400 and 900 cfm in an 8 inch diameter schedule 40 exhaust duct [8].

#### 4.1.2 Particle Characteristics:

The filtration system upstream of the sampling point consists of bag filters that remove particle sizes above 10 μm in diameter [8].

The material being vitrified in the furnace is clean soil from a lake bed that was used as a dump for hazardous waste and radioactive materials. Earlier tests with the furnace will use this clean feed while later tests will involve hot (radioactive) material.

The off gas will contain entrained effluents consisting mostly of metal/soil particulate. A sample of the clean lake bed soil was analyzed (See Table 2, p.63). The exhaust gas will contain trace amounts of these elements.

Due to the great amount of cooling air added to the furnace, the gas-particulate suspension in the region of interest is extremely dilute, that is, the volume occupied by the particulate compared to that of the gas is negligible. What this means in turn, is that the flow behavior of the exhaust gas should not be significantly influenced by the presence of the suspended particulate [10]. The solids profiles, however, will indeed be influenced by the gas behavior, as discussed in the previous chapter.

## 4.2 Experimental Apparatus:

The experimental setup was designed and constructed mostly by the author. The only fabricated component not designed by the author is the plasma torch setup itself (waveguide, starter, jets). The microwave equipment, spectrometer array, pump, manometer, and center steel pipe section are all off-the-shelf hardware. The remainder of the mechanism (sampling head, piping layouts, heat exchanger, main duct w/associated components, dust feed mechanism, etc.) were all designed and built by the author.

### 4.2.1 Main Duct:

A "replica" of the exhaust duct at SAIC was constructed in the laboratory (see Fig.8, p.78). This system consists of an 8-inch diameter schedule 40 PVC pipe approximately 20 feet in length. There is a center section made of steel with a 4" diameter 90-degree flange welded to it. This flange is the same as the one that is anticipated to be used out at SAIC during field tests.

The precise location in the SAIC exhaust duct in which the sampling will be performed has not been determined exactly. A straight run of pipe at least 8 pipe diameters in length has been requested so that the effects due to upstream geometric factors (bends, etc.) that upset the solids profile will be minimized. The basic piping layout of the setup in the lab therefore assumes a straight run of pipe leading up to the sampling point.

A squirrel cage blower provides between 250 and 750 cfm of flow through the sample duct, approximately in the lower 2/3 of the range of expected flowrates to be encountered at SAIC. The volume flowrate is controlled with a diverter valve that has seven different graduations, hence seven different volume flowrates can be achieved.

**4.2.2 Flow Straightener:**

Due to size constraints in the lab, the ducted flow must pass through two 90-degree elbows before it reaches the main duct. During earlier work, it was noticed that there was a helical component to the flow in the earlier stages of the duct. This was measured with a hot wire anemometer by holding it perpendicular to the axis of the duct. The profile in the axial flow direction was also a bit of a mess. This is not good because the particulate were going to be introduced shortly after the elbow. A significant helical component in the flow could upset the solids distribution and possibly result in abnormal deposition. Needless to say, this is not adequate for the simulation of a straight flow.

For this reason, a flow straightener was constructed (see Fig.9 ,p.79) by packing a three-foot section of 8-in. PVC pipe with 2-foot long tubes of different diameters. Tubes of larger diameter (~2 in.) were located on the outside while tubes of smaller diameter (~1 in.) were located toward the center. This was performed to try to

force a more fully developed flow profile in addition to straightening the flow. The larger pipes provide less flow resistance than the ones in the center, encouraging a flatter profile.

**4.2.3 Isokinetic Method:**

As mentioned in Section 3.2.3, one typically has a number of options in designing an isokinetic sampling system. In selecting a particular scheme, the primary factor is system simplicity allowing easy and reliable operation. It is for this reason the method described in 3.3.3 has been chosen. Its major advantage is that one does not have to account for temperature changes of the duct gas with time (as long as those changes are not too rapid). If the nozzle has to be calibrated for different velocities, a pitot tube can be mounted next to the nozzle to measure the local velocity (See Fig.10, p.80).

**4.2.4 Sampling Train:**

The isokinetic sampling train consists of the sampling nozzle, the plasma torch unit consisting of starter, swirl jets and waveguide, the primary exhaust section with a window, a heat exchanger, a suction pump, and a suction adjusting system (See Fig.8, p.78).

**4.2.4.1 Sizing of Sampling Head and Choice of Manometer:**

The size of the inlet to the nozzle has to be chosen such that the amount of flow that it has to intercept during isokinetic matching conditions will not exceed operational parameters of the torch. The maximum value for the torch was chosen to be 1.5 cfm of straight flow. The maximum flow velocity expected out at SAIC for 900 cfm of volume flow is approximately 45 ft/s. Based on these parameters, a nozzle with a frontal opening of 5/16-in. diameter was appropriate.

The manometer size was selected on the basis of the

maximum velocity head that could be encountered at SAIC. Based on a value of 45 ft/s for maximum local airflow, the maximum head was found to be ~0.4 in. $H_2O$ (using Eq.10).

This maximum differential would occur in the case that there were no flow through the nozzle with the duct operating at maximum flowrate.

A differential manometer was chosen (i.e. taken out of the junk pile in the NW-16 basement) that operated on that scale.

#### 4.2.4.2 Plasma Torch:

The plasma (See Fig.11, p.81) resides in a reduced width waveguide to increase microwave power density. This increases the number of ionizations per unit volume and robustness of the plasma. Immediately upstream of the waveguide is a tangential flow injection collar (to add vorticity to the flow), and a spark plug starting mechanism.

#### 4.2.4.3 Starting Mechanism:

Starting the plasma entails striking an arc between the two electrodes (in this case, spark plugs serve the purpose nicely). The electrical potential difference is provided by a Tesla coil. The arc is essentially a small plasma. The longitudinal flow from the gas flowing through the sampling nozzle transports these ionized particles to the waveguide where they act as a source for the electron cascade that causes the main plasma to form.

This starting mechanism, designed by Paul Thomas, a research engineer in the group, is essential to the operation of the device in a sealed environment. Without this advancement, use of this device in a non accessible area (i.e. sealed flowpath or in-situ placement) would have been very difficult. With this mechanism, starting the plasma is simply the act of pressing a button.

#### 4.2.4.4 Primary Exhaust:

Immediately after the plasma torch there is a series of KF-40 kwik-connect fittings that make up the first part of the exhaust system (primary exhaust). All of the components are stainless steel, and terminate at a 3/8-inch O.D. copper tube that leads to a heat exchanger. The exhaust from the plasma torch is very hot (several hundred degrees centigrade).

This initial run of fairly large diameter piping is very important for plasma operation. If the open region immediately after the plasma is not of sufficient volume one can obtain audible harmonics that cause the plasma to undergo cyclic perturbations that may cause it to extinguish.

Having a "reservoir" for the hot gases to travel through for a short time before they are drawn into a small orifice definitely helps keep the plasma in a stable operating mode. A window was installed at the end of the straight run to observe starting and operational behavior.

#### 4.2.4.5 Heat Exchanger:

As mentioned in the last section, the purge gas exiting the plasma is very hot, so it must be cooled before it is run through any flowmeters or suction pumps because of possible damage. A heat exchanger capable of removing at least one kilowatt of heat was required due to the fact that although some of the microwave energy is given off as light, the vast majority of that energy remains in the gas. One was designed and constructed from existing components.

The heat exchanger is a simple once-through cross flow design (See Fig.12, p.82) where hot gas flowing through a copper coil is cooled by water flowing across it. It was intended to over-design the unit from the beginning (since the materials were available) and also due to the fact that the research group has a 2.5 kW microwave power supply.

Should that unit ever be used in the lab in a similar application at high power, it would be a good idea to have this unit handy.

It was mentioned in Chapter 3 that the sampling scheme chosen would not need a heat exchanger or a flowmeter. This statement was based on the fact that the suction pump would likely be a large venturi pump that has no moving parts and is not heat-sensitive. To use a unit such as this in the lab setup would require a compressed air source capable of delivering at least 12 cfm. The system in the lab in NW-21 can only deliver 5 cfm. So a conventional pump had to be used in the lab which does have moving parts and can therefore be damaged by the hot gases. That is the reason the heat exchanger was needed. In the field, sufficient compressed air will be available to power a jet pump.

#### 4.2.4.6 Suction Pump and Adjustment:

Suction is applied to the system via a 3/4 HP double-diaphragm pump capable of pulling up to 5 cfm. In order to vary the amount of total suction through the torch exhaust there is a needle valve in the inlet to the pump that permits suction at the pump directly from atmosphere if less than total suction is needed. Using this alone it was only possible to reduce the suction from 5 to 2.5 cfm. To get the suction flowrate lower an additional valve was added in the flowpath. Considerable head loss was also added via the small diameter tube running through the heat exchanger. The end result was a capability to pull as little as 0.5 cfm and as much as 4 cfm through the exhaust system. The plasma can therefore operate with almost no flow at all through the sampling nozzle if necessary due to the air input in the swirl jets, which is typically 0.5 cfm.

## 4.3 Particulate Introduction system:

A system was devised to feed dust into the duct at a constant feed rate in order to help simulate conditions at SAIC for calibrating the plasma torch.

As was mentioned previously, it is known that the conditions at SAIC include particle diameters equal to or less than 10 μm in diameter [8]. The material being vitrified is soil from a particular lake bed in Idaho.

The Mark II plasma Arc Furnace in NW-21 uses clean soil from the same lake bed in Idaho for vitrification purposes. To simulate a likely ash at SAIC, a 50 kg sample of this soil was sent out to the Jet Pulverizer Company in Palmyra, NJ.

At Jet Pulverizer, the soil was run through an air-attrition mill which breaks up the soil through abrasive action with itself in a high speed air stream [11]. The walls of the mill chamber and the pump injector nozzle are hardened stainless steel, so contamination of the sample is claimed not to occur by the company.

Jet Pulverizer can produce a mix with a mean particle size of less than 10 μm, with a narrow size distribution [11].

A mechanism was designed to introduce this dust into the duct flow at a steady rate. In this mechanism, dust is stored in a hopper (see Fig.13,p.83) that has a cavity and matching rotor that are conical in shape (See Fig.14, p.84). The rotor is connected to a 3-phase motor running on a 115 V feed @ 60 Hz with an RC circuit to create the phase delay for the third phase. The motor rotates at a constant 72 RPM. The motor height may be raised or lowered by rotating the upper part of the PVC housing against the lower section (See Fig.15, p.85). This change in height changes the cross sectional area of the annulus for the dust to fall through thereby increasing or decreasing the feed-rate.

The rotor has agitator paddles that keep the dust from sticking together. The blades are in an arrangement that allows the entire chamber to be "swept out" in a single rotation of the rotor.

After falling through the hopper annulus, the dust travels through a vertical 2 in. I.D. pipe to a reducing section connected to the inlet port of a jet pump (See Fig.16, p.86). The jet pump mixes the suspended dust feed with a high velocity air stream (which also provides the suction) and atomizes the particles as it sprays them into the center of the duct. There is another height adjustment mechanism that enables one to translate the vertical position of the entire mechanism should it be desired to deposit particles in the top or bottom sections of the duct.

The entrainment length, $\lambda_{ent}$, was discussed in section 3.4.1. Based on properties of air at room temperature, it was found to be on the order of millimeters. This is the distance it takes for a 5 μm particle to become entrained in the duct flow at velocities in the operating range of interest. There should be no problem with particulate being fully entrained in the flow by the time it reaches the sampling nozzle (or at any point).

**4.4 Plasma Torch Operation:**

The objective of the torch operation is to achieve a steady time-averaged spectrometer signal for a particular transition of a certain element. The purpose of the dust feed mechanism is to entrain the particles in the duct flow.

Spectroscopic data will be obtained in the following manner.

With the entire system (main duct flow, dust feed, and sample train) operating isokinetically at a particular point, two tests will be performed. The first will entail normal operation of the plasma torch for a specified amount

of time. Spectroscopic transitions for a particular element will be monitored and accumulated for that time in the form of an intensity vs. time trace as a result of the dust being excited in the plasma. This will be repeated many times to ensure data correlation.

After this, the plasma will be shut off and removed from the sampling train. A housing containing a HEPA filter will be inserted in its place (See Fig.17, p.87). The setup will be run again, isokinetic flow will have to be re-established (due to the fact that the filter mechanism will contribute significant head loss) and the run times will be equal to those of the first tests. After the runs, the differences in weights of accumulated dust will be noted via use of an analytical balance. This second test will be performed to ensure that the solids flux at the point is steady over time. If this solids flux is constant over time, then hopefully the accumulated light signal will also be constant over time. The goal of this experiment is to verify that a steady particle flux will produce a steady signal over time.

This procedure will be performed at one point in the main duct many times to ensure data correlation. The objective is to obtain consistent results of accumulated light levels during different 5-minute runs. Duct sampling times less than five minutes may lead to spurious results (i.e. feed mechanism feedrate may fluctuate slightly in time, particles may become re-entrained causing solids flux spikes, etc.).

## 5.0 Results

### 5.1 Accuracy of Sampling Scheme:

In principle, isokinetic sampling should occur when the pressure difference between the inner and outer pressure taps is zero. However, to just assume that this is the case would be naive. As was previously mentioned, the EPA requires that when isokinetic sampling conditions are said to be met with whatever method has been chosen, that value must be within ten percent of true isokinetic sampling.

To characterize system performance then, it is necessary to establish true isokinetic sampling, where the gas velocity through the probe and the local velocity where the probe is located are measured and matched directly. This can be done over a wide range of duct flowrates. The manometer behavior can then be observed.

If the manometer behavior is consistent, one can then accurately predict when isokinetic sampling conditions exist well within the margin of error of ten percent.

So, following the above prescription, a direct measurement of the undisturbed velocity profile at the discrete sampling points was performed. The direct freestream flow measurements were made with a hot wire anemometer that uses a heated probe to calculate the passing air stream's local velocity. It is accurate to within 1 percent of the total flow [12].

The velocity profile across the center of the duct is given in Figure 23, p.93 for a series of volume flowrates. Figures 18-22 are discussed at a later point. The same data is tabulated in Table 4, p.65. The volume flowrate through the main duct was varied via use of an adjustable valve that has seven graduated positions between 0 and 90 degrees (fully closed to fully open). The velocity profile is skewed to one side, with the higher velocities flowing closer to the flange.

In order to match these local velocities to establish true isokinetic sampling, calculations were performed to find out what volume flow rate needed to be pulled through the sampling nozzle. Results are summarized in column 2 of Table 3, p. 64.

It is assumed that there is no variation in local flow velocity across the face of the probe. The volume flow is therefore just considered as the probe area multiplied by the local duct velocity. It is for this reason that one should not sample too close to the wall (i.e. in the viscous sublayer), because of the sharp velocity gradient with changing radius in addition to eddy flows that could invalidate any measurements [3].

In order to determine the flowrate going through the sample nozzle only, a flowmeter was installed between the pick-off tube and the primary exhaust before the torch See Fig 18, p.88). This avoids any errors that may be caused by suction inflow through the waveguide, starter assembly, or having to subtract the swirl jet flow.

This flowmeter was installed at this location for this series of characterization tests only. Clearly, this flowmeter could not be present during runs with suspended particulate because it would cause severe deposition. Once this system has been fully characterized, one can depend on the pressure taps to monitor the flow non-invasively, thereby minimizing particulate settling.

**System Accuracy:**

True isokinetic sampling was established in the following manner. The local duct velocity at the sampling point was measured with a hot-wire anemometer without the sampling head present. The volume flowrate that had to be pulled through the head to establish isokinetic flow was calculated by multiplying this value by the cross-sectional

area of the inlet tube. This volume flow was then established with the probe in the airstream.

When true isokinetic sampling was established, the manometer reading was not zero, but instead was consistently off zero in one direction. This indicates that at true isokinetic conditions, the pressure reading at the inner pressure tap was always lower than the outer pressure tap. This deviation in velocity head was not constant, but instead increased with the velocity that was being observed.

Measurements were performed at local duct flowrates between 825 and 2400 ft/min. Readings on average were taken in increments of 50 ft/min. A calibration chart was developed (see Fig.24, p.94) based on this data. The discrepancy appears to go linearly with increasing velocity.

This discrepancy must arise from a number of competing factors. Intuitively, one would not expect a linear dependence due to the fact that head scales as the square of velocity [9]. So the linear dependence is a unique characteristic of this particular nozzle where the coincidental linear behavior results from competing effects of local flow deceleration, boundary layer development, and turbulence.

One would expect the flow on the exterior to be lower at true isokinetic sampling conditions than the inside because if one has two control volumes, each with a characteristic thickness, one just inside the tip of the probe, and one directly outside of it (See Fig.19, p.89), as these control volumes move over the probe, the one on the inside remains much the same, while the one on the exterior increases in area by a factor of $r_o/r_i$. From conservation of mass, one would expect the velocity to decrease on the exterior by a factor of $r_i/r_o$. The corresponding head difference would then go like the square of this velocity difference.

To see if this behavior is a major contributor to the error, the volume flow required for pressure balance on the manometer was also recorded at all of these points (See Table 3, p.64). The manometer was set up to have pressure equilibrium at +.3 in. of water. The system was run and manometer pressure balance was achieved. The volume flowrate going through the sample nozzle at this state was recorded. This was then subtracted from the volume flow necessary for isokinetic sampling at each point. This was converted to a velocity in feet per second and a velocity head in inches of water was calculated. As can be seen in the last 2 columns of this table, the head that would result from this velocity difference is two orders of magnitude smaller than that which was observed.

Based on this analysis and its failure to describe the situation, one may conclude that it is best to try to avoid trying to predict theoretically why the discrepancy arises and just live with it. The source from which this design was acquired [6] used a nozzle with a slightly more reduced profile. Although the reference did not mention it, it is likely that the ratio of inner to outer probe diameters is a very significant quantity. Even if the above effect does not dominate, other geometrically dependent effects most likely do. This factor is the only one that was not incorporated into the nozzle design that was used for the purposes of this thesis.

So where does that leave the issues of isokinetic sampling with this technique?

The simplest solution is to include a pitot tube in the design, mounted just next to the nozzle (See Fig.10, p.80). If the velocity dependence of the error can be quantified, then one simply needs a local velocity measurement to tell the operator what discrepancy is necessary to ensure isokinetic sampling.

**Operation of This System:**

During operation then, one would obtain a local velocity measurement with the pitot tube, refer to the calibration chart for the nozzle, and make the necessary suction adjustment so the head reading was the correct value for that flowrate. Isokinetic sampling conditions should then exist. There is nothing wrong with this technique, and it should provide sampling well within 5% of true isokinetic, let alone ten.

**5.1.1 Temperature Effects:**

Unfortunately, this nozzle could only be tested at room temperature. It would have been ideal if tests could have been performed at higher temperatures, but the elevated temperatures at which effects would have been noticeable (above 200 degrees Centigrade ), could not be reproduced in the laboratory with the existing equipment. Certainly, one could have installed a large heat exchanger to heat up the entire duct flow, but this would have been impractical.

**5.1.2 Device Sensitivity:**

The manometer is extremely sensitive to changes in flow. It is possible to observe a manometer difference for a flowrate change as small as .015 cfm. This amount of change in flowrate will result in a head change of approximately .0025 in.$H_2O$, which is the smallest practical observable change in the manometer. Graduations are placed every .01 in. on the manometer. Being within .01 cfm is adequate because that corresponds to less than 3% of the flow, even at the lowest volume flowrates. So there is no danger of exceeding the 10% isokinetic sampling limit.

**5.1.3 Effect of Plasma Torch Operation on Manometer:**

The plasma torch was run on many occasions during isokinetic sampling. There was no difference in manometer

setting between the torch being on or off during normal operation. However, a suction velocity fluctuation did exist when the plasma was in an unstable operating mode.

## 5.2 Results of Particulate Studies:

### 5.2.1 Particle Characteristics:

The particulate that was run through the duct was from one of ten batches that was processed by the Jet Pulverizer Co. The particulate from the ninth run was used in the particulate studies. As can be seen, the size distribution of this batch is indeed narrow (See Fig.25, p.95). Almost all of the particles are under ten microns in diameter. This should therefore be a very close approximation to the particulate in the SAIC duct.

The soil was also sent to IEA for chemical analysis. As can be seen from the results (See Table 2, p.63), there is a significant iron impurity in the soil. This is highly desirable because it is very easy to monitor iron spectroscopic transitions with the spectrometer.

Since the particles are so small it is likely that they will be fully volatilized in the plasma as long as the mass flow rate of particulate is not too high.

### 5.2.2 Flow Characteristics:

A detailed flow study was performed of the duct to ensure that it would be suitable for particle transport. Flow measurements were taken across the duct along four separate radial axes such that measurements were no further than 45 degrees apart from each other at any given radius (See Fig.20, p.90).

The development of the profiles along these axes along the duct's length are given in Figures 26-29, p.96-99. The raw data is tabulated in Table 5, p.66. The velocity profile across the whole duct appears to be skewed

preferentially toward the inboard (flange) side. This is a characteristic of the mechanism itself.

#### 5.2.2.1 Flow Straightener Performance:

As mentioned, the flow straightener was installed to remove the helical component of the flow that resulted from the elbows upstream of the main duct. It performed fine, and there were no signs of helical flow in the device.

This profile is as good as any other because it is unknown what point at which the diagnostic will be set up in the furnace exhaust train (i.e. precise upstream conditions are unknown). However, it is more than likely that it will be an almost fully developed profile, as in this case.

The flow development is important from the standpoint of feeding particulate into the duct because if it is not of the correct nature, the particles may settle out of the flow or be distributed abnormally across the duct.

The feed nozzle was placed in the geometric center of the main duct for all data taken in this experiment.

### 5.2.3 Entrained Solids Distribution:

The solids flux was measured across the sampling (0-degree) axis isokinetically by replacing the plasma torch unit with a HEPA filter element in a housing equipped with KWIK-Connect flanges for ease of installation (See Fig.17, p.87). Three five-minute runs were performed at each of the nine locations across the duct. These results correlated closely and were subsequently plotted as a function of radius (see Fig.30, p.100). The related data can be found in Table 6, p.68. As can be seen, the solids distribution is also skewed toward the inboard side of the duct, but sharper in nature. This is typical of higher speed heavily laden flows as outlined in [3] and as demonstrated in [6].

#### 5.2.3.1 Sampling Concerns:

The only real concern in particulate sampling is to keep away from the duct walls. Evidence in [7] demonstrates that particulate distributions tend to drop off almost to zero in the viscous sublayer leading to spurious results.

### 5.2.4 Calibration of Particle Feeder:

In order to determine what fraction of the total particles flowing through the duct are being sampled, it was necessary to calibrate the feed mechanism. This was performed by placing the feeder above an analytical balance and operating it for 10-minute runs. The feed rate of the mechanism is adjustable, but the most reliable results it provided were those that are outlined for this feed setting in Table 7, p. 69. A best-fit line was fit to this data, and plotted in Figure 31, p.101. On average then, the particulate feed-rate was approximately 2.5 g/min delivered into the main duct.

### 5.2.5 Plasma Torch Studies:

The plasma torch was run with the sampling nozzle at a radial location of + .875 inches at a local duct flowrate of 2250 ft/min with 800 Watts of microwave power input. The corresponding plasma torch axial flowrate to maintain isokinetic sampling at this location was 1.2 cfm.

The objective for monitoring was to observe a particular spectroscopic transition for iron, which is a trace element in the soil. The observed region of the spectrum is shown in Figure 32, p.102. The iron line that was observed in the intensity vs. time traces is located at 358.1190 nm. This is the strongest line in this region.

The area under this peak was recorded as a function of time for a number of five-minute runs. These time spectra are displayed in Figures 33-37, p.103-107. The accumulated light signature per unit time is located at the top of each

chart. The average value for light collection was found to be 1452 I.U./sec, where I.U. is a generic light intensity unit. The discrepancy of the data from this average was quite small for the plasma torch.

This data reflects that the light signal was fairly steady over time with a constant feedrate. The feed rate to the torch was shown to be constant over time at the sampling point. This demonstrates that a steadily metered flux of material over time will provide a steady signal. This may sound trivial, but it is very important. The signal level depends on so many variables that this device might not be capable of steady performance. This data shows that if power input, flow and particle input are carefully monitored, one may obtain good results. Superficially, error bars of +/- 20% in light level sound bad. However, this is a significant improvement from earlier results with direct sample insertion that produced error bars of +/- 250%.

Fluctuations in the signal correspond to fluctuations in the mass flux. A particularly large spike could correspond to an amount of deposited material being re-entrained in the flow, or a transient of the feed mechanism.

It was certainly possible to run this device at different mass flow rates of particulate and air to chart plasma performance, but for it to be meaningful a huge database (of hundreds of data points) must be obtained. If that were done on this setup it would require running large amounts of custom ground material. That is clearly not practical. A system is recommended in section 6.2.1 to achieve this goal using minuscule amounts of feed material.

## 5.3 Summary:

Fortunately, everything worked. The nozzle did not operate in quite the way that was hoped, but with the attached pitot tube, it will sample isokinetically well within the required limits.

The particulate studies yielded encouraging results on plasma torch operation. This work will provide an appropriate basis for further studies. It is likely that nearly all of the particulate was volatilized due to the low solids mass flow rate through the torch, and the small particle diameter.

Ideas for future work are covered in the next Chapter.

## 6.0 Conclusions:

### 6.1 Research to Date:

The development of the microwave plasma torch monitor for real-time emissions measurements to date has made a great deal of progress. It is likely that it is not too far from being commercialized. Most of the challenging technical problems (starting, continuous operation, and isokinetic sampling) have been resolved. The major one that remains is calibration. However, experience in this work points to the fact that most calibration is application specific. The work that has been performed for this thesis seems to have promise as a model for developing calibration schemes in similar applications.

The development of isokinetic sampling for this system has been successful. For application at SAIC, it is safe to say that the device will meet the EPA requirement of sampling within 10% of true isokinetic sampling.

The challenge of the present work was to create a reliable self-contained plasma torch system that could sample isokinetically from a flowstream. Careful design in the sizing of the sample probe and designing for application specific worst case scenarios (high-end duct flowrates)was the crucial factor.

### 6.2 Future Work:

#### 6.2.1 Future Plasma Torch Studies:

Much would be gained by a great deal more work in characterizing the effect of particulate sizes on light signal and how that behavior correlates with changes in plasma power input, and residence time.

Since the plasma torch diagnostic is so sensitive to small quantities of material, a small scale experiment may be appropriate. A sample calibration gun similar to that in Figure 21, p.91 would be a good start. The basic way that a device such as this would work is the following.

Feed would be fed into a cylinder where a piston could push the material through an orifice in another piston. Excess material would spill out the other side of the orifice, preventing excess compaction of material.

Next the shear piston would be pushed up so that small volume of particulate (which would have the same cross section as the shear piston orifice), could then be shot with compressed air into the torch. An intensity vs. time trace could be obtained for the pulse of effluent. Hence calibration could be achieved after many trials.

A system such as this would be advantageous because one could take hundreds of data points per day and use very small amounts of test material. When the plasma torch is commercialized, a device of this nature could be built into the system for periodic device calibration.

### 6.2.2 Future Applications of the Diagnostic:

This diagnostic will be in use at Pacific Northwest Laboratory later this year in the exhaust stream of another vitrification furnace. The design explored for this application will be modified for use on that system. The duct size is smaller as well as the gas flowrate. Even so, the gas velocity is almost the same (~30-35 ft/s) so the same sampling nozzle can be used. This test will involve radioactive material though, so whatever equipment goes out to the test site will become contaminated and remain there.

The exhaust temperatures at the PNL furnace where the probe will be located are estimated to be about 300 C. Temperature effects on isokinetic sampling will therefore not be significant.

In these field applications, the solids and volume flow profiles will have to be estimated with the techniques outlined in Section 3.2.1. This will necessitate sampling with an isokinetic cyclone probe from at least 2 directions

(e.g. 0 and 90-Degree planes). The mass flowrate could then be estimated.

These estimations were not necessary for the in-lab tests because in the characterization of the sampling nozzle, the important quantity was local duct flowrate, and the mass flowrate through the duct was already quantified at 2.5 g/min. These estimations could have been made anyway, but sampling with the isokinetic probe could only be made along the 0-Degree plane since there was only one flange.

### 6.2.3 Commercialization of the Diagnostic:

This diagnostic will eventually be used in large scale commercial applications whether it involves detecting metal emissions from commercial incinerators or in manufacturing processes (e.g. alloy production). The exhaust ducts for these systems will probably be quite large, so in-situ placement may be a practical possibility (see Fig.22, p.92).

This would be beneficial, particularly in hostile environments where bringing the contaminated exhaust out of the duct and piping it back in may be a safety concern in the event of leakage or rupture.

### 6.2.4 Future Nozzle Designs:

The work with sampling nozzles is far from over. It should be possible to get the sampling system to operate reliably with the manometer alone and no pitot tube. This will necessitate the construction of more nozzles and the performance of more testing to ascertain their characteristics. After a few more iterations, it should be possible to have desirable operational characteristics.

## 6.3 Overall Perspective of Plasma Torch Diagnostic:

The plasma torch diagnostic holds a great deal of promise for environmental monitoring. Its robustness and capacity for untreated effluents give it a clear advantage over competing technologies (ICP, Laser-Spark Detectors).

The device will only turn into something big if proper care is taken to calibrate it for the respective applications that it will be used for. The potential is there waiting to be tapped.

## 7.0 References:

### 7.1 Cited:


1) P.P.Woskov; D.Y.Rhee; P.Thomas; D.R.Cohn; J.E.Surma; C.H.Titus; "Microwave Plasma Continuous Emissions Monitor for Trace Metals", PFC Report, March, 1996

2) Liboff, R.L.; "Introductory Quantum Mechanics", 2nd Ed., © 1992, Addison Wesley, 782 pp.

3) Hawksley, P.G.W.; Badzioch, S; Blackett, J.H.; "Measurement of Solids in Flue Gases", 2nd Ed. © 1977, The Institute of Fuel, London, Printed by Adlard & Son Ltd., Dorking, U.K., 248pp.

4) Willeke, Klaus; Baron, Paul A.; Ed.; "Aerosol Measurement: Principles, Techniques and Applications", © 1993 by Van Nostrand Reinhold, 876 pp.

5) Environmental Protection Agency; "EPA Stationary Source Sampling Methods", Rev 2, 6/94.

6) Van Breugel, J.W.; Stein,J.J.M.; De Vries,R.J.; "Isokinetic Sampling in a Dense Gas-Solids Stream", Proc. Instn. Mech. Engrs., 1969-70, pp.18-23.

7) Friedlander, S.K.; "Smoke, Dust and Haze; Fundamentals of Aerosol Behavior", John Wiley and Sons, © 1977, 317pp.

8) Cornelison, C.; DeWitt, L.M.; Hassel, G.R.; Leatherman, G.L.; "Final Report for the Advanced Analytical Instrumentation Demonstration", SAIC Waste Management Technology Division, 1985.

9) Fay, J.A.; "Introduction to Fluid Mechanics", © 1994 MIT Press, Cambridge, MA., 605 pp.

10) Di Giacinto, M.; Sabetta, F.; Piva,R.; "Two-Way Coupling Effects in Dilute Gas-Particulate Flows", Transactions of the ASME, Vol 104, September, 1982, pp.304-312.

11) The Jet Pulverizer Co., Assorted Technical Equipment Data (Brochures) and Analysis of Feed Material, 1996

12) Omega Engineering, Inc.; "HHF600 Series Omega Air Velocity Meter Operator's Manual", © 1992, Omega Engineering Inc. 21pp.

**7.2 Non-Cited:**

13) Apazidis, Nicholas; "On Two-Dimensional Laminar Flows of a Particulate Suspension in the Presence of Gravity Field", International Journal of Multiphase Flow, Vol.11, No.5, pp.675-698, 1985.

14) Blades, M.W.; "Application of Weakly Ionized Plasmas for Materials Sampling and Analysis", IEEE Transactions on Plasma Science, V.19, No.6, Dec. 1991, pp.1090-1113.

15) Feinman, J.; "Plasma Technology in Metallurgical Processing", © 1987, Iron & Steel Society, 208 pp.

16) Fox, R.W.; McDonald, A.T.; "Introduction to Fluid Mechanics", 4th Ed., © 1992, John Wiley & Sons, New York, 829 pp.

17) Harrison, George R.; "MIT Wavelength Tables", © 1969, MIT Press, 429 pp.

18) Hayashi, K; Branch, M.C.; "Concentration, Velocity, and Particle Size Measurements in Gas-Solid Two Phase Jets", Journal of Energy, Sept.-Oct.1980, pp.193-198.

19) Hesketh, Howard E.; El-Shobokshy, M.S., "Predicting and Measuring Fugitive Dust", © 1985, Technomic Publishing Co., 131 pp.

20) Kennard, E.H.; "Kinetic Theory of Gases", © 1938 McGraw-Hill, New York, 483 pp.

21) Orlemann,J.A.; Kalman, T.J.; Cummings, J.A.; Lim, E.Y.; "Fugitive Dust Control Technology", © 1983, Noyes Data Corporation, Park Ridge, N.J., 534 pp.

22) Spedden, S.E.; "Adjustable Isokinetic Sampling Horn", IBM Technical Disclosure Bulletin, Vol.26, No.2, July 1983, pp.853-857.

23) Wright, B.M.; "A New Dust Feed Mechanism", British Journal of Industrialized Medicine, Vol. 27, January 1950, pp.12-15.

# Appendix A: Tables

# Table 1

## Torch Detection Limits

| Toxic Metal | Transition (nm) | Burn Off (sec) | Detection Limit (ng) | (ppb) |
|---|---|---|---|---|
| Be | 234.9 | 17 | 0.16 | 0.1 |
| Cd | 228.8 | 6.8 | 0.17 | 0.02 |
| Ag | 328.1 | >11 | <.24 | <.02 |
| Ba | 553.6 | >32 | <.68 | <.01 |
| Sb | 231.1 | >30 | <.89 | <.02 |
| Pb | 283.3 | 4.2 | 1.1 | 0.2 |
| Ni | 341.4 | >36 | <1.1 | <.05 |
| Cr | 357.8 | 2.6 | 1.3 | 0.8 |
| Hg | 253.7 | 4.2 | 2.9 | 0.3 |
| As | 235 | 6.4 | 5.8 | 1 |

Limits were obtained by inserting ceramic probes into edge of plasma with test material on tip of rod.

Burn off refers to evaporation of material from inserted probe and subsequent excitation in the plasma.

# Table 2

## Soil Composition

| Metal | wt sample/wt soil (mg/kg) |
|---|---|
| Aluminum | 19300 |
| Arsenic | 13 |
| Barium | 257 |
| Boron | 7 |
| Cadmium | 1.04 |
| Calcium | 42,200 |
| Chromium | 27.9 |
| Copper | 244 |
| Iron | 20300 |
| Lead | 22 |
| Lithium | 20.1 |
| Magnesium | 10300 |
| Manganese | 344 |
| Nickel | 28.1 |
| Sodium | 310 |
| Silicon | 184 |
| Titanium | 345 |

## Table 3, Analysis of Manometer Discrepancy

| Duct Flow Velocity | Required Volume Flow | Measured Head Difference (at isokinetic conds.) | Volume Flow at Pressure Equilibrium | Volume Flow at Pressure Equilibrium | Difference in Volume Flow Between Pressure Tap Equilibrium and Isokinetic Conds. | Corresponding Flow Velocity Difference | Corresponding Head Difference | Actual Head Discrepancy (Manometer Imbalance) |
|---|---|---|---|---|---|---|---|---|
| (ft/min) | (cfm) | (in. Water) | (cfh) | (cfm) | (cfm) | (ft/s) | (in.water) | (in.water) |
| 825 | 0.439421 | 0.515 | 12.5 | 0.208333333 | 0.231088067 | 7.231010863 | 0.009743018 | 0.215 |
| 875 | 0.466053 | 0.52 | 14.5 | 0.241666667 | 0.278333333 | 8.709369488 | 0.014134121 | 0.22 |
| 900 | 0.479369 | 0.525 | 16 | 0.266666667 | 0.258333333 | 8.08354653 | 0.012175849 | 0.225 |
| 950 | 0.506 | 0.535 | 17 | 0.283333333 | 0.251666667 | 7.874938878 | 0.011555527 | 0.235 |
| 1000 | 0.532632 | 0.537 | 18 | 0.3 | 0.237 | 7.416002043 | 0.010247904 | 0.237 |
| 1050 | 0.559264 | 0.54 | 18.5 | 0.308333333 | 0.231666667 | 7.249115921 | 0.009791866 | 0.24 |
| 1100 | 0.585895 | 0.545 | 20 | 0.333333333 | 0.211666667 | 6.623292964 | 0.008174163 | 0.245 |
| 1150 | 0.612527 | 0.552 | 23 | 0.383333333 | 0.168666667 | 5.277773606 | 0.005190353 | 0.252 |
| 1225 | 0.652474 | 0.556 | 23.5 | 0.391666667 | 0.166333333 | 5.204760927 | 0.00504774 | 0.258 |
| 1250 | 0.66579 | 0.57 | 24 | 0.4 | 0.17 | 5.319495136 | 0.005272738 | 0.27 |
| 1300 | 0.692422 | 0.573 | 24.5 | 0.408333333 | 0.164666667 | 5.152609014 | 0.004947089 | 0.273 |
| 1350 | 0.719053 | 0.585 | 25 | 0.416666667 | 0.168333333 | 5.267343223 | 0.005169858 | 0.285 |
| 1400 | 0.745685 | 0.57 | 26 | 0.433333333 | 0.136666667 | 4.276456874 | 0.003407717 | 0.27 |
| 1450 | 0.772316 | 0.58 | 27 | 0.45 | 0.13 | 4.067849222 | 0.003083366 | 0.28 |
| 1500 | 0.798948 | 0.59 | 27.5 | 0.458333333 | 0.131666667 | 4.120001135 | 0.003162933 | 0.29 |
| 1550 | 0.82558 | 0.605 | 27 | 0.45 | 0.155 | 4.850127918 | 0.004383306 | 0.305 |
| 1600 | 0.852211 | 0.628 | 28 | 0.466666667 | 0.161333333 | 5.048305188 | 0.00474883 | 0.328 |
| 1650 | 0.878843 | 0.625 | 29.75 | 0.495833333 | 0.129166667 | 4.041773265 | 0.003043962 | 0.325 |
| 1700 | 0.905474 | 0.63 | 29.5 | 0.491666667 | 0.138333333 | 4.328606787 | 0.003491339 | 0.33 |
| 1750 | 0.932106 | 0.638 | 30.5 | 0.508333333 | 0.129666667 | 4.057418839 | 0.003067574 | 0.338 |
| 1800 | 0.958738 | 0.64 | 29.75 | 0.495833333 | 0.144166667 | 4.511140483 | 0.003791998 | 0.34 |
| 1850 | 0.985369 | 0.665 | 30.5 | 0.508333333 | 0.156666667 | 4.902279831 | 0.004478077 | 0.365 |
| 1900 | 1.012001 | 0.663 | 33 | 0.55 | 0.113 | 3.535899708 | 0.002329675 | 0.363 |
| 1950 | 1.038632 | 0.67 | 33 | 0.55 | 0.12 | 3.754937743 | 0.002627247 | 0.37 |
| 2000 | 1.065264 | 0.687 | 32.5 | 0.541666667 | 0.145333333 | 4.547646822 | 0.00385362 | 0.387 |
| 2050 | 1.091896 | 0.705 | 34 | 0.566666667 | 0.138333333 | 4.328606787 | 0.003491339 | 0.405 |
| 2100 | 1.118527 | 0.72 | 37.5 | 0.625 | 0.095 | 2.972659047 | 0.00164659 | 0.42 |
| 2150 | 1.145159 | 0.73 | 37 | 0.616666667 | 0.113333333 | 3.546330091 | 0.002343439 | 0.43 |
| 2200 | 1.17179 | 0.74 | 37.5 | 0.625 | 0.115 | 3.598482004 | 0.002412871 | 0.44 |
| 2250 | 1.198422 | 0.745 | 38 | 0.633333333 | 0.111666667 | 3.494178178 | 0.002275021 | 0.445 |
| 2300 | 1.225054 | 0.748 | 38 | 0.633333333 | 0.114666667 | 3.588051621 | 0.002398903 | 0.448 |
| 2350 | 1.251685 | 0.75 | 38.5 | 0.641666667 | 0.108333333 | 3.389874351 | 0.002141226 | 0.45 |
| 2400 | 1.278317 | 0.76 | 39.5 | 0.658333333 | 0.101666667 | 3.181266699 | 0.0018858 | 0.46 |

| | | Table 4,Variable Flow Data for Main Duct | | | | | | | | |
|---|---|---|---|---|---|---|---|---|---|---|
| Valve | Angular | | | | | | | | | |
| Position | Position | -3.5 | -2.625 | -1.75 | -0.875 | 0 | 0.875 | 1.75 | 2.625 | 3.5 |
| Closed 1 | 0 | 1875 | 2350 | 2400 | 2400 | 2350 | 2275 | 2225 | 2200 | 2100 |
| 2 | 15 | 1750 | 2200 | 2250 | 2250 | 2200 | 2150 | 2100 | 2000 | 1925 |
| 3 | 30 | 1700 | 2000 | 2050 | 2050 | 2000 | 1950 | 1900 | 1850 | 1750 |
| 4 | 45 | 1600 | 1850 | 1850 | 1850 | 1800 | 1750 | 1650 | 1650 | 1500 |
| 5 | 60 | 1450 | 1600 | 1650 | 1600 | 1550 | 1500 | 1450 | 1400 | 1250 |
| 6 | 75 | 1150 | 1400 | 1400 | 1400 | 1350 | 1300 | 1250 | 1225 | 1100 |
| Open 7 | 90 | 875 | 1025 | 1050 | 1050 | 1000 | 950 | 925 | 900 | 825 |

# Table 5

## Flow Study Data

| Distance Downstream From Feeder (ft) | | | | | | | | | | |
|---|---|---|---|---|---|---|---|---|---|---|
| | | *All velocities in (ft/min) | | | | | | | | |
| | | * Study performed with PVC elbow in place of main duct diverter valve | | | | | | | | |
| | Radius: | -3.5 | -2.625 | -1.75 | -0.875 | 0 | 0.875 | 1.75 | 2.625 | 3.5 |
| 0 | 0 Degrees | 2200 | 2300 | 2300 | 1900 | 1850 | 2000 | 2400 | 2400 | 2300 |
| | 45 Degrees | 2400 | 2200 | 2100 | 1950 | 1850 | 1950 | 2200 | 2400 | 2500 |
| | 90 Degrees | 1800 | 1800 | 1900 | 1900 | 1850 | 1900 | 2000 | 1900 | 1950 |
| | 135 Degrees | 2200 | 2050 | 1900 | 1850 | 1850 | 1950 | 2200 | 2400 | 2550 |
| | | | | | | | | | | |
| | Radius: | -3.5 | -2.625 | -1.75 | -0.875 | 0 | 0.875 | 1.75 | 2.625 | 3.5 |
| 0.5 | 0 Degrees | 2200 | 2300 | 2200 | 2000 | 1950 | 2050 | 2250 | 2350 | 2250 |
| | 45 Degrees | 2100 | 2100 | 2050 | 1950 | 1900 | 2100 | 2250 | 2250 | 2200 |
| | 90 Degrees | 1850 | 1875 | 1900 | 1975 | 1975 | 2050 | 2100 | 2050 | 1875 |
| | 135 Degrees | 2250 | 2100 | 1950 | 1925 | 1975 | 2100 | 2250 | 2300 | 2300 |
| | | | | | | | | | | |
| | Radius: | -3.5 | -2.625 | -1.75 | -0.875 | 0 | 0.875 | 1.75 | 2.625 | 3.5 |
| 1.5 | 0 Degrees | 2350 | 2350 | 2250 | 2150 | 2100 | 2150 | 2250 | 2250 | 2100 |
| | 45 Degrees | 2150 | 2200 | 2150 | 2050 | 2000 | 2100 | 2200 | 2200 | 2100 |
| | 90 Degrees | 1950 | 1950 | 1975 | 2000 | 2000 | 2150 | 2150 | 2050 | 2050 |
| | 135 Degrees | 2250 | 2150 | 2000 | 2000 | 2100 | 2200 | 2200 | 2150 | 2300 |
| | | | | | | | | | | |
| | Radius: | -3.5 | -2.625 | -1.75 | -0.875 | 0 | 0.875 | 1.75 | 2.625 | 3.5 |
| 2 | 0 Degrees | 2350 | 2350 | 2250 | 2150 | 2100 | 2100 | 2150 | 2150 | 2200 |
| | 45 Degrees | 2150 | 2200 | 2150 | 2100 | 2100 | 2150 | 2175 | 2150 | 2050 |
| | 90 Degrees | 1925 | 1975 | 2000 | 2000 | 2100 | 2150 | 2150 | 2000 | 2100 |
| | 135 Degrees | 2150 | 2200 | 2100 | 2100 | 2125 | 2250 | 2200 | 2200 | 2050 |
| | | | | | | | | | | |
| | Radius: | -3.5 | -2.625 | -1.75 | -0.875 | 0 | 0.875 | 1.75 | 2.625 | 3.5 |
| 2.5 | 0 Degrees | 2350 | 2300 | 2250 | 2200 | 2200 | 2150 | 2150 | 2150 | 2050 |
| | 45 Degrees | 2100 | 2200 | 2200 | 2150 | 2150 | 2200 | 2150 | 2100 | 2050 |
| | 90 Degrees | 2000 | 2000 | 2050 | 2100 | 2175 | 2200 | 2150 | 2050 | 2050 |
| | 135 Degrees | 2150 | 2150 | 2050 | 2100 | 2200 | 2250 | 2150 | 2150 | 2100 |
| | | | | | | | | | | |
| | Radius: | -3.5 | -2.625 | -1.75 | -0.875 | 0 | 0.875 | 1.75 | 2.625 | 3.5 |
| 3 | 0 Degrees | 2300 | 2300 | 2250 | 2200 | 2200 | 2150 | 2100 | 2050 | 2050 |
| | 45 Degrees | 2100 | 2200 | 2200 | 2200 | 2200 | 2200 | 2150 | 2150 | 2100 |
| | 90 Degrees | 2000 | 2100 | 2100 | 2150 | 2200 | 2200 | 2100 | 2050 | 2050 |
| | 135 Degrees | 2300 | 2150 | 2100 | 2150 | 2200 | 2250 | 2100 | 2150 | 2100 |
| | | | | | | | | | | |
| | Radius: | -3.5 | -2.625 | -1.75 | -0.875 | 0 | 0.875 | 1.75 | 2.625 | 3.5 |
| 3.5 | 0 Degrees | 2350 | 2350 | 2300 | 2300 | 2300 | 2200 | 2150 | 2050 | 2000 |
| | 45 Degrees | 2050 | 2200 | 2250 | 2250 | 2300 | 2250 | 2150 | 2150 | 1950 |
| | 90 Degrees | 2000 | 2100 | 2150 | 2200 | 2250 | 2250 | 2150 | 2050 | 1900 |
| | 135 Degrees | 2100 | 2200 | 2200 | 2200 | 2300 | 2250 | 2250 | 2250 | 2100 |
| | | | | | | | | | | |
| | Radius: | -3.5 | -2.625 | -1.75 | -0.875 | 0 | 0.875 | 1.75 | 2.625 | 3.5 |
| 4 | 0 Degrees | 2250 | 2350 | 2300 | 2300 | 2250 | 2200 | 2150 | 2100 | 2100 |
| | 45 Degrees | 2200 | 2250 | 2250 | 2300 | 2300 | 2300 | 2150 | 2100 | 1900 |
| | 90 Degrees | 2050 | 2100 | 2150 | 2200 | 2300 | 2250 | 2150 | 2050 | 1950 |
| | 135 Degrees | 2200 | 2250 | 2200 | 2250 | 2250 | 2200 | 2150 | 2000 | 1900 |
| | | | | | | | | | | |
| | Radius: | -3.5 | -2.625 | -1.75 | -0.875 | 0 | 0.875 | 1.75 | 2.625 | 3.5 |
| 5 | 0 Degrees | 2200 | 2300 | 2350 | 2350 | 2250 | 2200 | 2050 | 2000 | 1900 |
| | 45 Degrees | 2050 | 2200 | 2250 | 2250 | 2250 | 2200 | 2150 | 2075 | 1875 |
| | 90 Degrees | 1925 | 2150 | 2225 | 2250 | 2350 | 2250 | 2200 | 2100 | 1850 |
| | 135 Degrees | 2050 | 2250 | 2275 | 2300 | 2350 | 2250 | 2150 | 2050 | 1850 |

| | Radius: | -3.5 | -2.625 | -1.75 | -0.875 | 0 | 0.875 | 1.75 | 2.625 | 3.5 |
|---|---|---|---|---|---|---|---|---|---|---|
| 6 | 0 Degrees | 2250 | 2350 | 2350 | 2400 | 2350 | 2250 | 2150 | 2150 | 1950 |
| | 45 Degrees | 2100 | 2250 | 2350 | 2350 | 2350 | 2250 | 2250 | 2150 | 1950 |
| | 90 Degrees | 1950 | 2250 | 2300 | 2350 | 2400 | 2350 | 2250 | 2150 | 1950 |
| | 135 Degrees | 2150 | 2300 | 2300 | 2350 | 2350 | 2200 | 2150 | 2050 | 1750 |
| | | | | | | | | | | |
| | Radius: | -3.5 | -2.625 | -1.75 | -0.875 | 0 | 0.875 | 1.75 | 2.625 | 3.5 |
| 6.5 | 0 Degrees | 2200 | 2350 | 2400 | 2400 | 2375 | 2250 | 2200 | 2150 | 1975 |
| | 45 Degrees | 2200 | 2350 | 2350 | 2375 | 2300 | 2200 | 2200 | 2150 | 1750 |
| | 90 Degrees | 1925 | 2250 | 2350 | 2400 | 2400 | 2300 | 2200 | 2150 | 1925 |
| | 135 Degrees | 2150 | 2350 | 2400 | 2350 | 2350 | 2225 | 2200 | 2050 | 1850 |
| | | | | | | | | | | |
| | Radius: | -3.5 | -2.625 | -1.75 | -0.875 | 0 | 0.875 | 1.75 | 2.625 | 3.5 |
| 7.5 | 0 Degrees | 2150 | 2650 | 2400 | 2400 | 2350 | 2400 | 2200 | 2100 | 1950 |
| | 45 Degrees | 2250 | 2350 | 2400 | 2400 | 2300 | 2200 | 2200 | 2050 | 1750 |
| | 90 Degrees | 1900 | 2300 | 2400 | 2400 | 2350 | 2200 | 2150 | 2050 | 1900 |
| | 135 Degrees | 2100 | 2350 | 2400 | 2400 | 2400 | 2200 | 2150 | 2050 | 1850 |
| | | | | | | | | | | |
| | Radius: | -3.5 | -2.625 | -1.75 | -0.875 | 0 | 0.875 | 1.75 | 2.625 | 3.5 |
| 8.5 | 0 Degrees | 2100 | 2250 | 2450 | 2450 | 2400 | 2300 | 2250 | 2200 | 2050 |
| | 45 Degrees | 2150 | 2300 | 2400 | 2400 | 2400 | 2300 | 2200 | 1250 | 1650 |
| | 90 Degrees | 1650 | 2200 | 2400 | 2400 | 2400 | 2350 | 2250 | 2150 | 1950 |
| | 135 Degrees | 2100 | 2400 | 2400 | 2400 | 2400 | 2300 | 2200 | 2100 | 1900 |
| | | | | | | | | | | |
| | Radius: | -3.5 | -2.625 | -1.75 | -0.875 | 0 | 0.875 | 1.75 | 2.625 | 3.5 |
| 10 | 0 Degrees | 2000 | 2400 | 2550 | 2600 | 2550 | 2500 | 2350 | 2250 | 2200 |
| | 45 Degrees | 2250 | 2400 | 2500 | 2550 | 2450 | 2400 | 2350 | 2200 | 1750 |
| | 90 Degrees | 1550 | 2300 | 2450 | 2550 | 2550 | 2450 | 2425 | 2350 | 2000 |
| | 135 Degrees | 2250 | 2400 | 2500 | 2550 | 2550 | 2450 | 2375 | 2200 | 1950 |
| | | | | | | | | | | |
| | Radius: | -3.5 | -2.625 | -1.75 | -0.875 | 0 | 0.875 | 1.75 | 2.625 | 3.5 |
| 11 | 0 Degrees | 2250 | 2450 | 2550 | 2550 | 2550 | 2450 | 2350 | 2250 | 2100 |
| | 45 Degrees | 2050 | 2350 | 2550 | 2500 | 2450 | 2400 | 2300 | 2150 | 1850 |
| | 90 Degrees | 1900 | 2300 | 2500 | 2500 | 2450 | 2400 | 2400 | 2200 | 1950 |
| | 135 Degrees | 2350 | 2500 | 2450 | 2425 | 2450 | 2400 | 2250 | 2000 | 1850 |
| | | | | | | | | | | |
| | Radius: | -3.5 | -2.625 | -1.75 | -0.875 | 0 | 0.875 | 1.75 | 2.625 | 3.5 |
| 11.5 | 0 Degrees | 2300 | 2450 | 2550 | 2550 | 2500 | 2400 | 2400 | 2250 | 2250 |
| | 45 Degrees | 2100 | 2400 | 2550 | 2500 | 2500 | 2400 | 2350 | 2050 | 2200 |
| | 90 Degrees | 2150 | 2400 | 2500 | 2450 | 2450 | 2400 | 2350 | 2150 | 1950 |
| | 135 Degrees | 2350 | 2450 | 2450 | 2450 | 2450 | 2400 | 2200 | 1900 | 1750 |
| | | | | | | | | | | |
| | Radius: | -3.5 | -2.625 | -1.75 | -0.875 | 0 | 0.875 | 1.75 | 2.625 | 3.5 |
| 12 | 0 Degrees | 2250 | 2450 | 2500 | 2500 | 2500 | 2450 | 2350 | 2250 | 2100 |
| | 45 Degrees | 2100 | 2300 | 2500 | 2450 | 2450 | 2400 | 2300 | 2000 | 2300 |
| | 90 Degrees | 2100 | 2350 | 2400 | 2450 | 2450 | 2450 | 2400 | 2150 | 1975 |
| | 135 Degrees | 2350 | 2500 | 2450 | 2400 | 2400 | 2350 | 2200 | 1900 | 1850 |
| | | | | | | | | | | |
| | Radius: | -3.5 | -2.625 | -1.75 | -0.875 | 0 | 0.875 | 1.75 | 2.625 | 3.5 |
| 12.5 | 0 Degrees | 2300 | 2500 | 2550 | 2500 | 2475 | 2400 | 2400 | 2250 | 2100 |
| | 45 Degrees | 2100 | 2300 | 2450 | 2450 | 2450 | 2400 | 2300 | 2000 | 2000 |
| | 90 Degrees | 2250 | 2400 | 2500 | 2450 | 2450 | 2400 | 2300 | 2100 | 1900 |
| | 135 Degrees | 2300 | 2550 | 2500 | 2400 | 2400 | 2350 | 2050 | 1850 | 1750 |
| | | | | | | | | | | |
| | Radius: | -3.5 | -2.625 | -1.75 | -0.875 | 0 | 0.875 | 1.75 | 2.625 | 3.5 |
| 13.5 | 0 Degrees | 2150 | 2400 | 2450 | 2500 | 2450 | 2400 | 2400 | 2200 | 1950 |
| | 45 Degrees | 2100 | 2300 | 2400 | 2400 | 2450 | 2300 | 2200 | 2000 | 1850 |
| | 90 Degrees | 2300 | 2450 | 2450 | 2450 | 2400 | 2400 | 2200 | 2000 | 1850 |
| | 135 Degrees | 2200 | 2500 | 2500 | 2450 | 2400 | 2300 | 2050 | 1850 | 1700 |

# Table 6, Particulate Collection Data for Main Duct

| Accumulations From 5 Minute Tests | | | | | | | | | |
|---|---|---|---|---|---|---|---|---|---|
| Position | -3.5 | -2.625 | -1.75 | -0.875 | 0 | 0.875 | 1.75 | 2.625 | 3.5 |
| | Mass (g) | Mass (g) | Mass (g) | Mass (g) | Mass (g) | Mass (g) | Mass (g) | Mass (g) | Mass (g) |
| Run 1 | 0.0173 | 0.0486 | 0.0528 | 0.0249 | 0.0203 | 0.0171 | 0.0165 | 0.0062 | 0.0084 |
| Run 2 | 0.0205 | 0.0475 | 0.052 | 0.0292 | 0.0197 | 0.0189 | 0.0109 | 0.009 | 0.0082 |
| Run 3 | 0.0188 | 0.0513 | 0.0504 | 0.0302 | 0.0206 | 0.0201 | 0.0143 | 0.0096 | 0.0093 |
| Average: | 0.018867 | 0.049133 | 0.051733 | 0.0281 | 0.0202 | 0.0187 | 0.0139 | 0.008267 | 0.008633 |

| Values Per Second | | | | | | | | | |
|---|---|---|---|---|---|---|---|---|---|
| Position | -3.5 | -2.625 | -1.75 | -0.875 | 0 | 0.875 | 1.75 | 2.625 | 3.5 |
| | Mass (g) | Mass (g) | Mass (g) | Mass (g) | Mass (g) | Mass (g) | Mass (g) | Mass (g) | Mass (g) |
| Run 1 | 5.77E-05 | 0.000162 | 0.000176 | 0.000083 | 6.77E-05 | 0.000057 | 0.000055 | 2.07E-05 | 0.000028 |
| Run 2 | 6.83E-05 | 0.000158 | 0.000173 | 9.73E-05 | 6.57E-05 | 0.000063 | 3.63E-05 | 0.00003 | 2.73E-05 |
| Run 3 | 6.27E-05 | 0.000171 | 0.000168 | 0.000101 | 6.87E-05 | 0.000067 | 4.77E-05 | 0.000032 | 0.000031 |
| Average | 6.29E-05 | 0.000164 | 0.000172 | 9.37E-05 | 6.73E-05 | 6.23E-05 | 4.63E-05 | 2.76E-05 | 2.88E-05 |

# Table 7, Dust Feed Mechanism Performance

| Time (minutes) | Test 1 | Test 2 | Test 3 | Average | Best Fit | |
|---|---|---|---|---|---|---|
| 0 | 0 | 0 | 0 | 0 | 0 | |
| 0.5 | 1.3 | 1.6 | 1.49 | 1.463333 | 1.32755 | |
| 1 | 2.8 | 3.15 | 2.42 | 2.79 | 2.6121 | |
| 1.5 | 4.24 | 4.5 | 3.2 | 3.98 | 3.89665 | |
| 2 | 5.6 | 5.96 | 4.55 | 5.37 | 5.1812 | |
| 2.5 | 7 | 7.47 | 5.2 | 6.556667 | 6.46575 | |
| 3 | 8.4 | 8.8 | 6.7 | 7.966667 | 7.7503 | |
| 3.5 | 9.7 | 10 | 7.7 | 9.133333 | 9.03485 | |
| 4 | 11.1 | 11 | 8.4 | 10.16667 | 10.3194 | |
| 4.5 | 12.6 | 11.7 | 9.1 | 11.13333 | 11.60395 | |
| 5 | 13.9 | 12.6 | 10.7 | 12.4 | 12.8885 | |
| 5.5 | 15.7 | 13.9 | 12.2 | 13.93333 | 14.17305 | |
| 6 | 17 | 15.2 | 14 | 15.4 | 15.4576 | |
| 6.5 | 18.3 | 16.2 | 15.25 | 16.58333 | 16.74215 | |
| 7 | 19.7 | 17.4 | 16.7 | 17.93333 | 18.0267 | |
| 7.5 | 21.2 | 18.6 | 18.3 | 19.36667 | 19.31125 | |
| 8 | 22.4 | 19.75 | 20 | 20.71667 | 20.5958 | |
| 8.5 | 23.5 | 21 | 21.5 | 22 | 21.88035 | |
| 9 | 24.5 | 22 | 22.8 | 23.1 | 23.1649 | |
| 9.5 | 26 | 23.7 | 24.1 | 24.6 | 24.44945 | |
| 10 | 27.5 | 25 | 25.7 | 26.06667 | 25.734 | |

# Appendix B: Figures

# Figure 1

## Basic MIP Setup

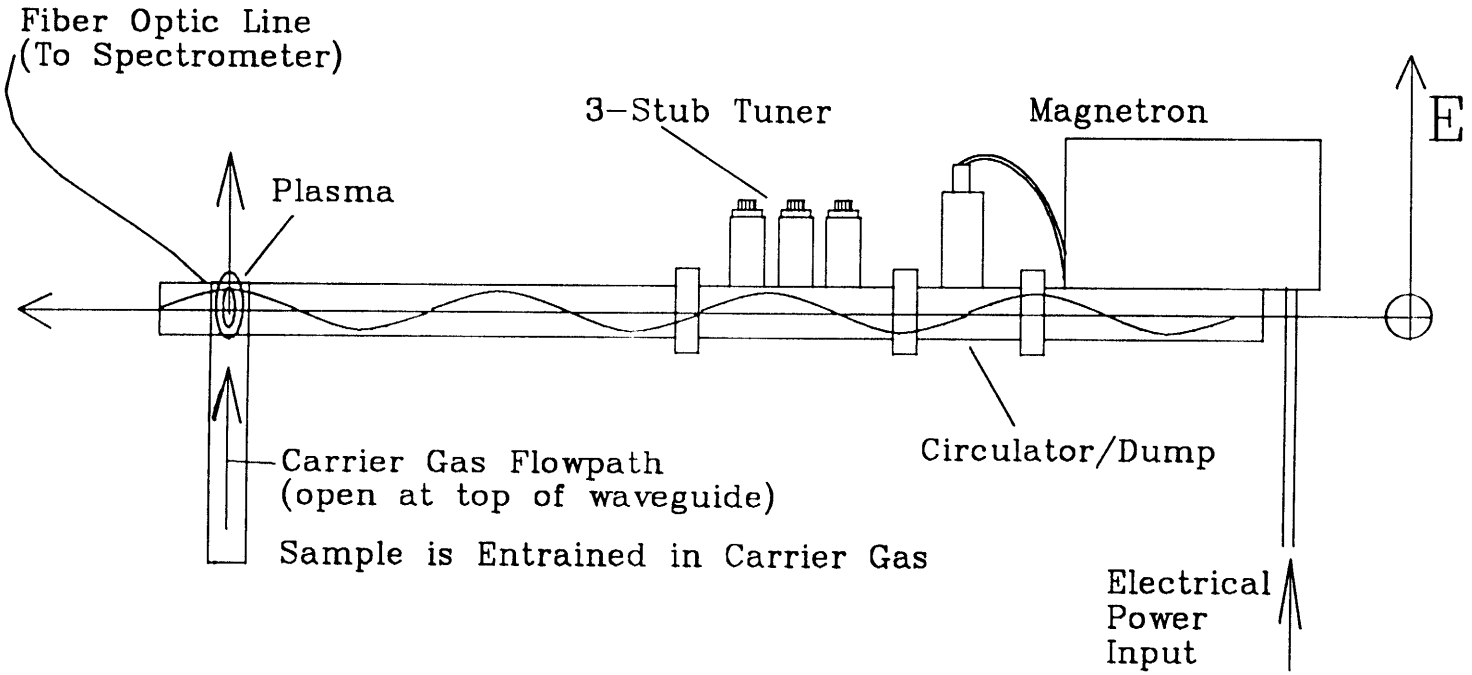

# Figure 2

# Isokinetic Sampling

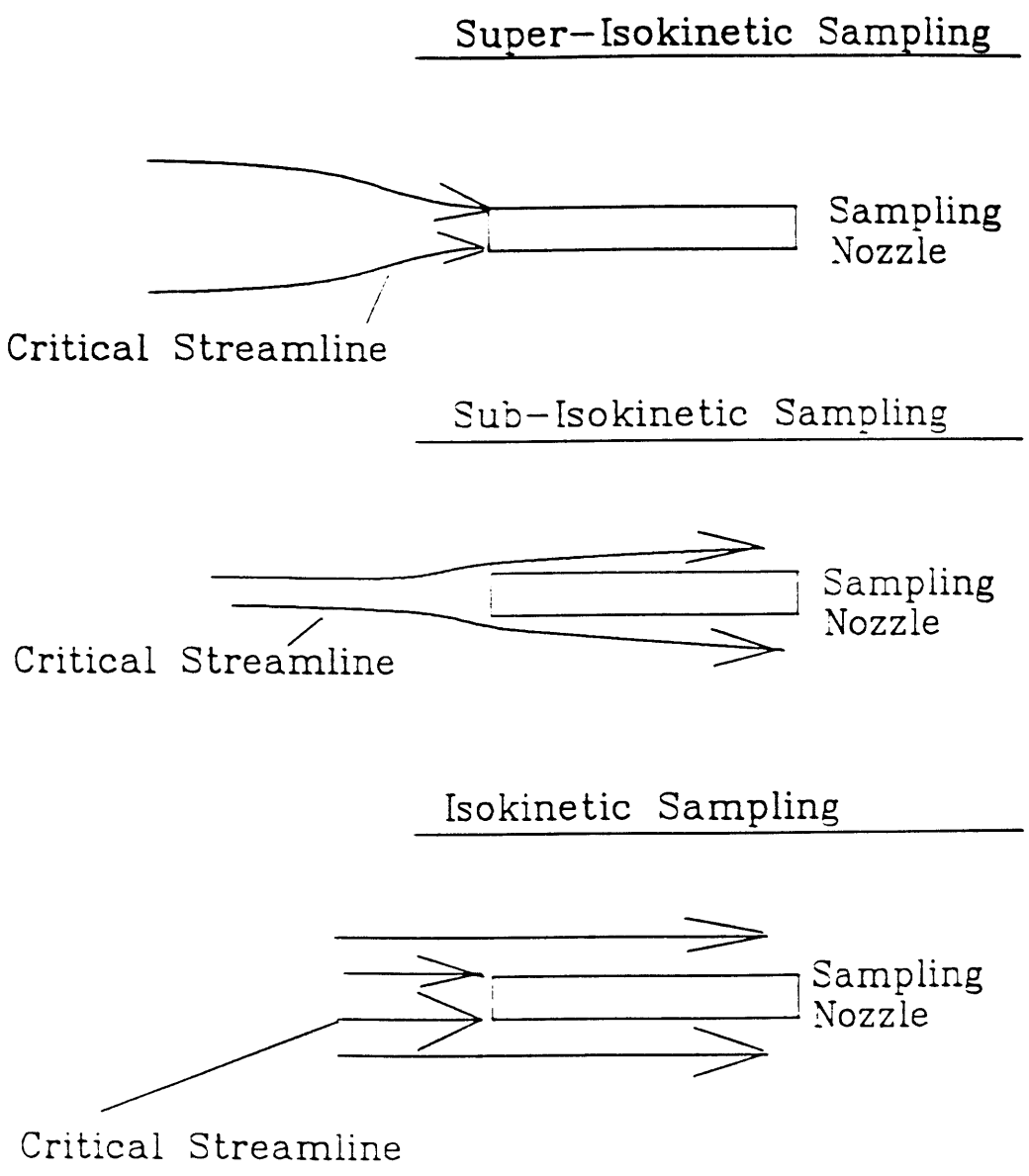

# Figure 3 Duct Sampling Points

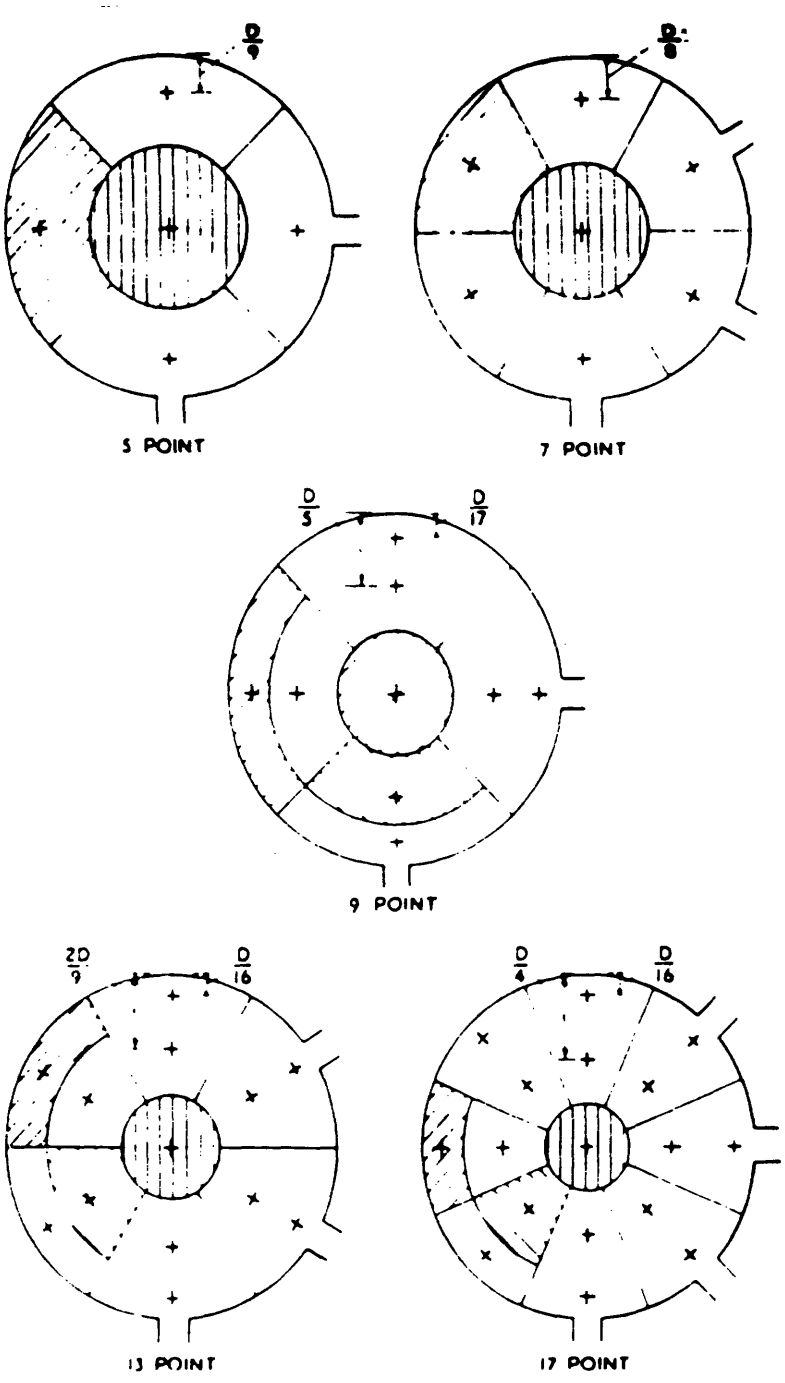


FIG. 15 Location of sampling points for circular flues including centre point (D is internal diameter of flue) Ref.[3]

# Figure 4

## Sampling Method No. 1

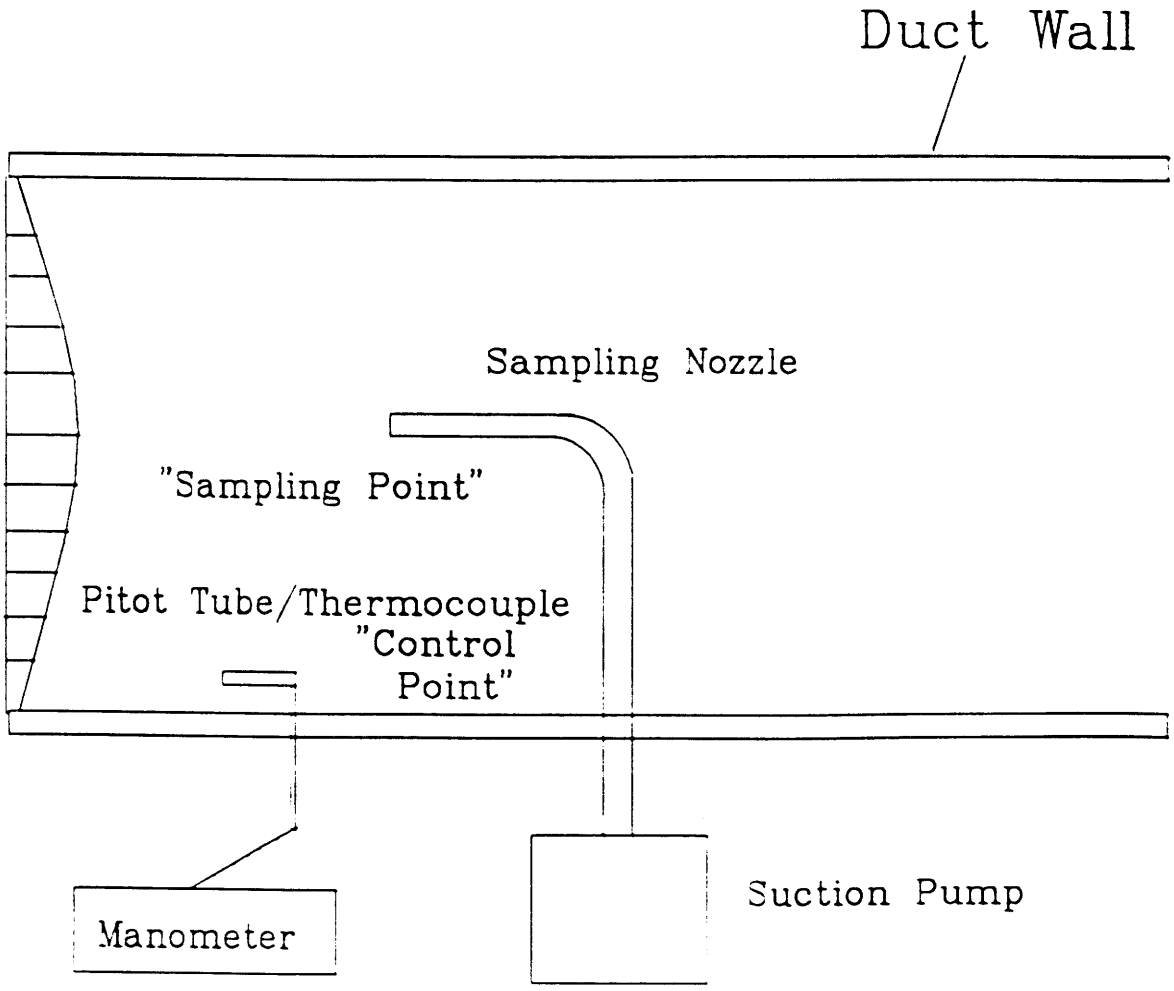

# Figure 5

## EPA Method No. 29

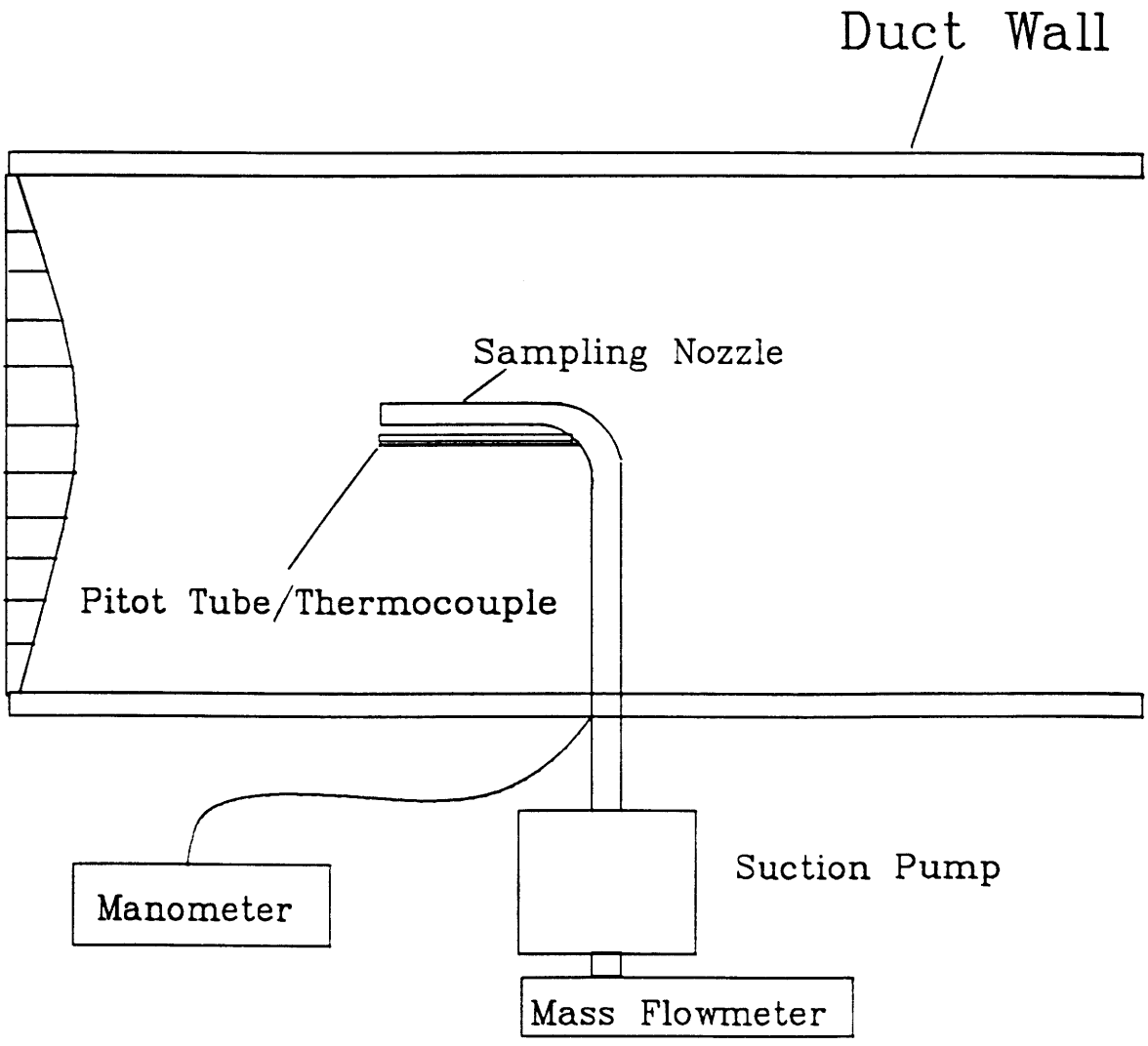

Figure 6

Method No.3 Static Pressure Taps

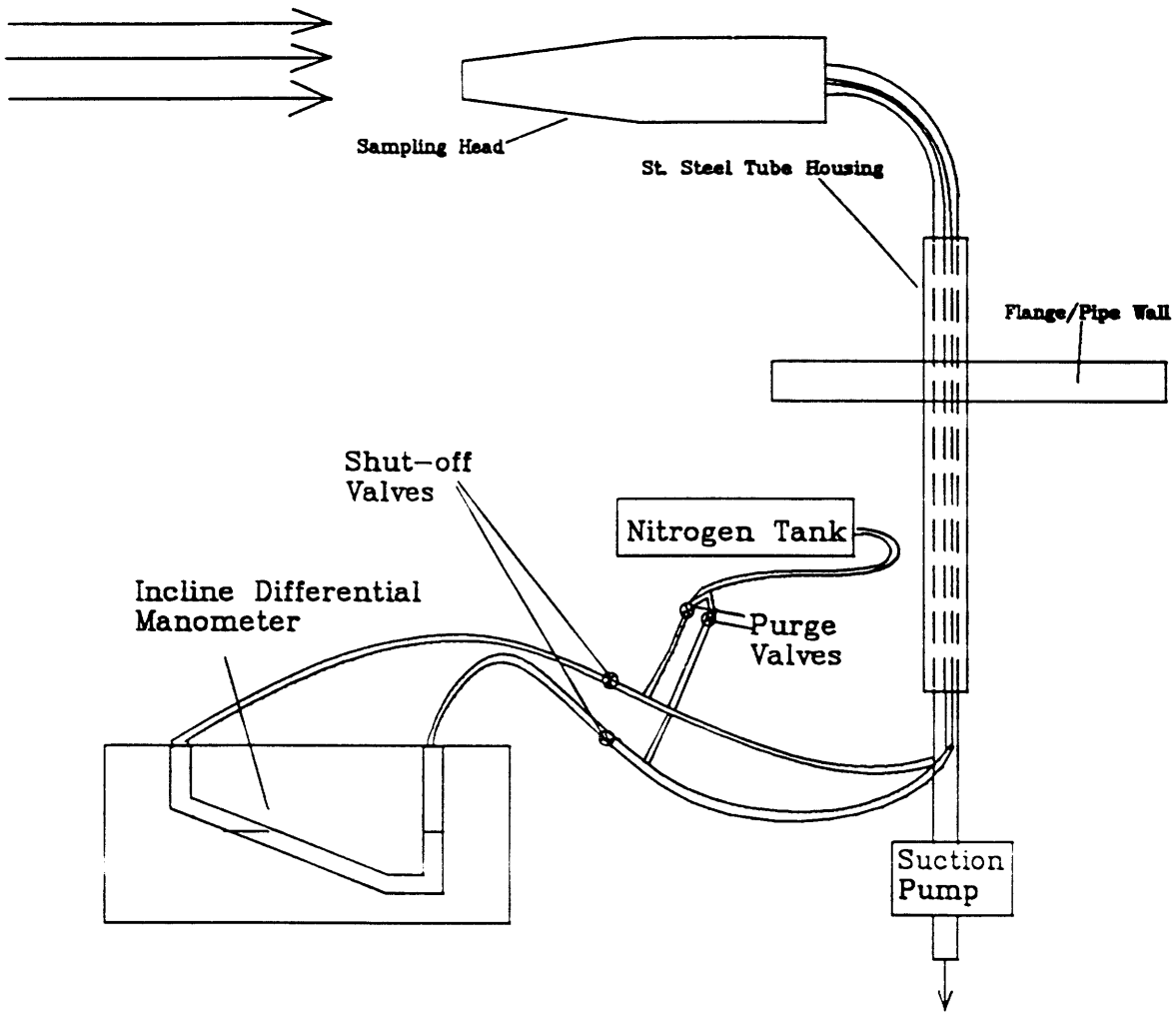

# Figure 7

## Isokinetic Sampling Head
## Side Cutaway View

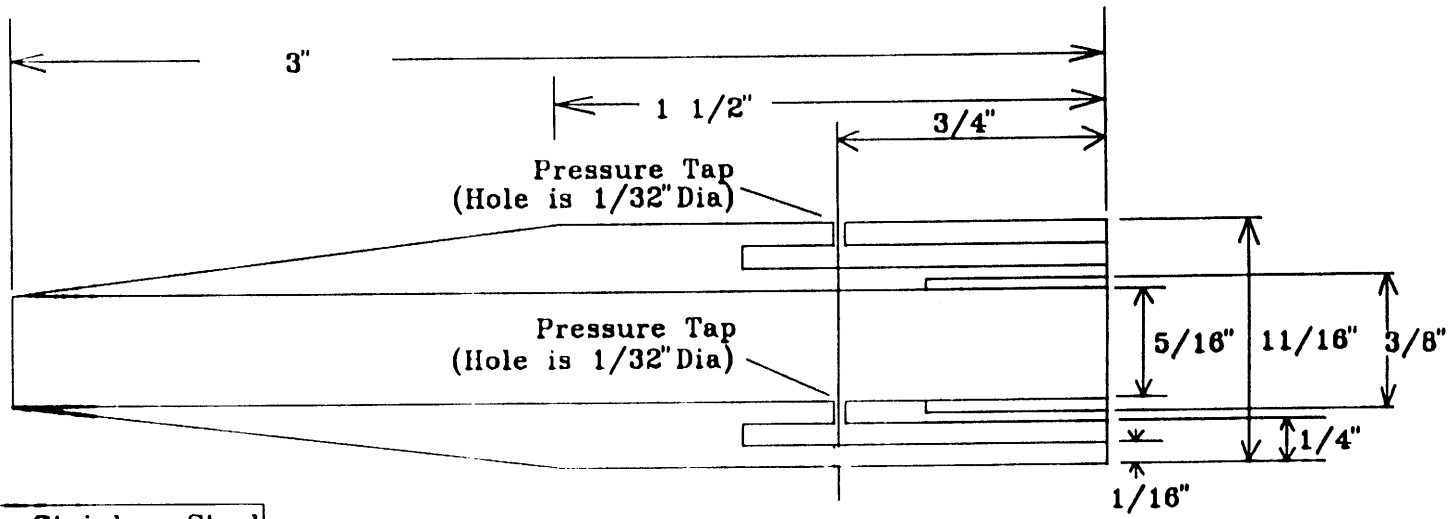


Material is Stainless Steel

# Figure 8

## Experimental Apparatus

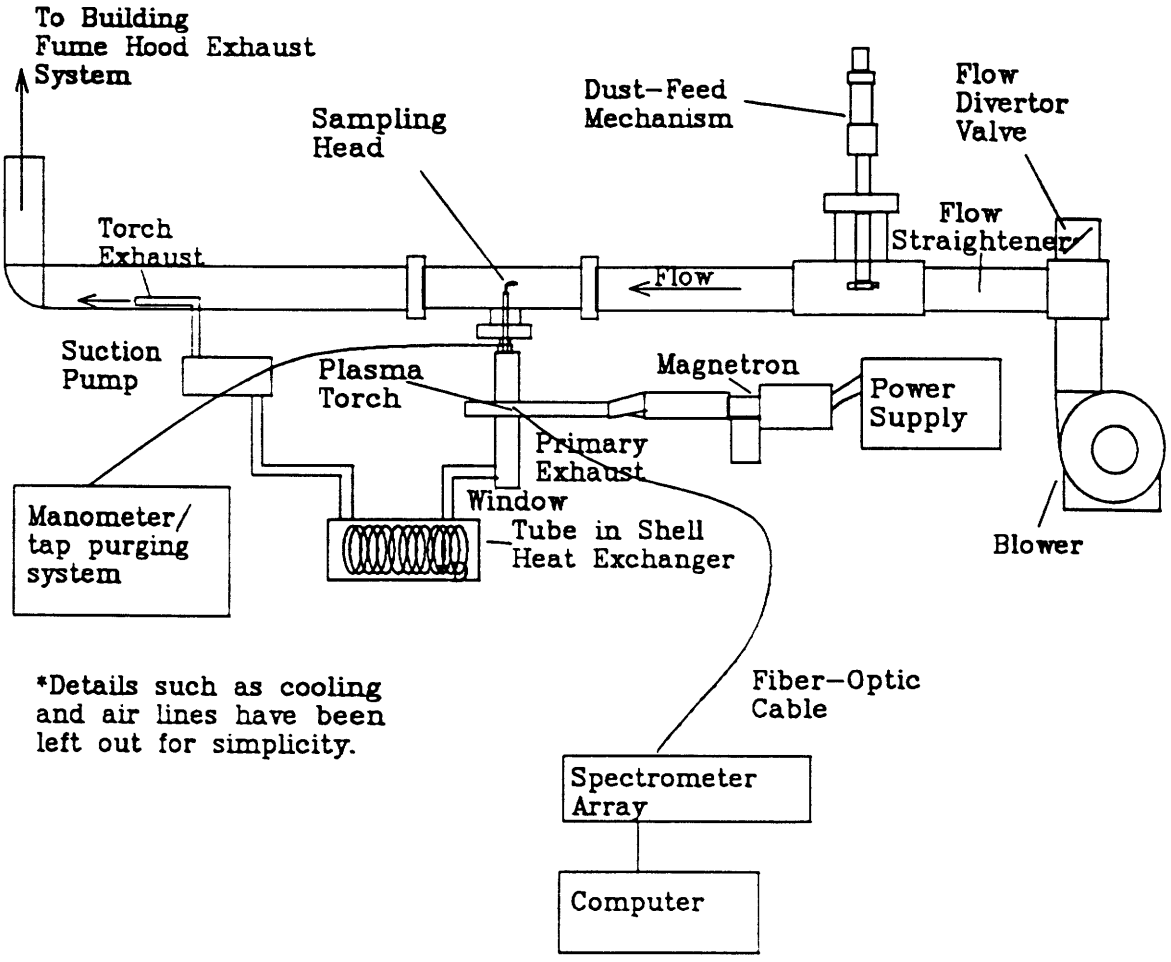

# Figure 9

## Flow Straightener

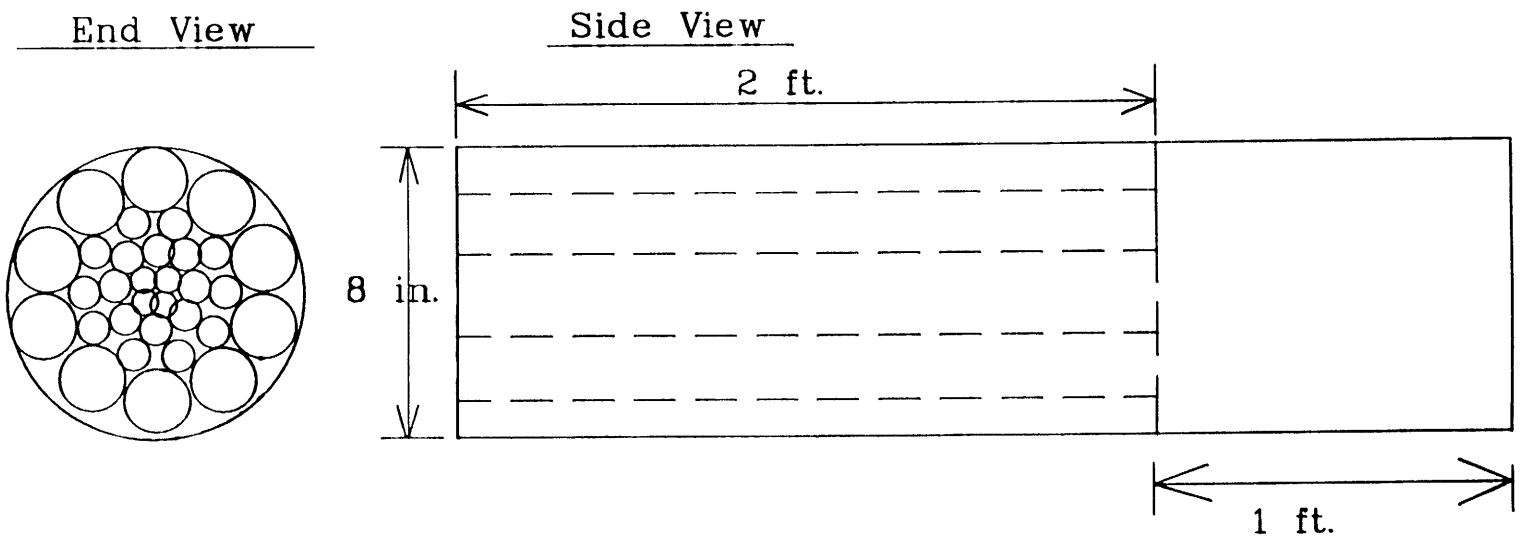

# Figure 10

## Sampling Method for SAIC

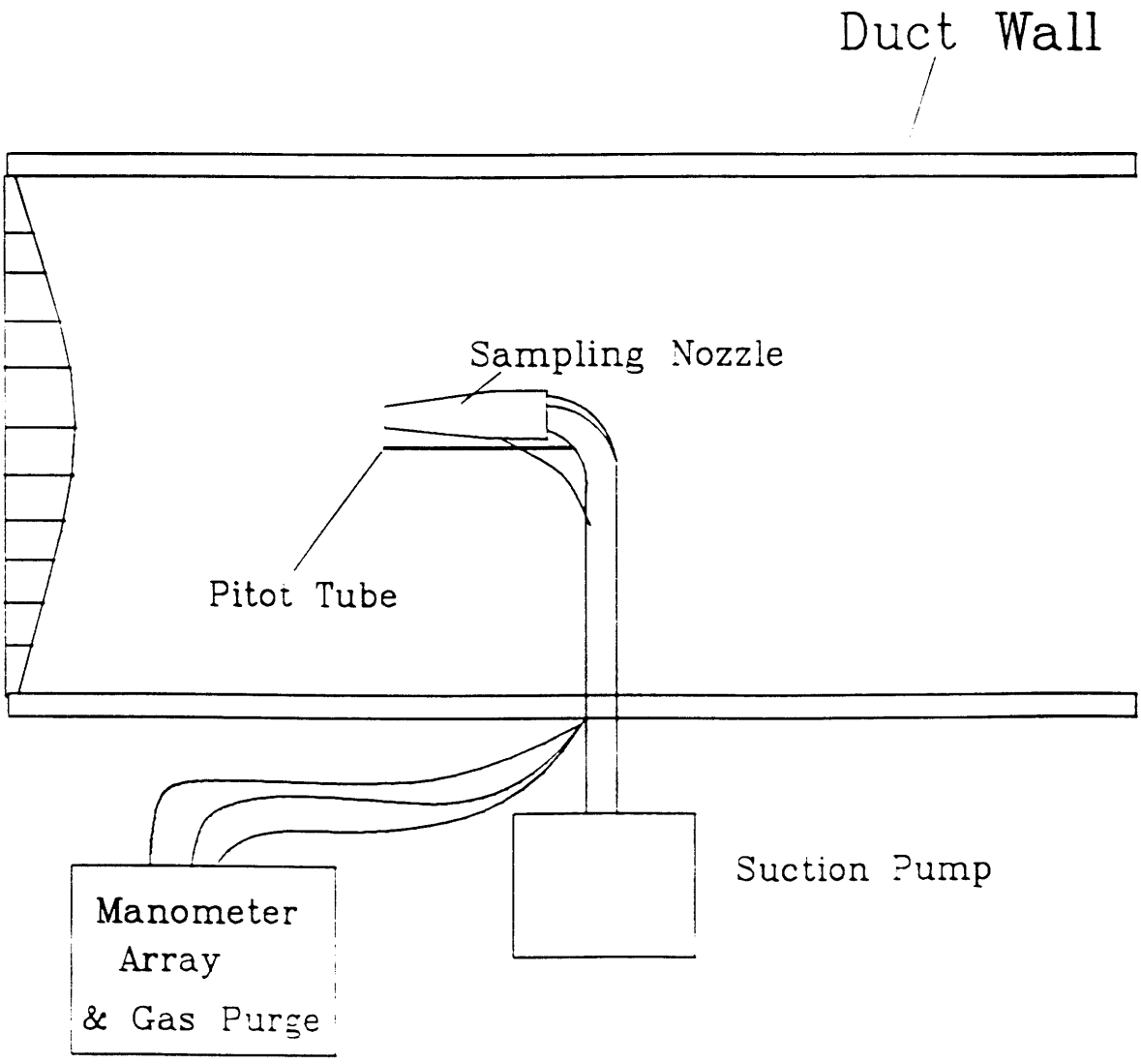

Figure 11

Plasma Torch Setup

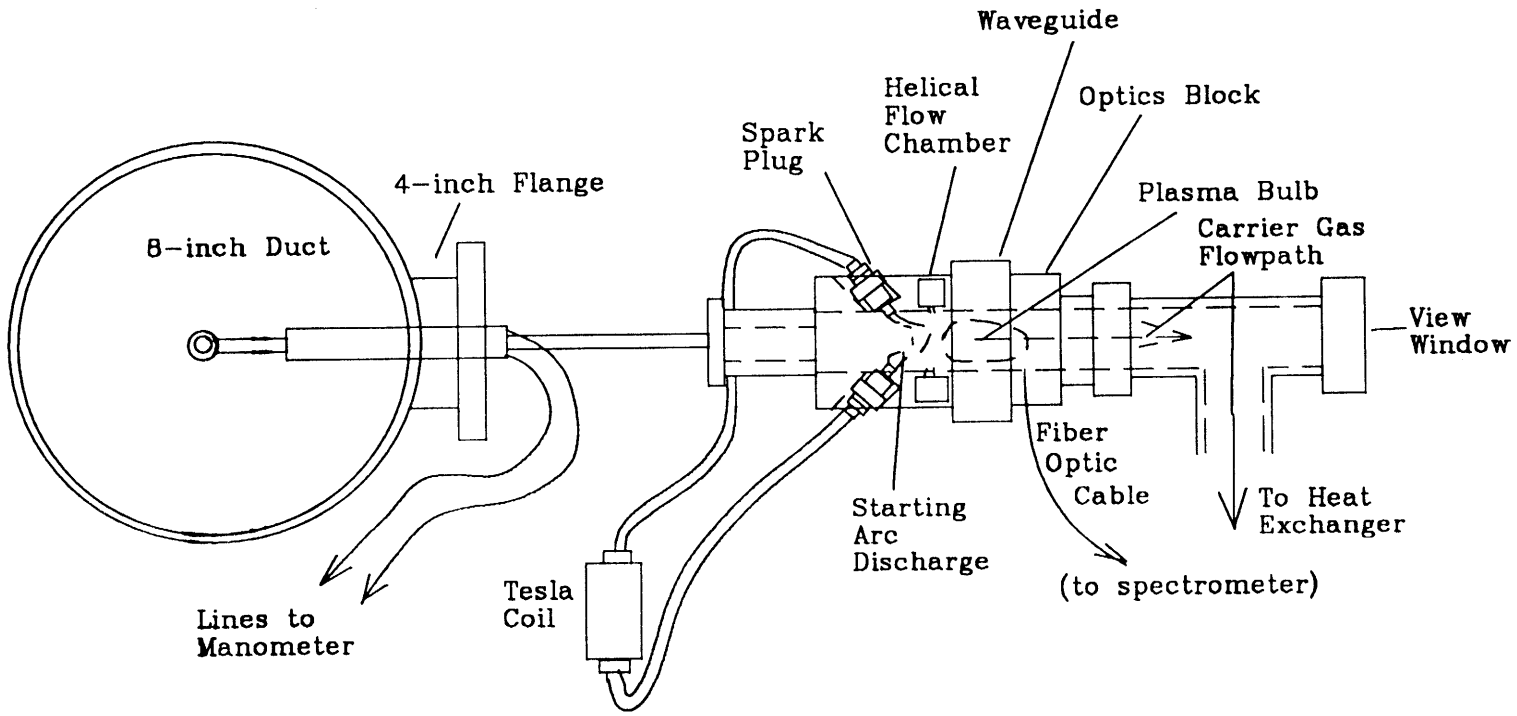

# Figure 12

## Heat Exchanger

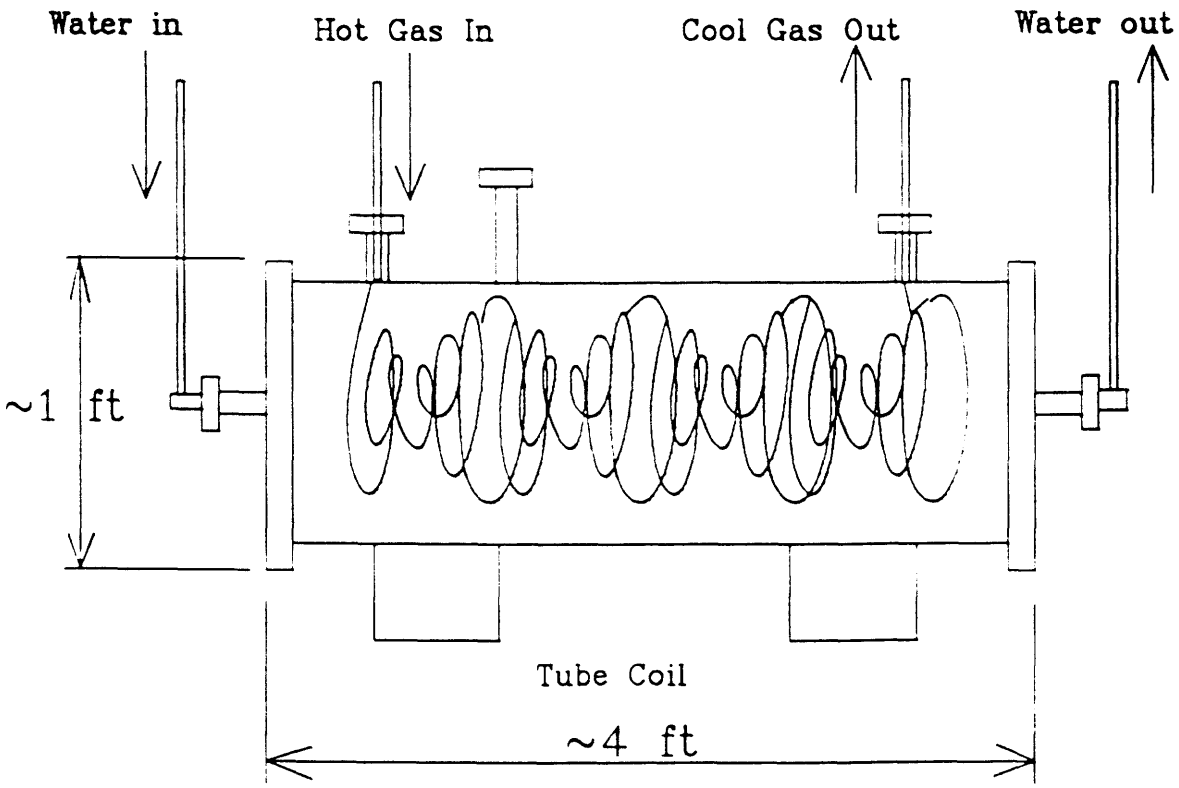

# Figure 13, Cross-Section of Feeder

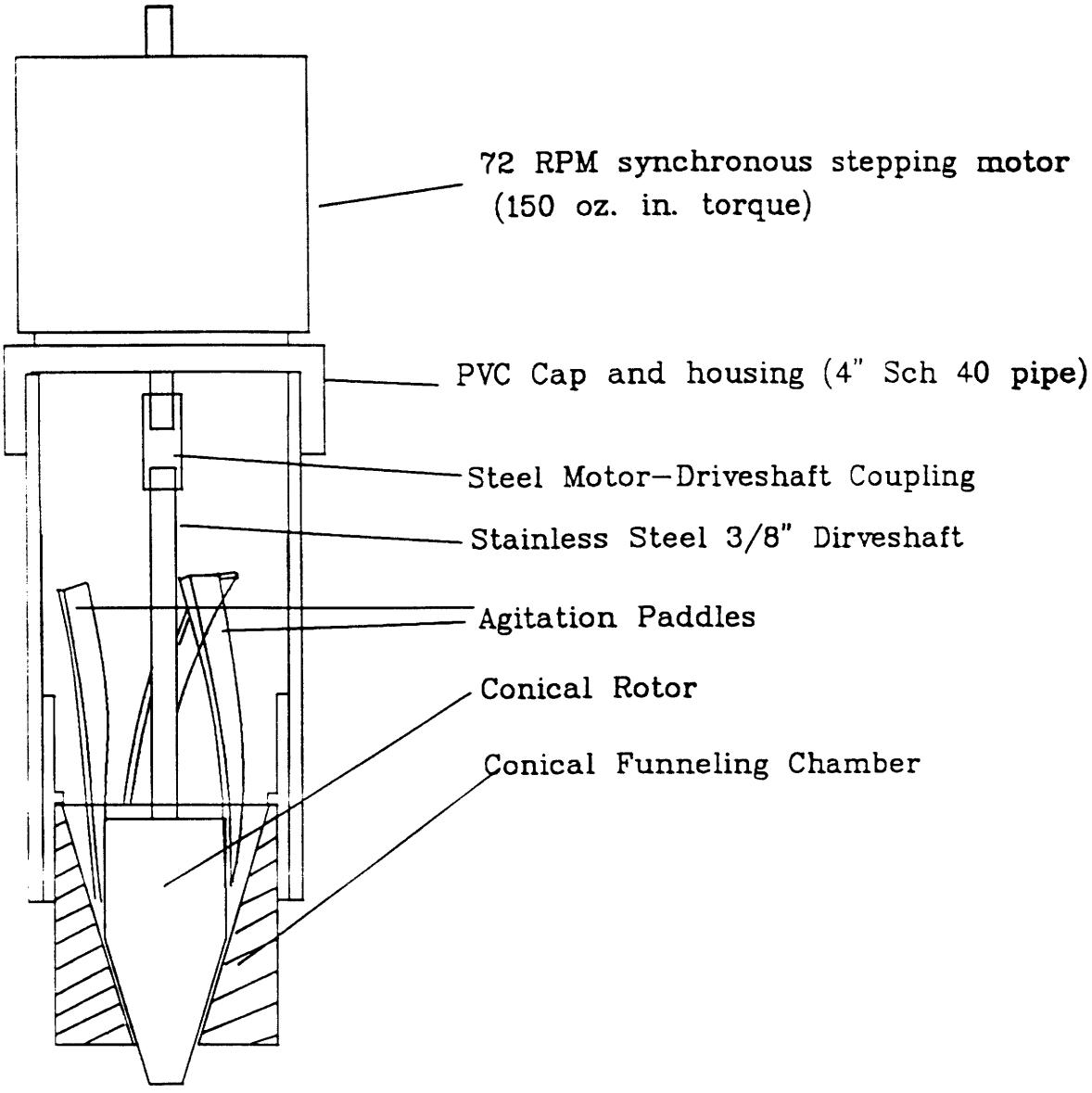

# Figure 14 Conical Funneling Chamber

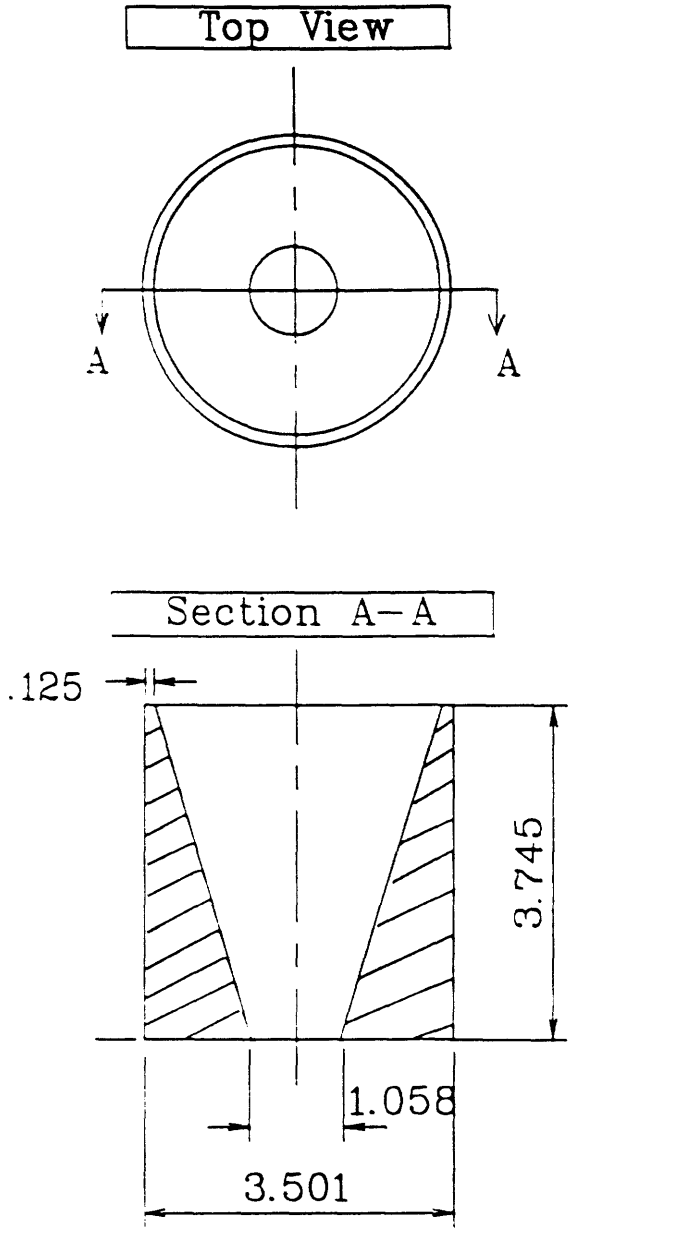


* Material is Aluminum

*All Dimensions are in Inches

# Figure 15, Outside view of Feeder

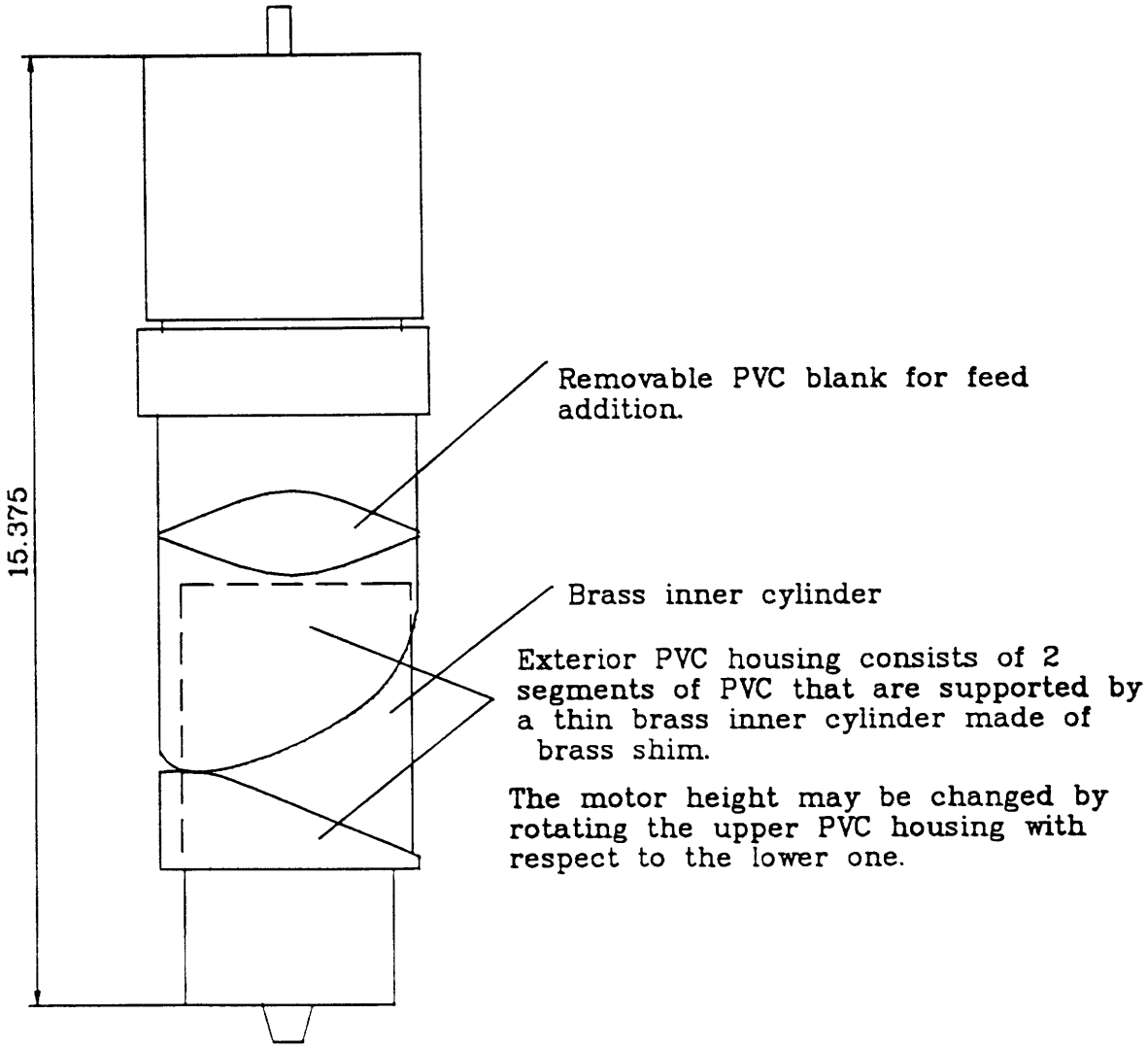

Figure 16

Complete Feed Apparatus

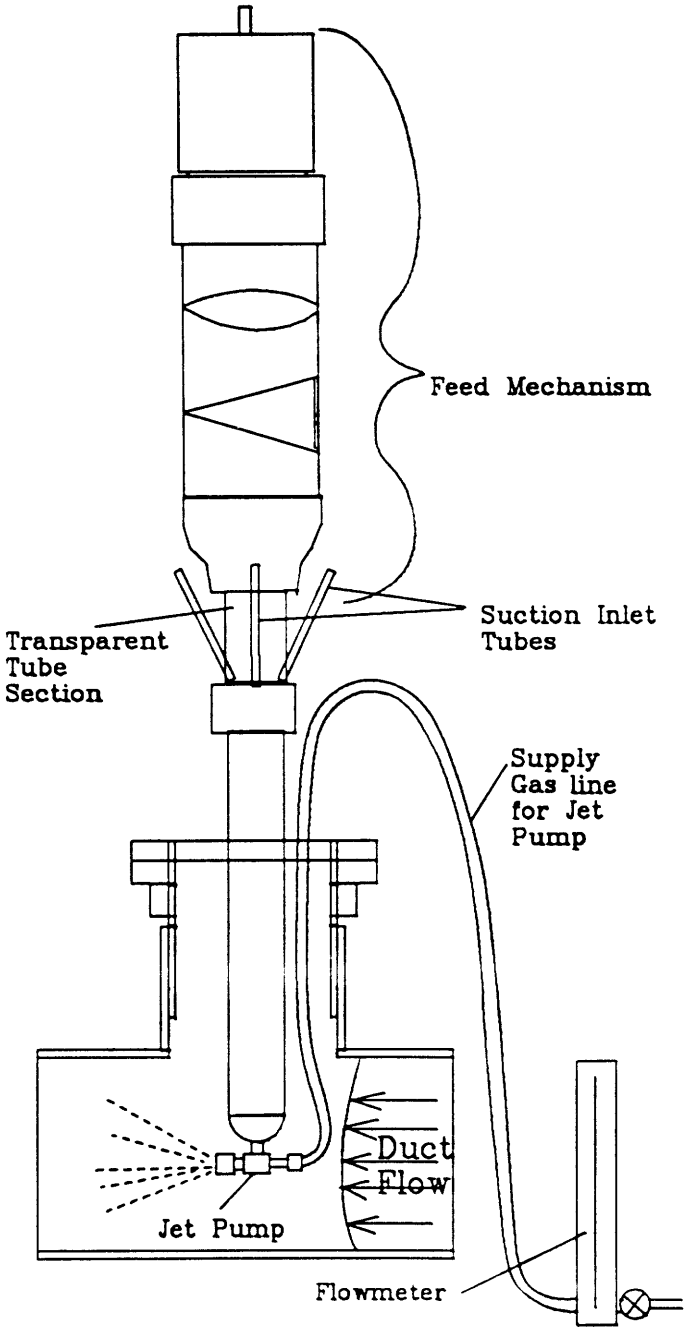

Figure 17

Dust Collector Assembly

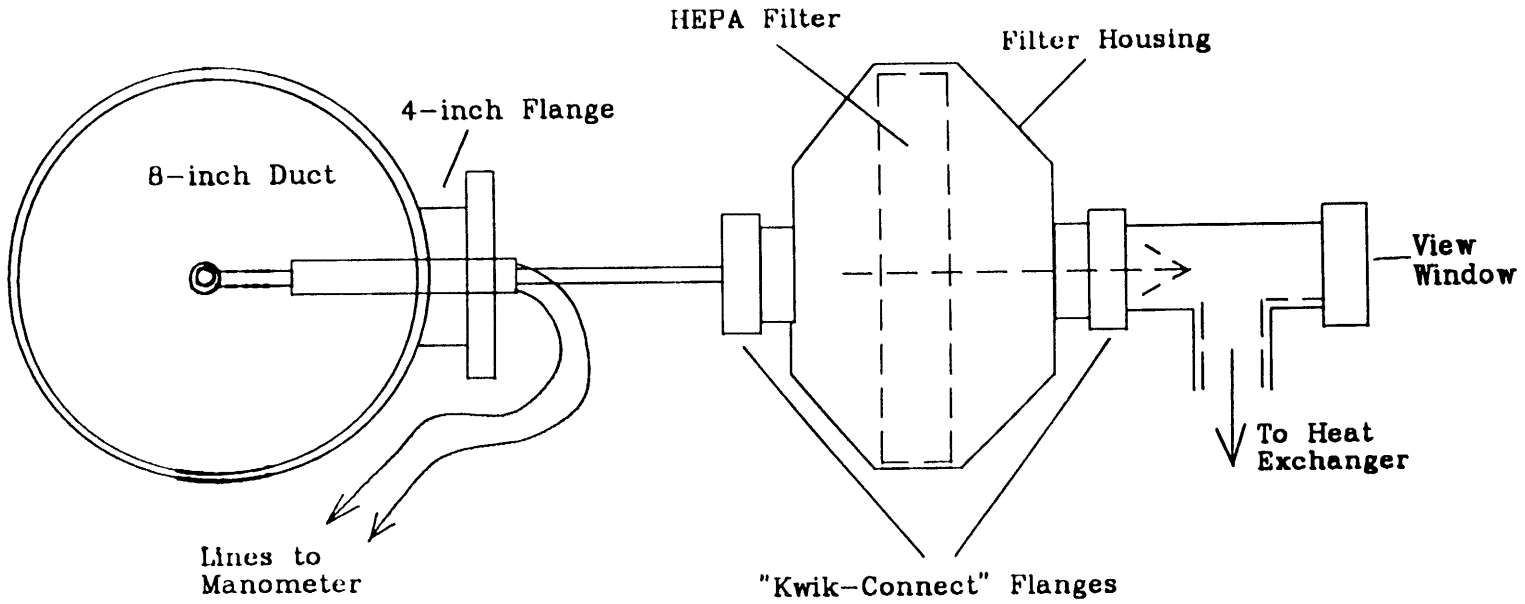

# Figure 18

## Sampling Calibration

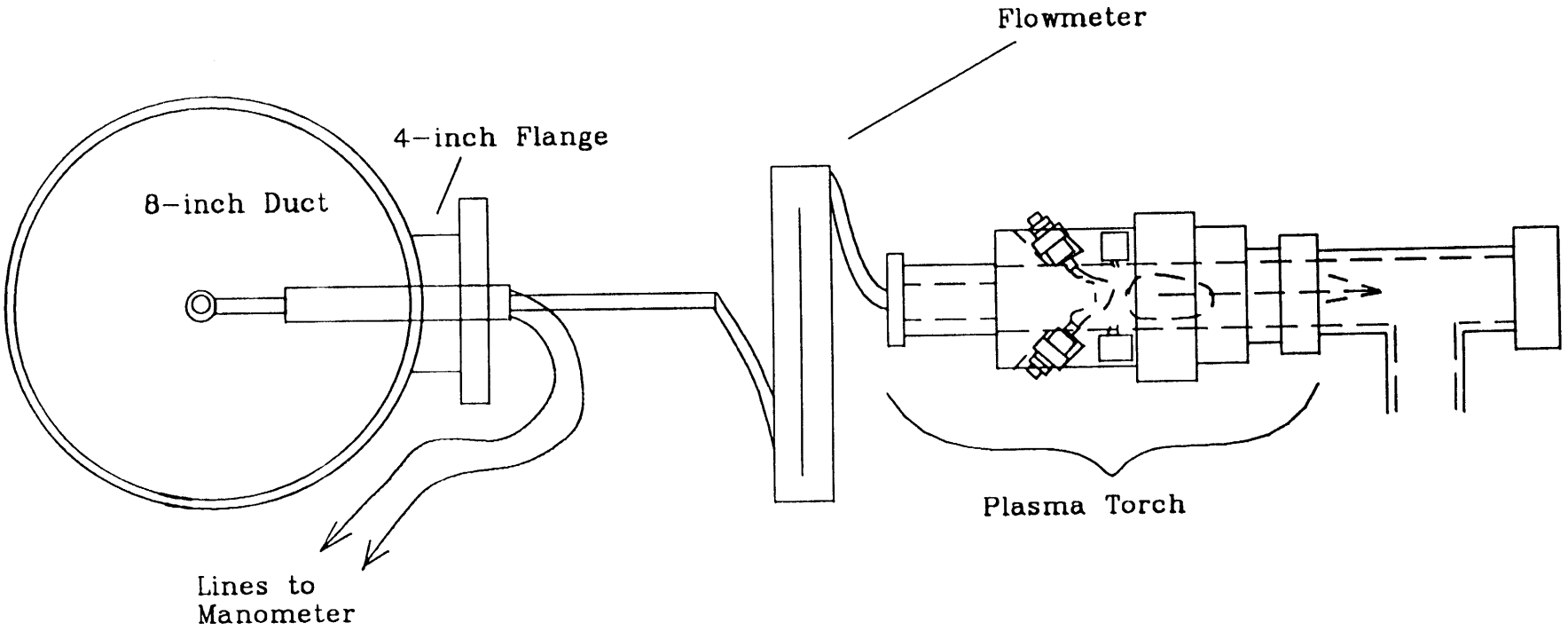

Figure 19

Flow Behavior Over Sampling Nozzle

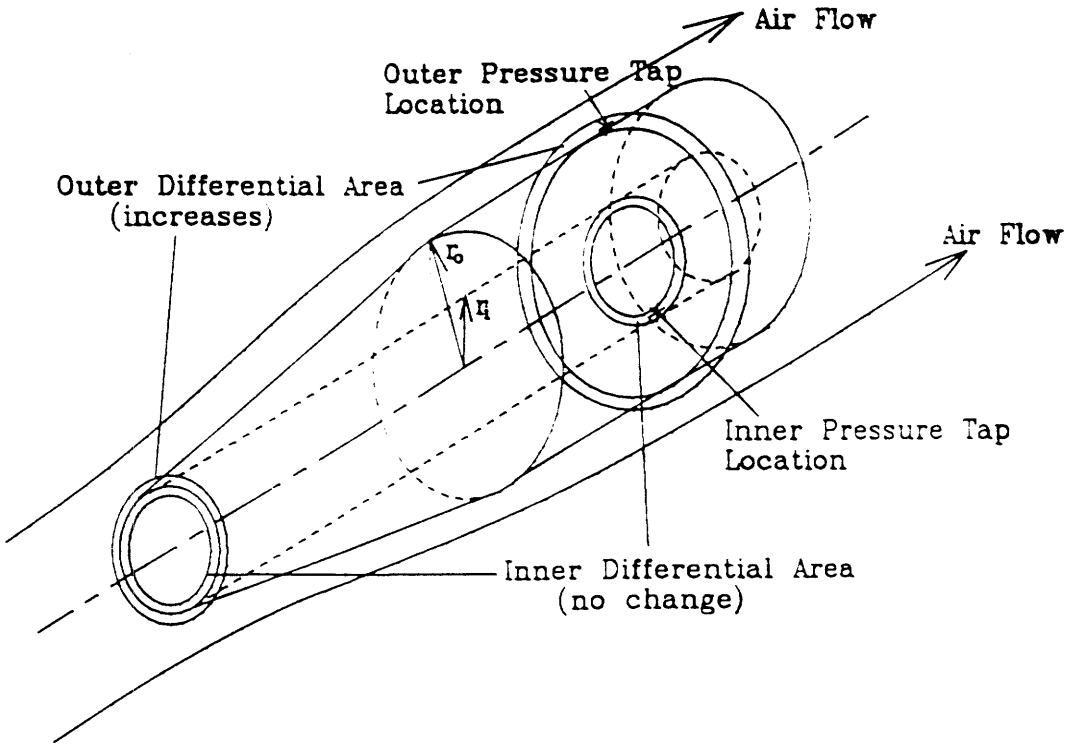

# Figure 20

## Flow Study Sampling Geometry

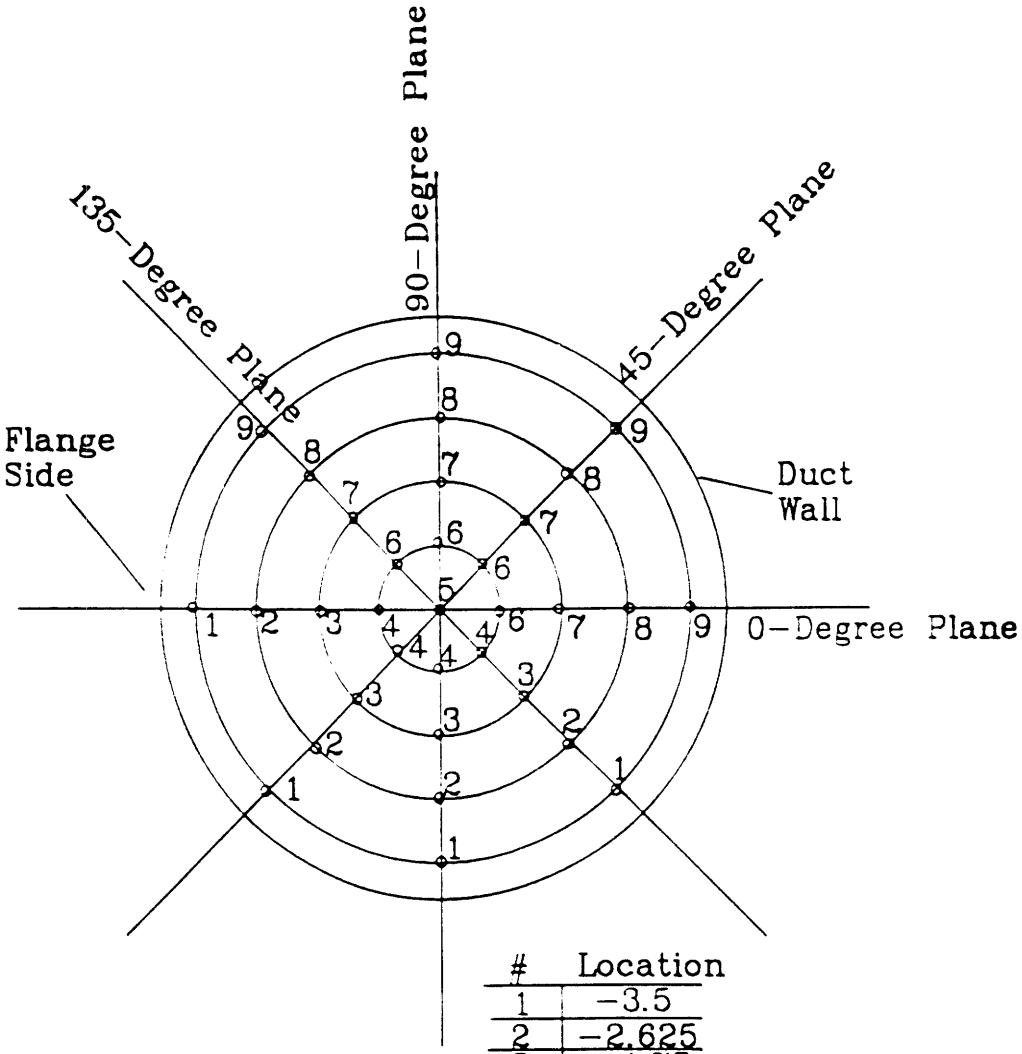


| # | Location |
|---|---|
| 1 | −3.5 |
| 2 | −2.625 |
| 3 | −1.75 |
| 4 | −.875 |
| 5 | 0 |
| 6 | .875 |
| 7 | 1.75 |
| 8 | 2.625 |
| 9 | 3.5 |

# Figure 21

## Sample Calibration Gun

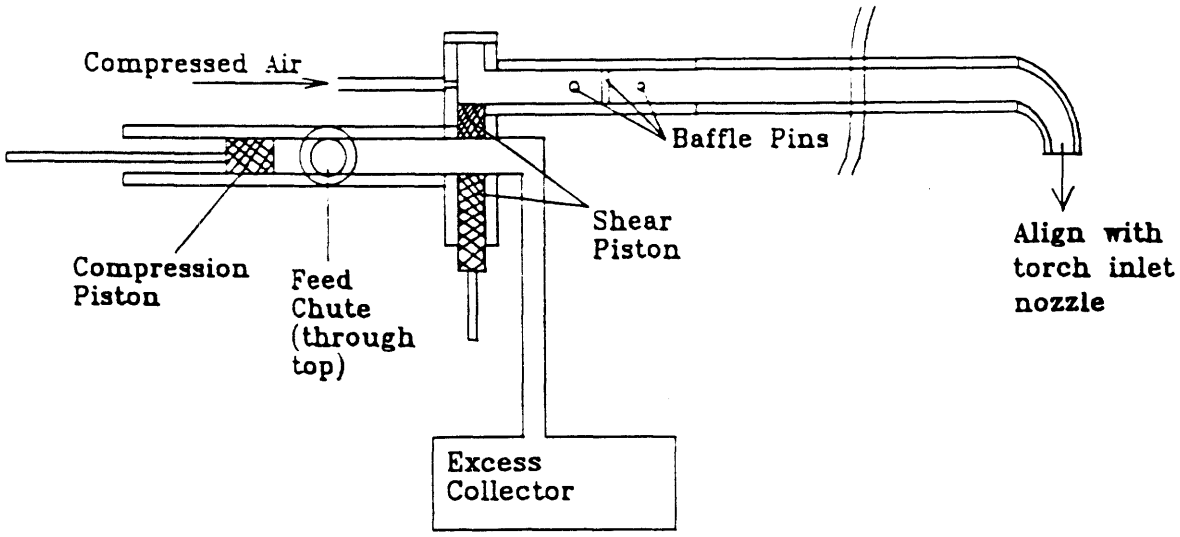

# Figure 22

## Basic In-Situ Arrangement

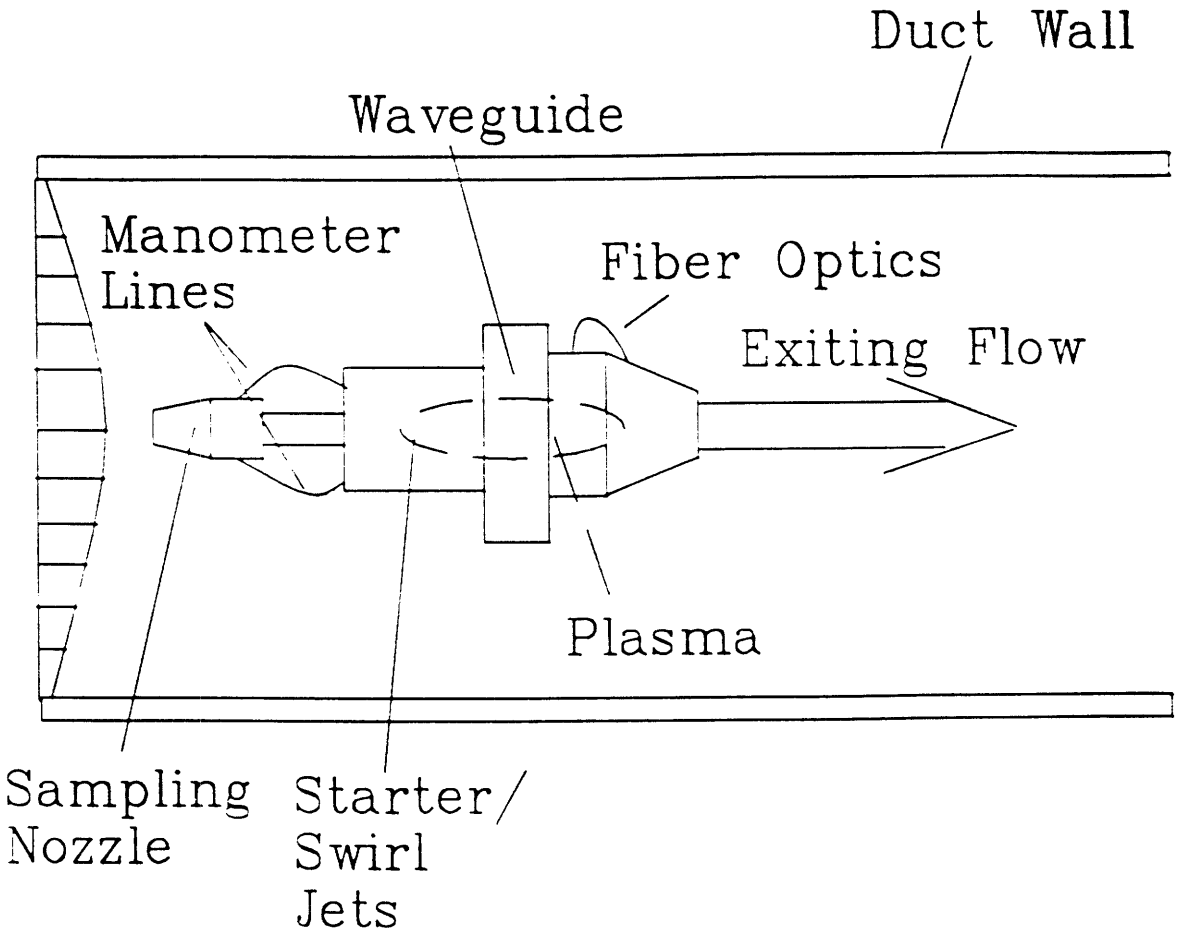

Figure 23, Duct Centerline Velocity Profiles at Sampling Location

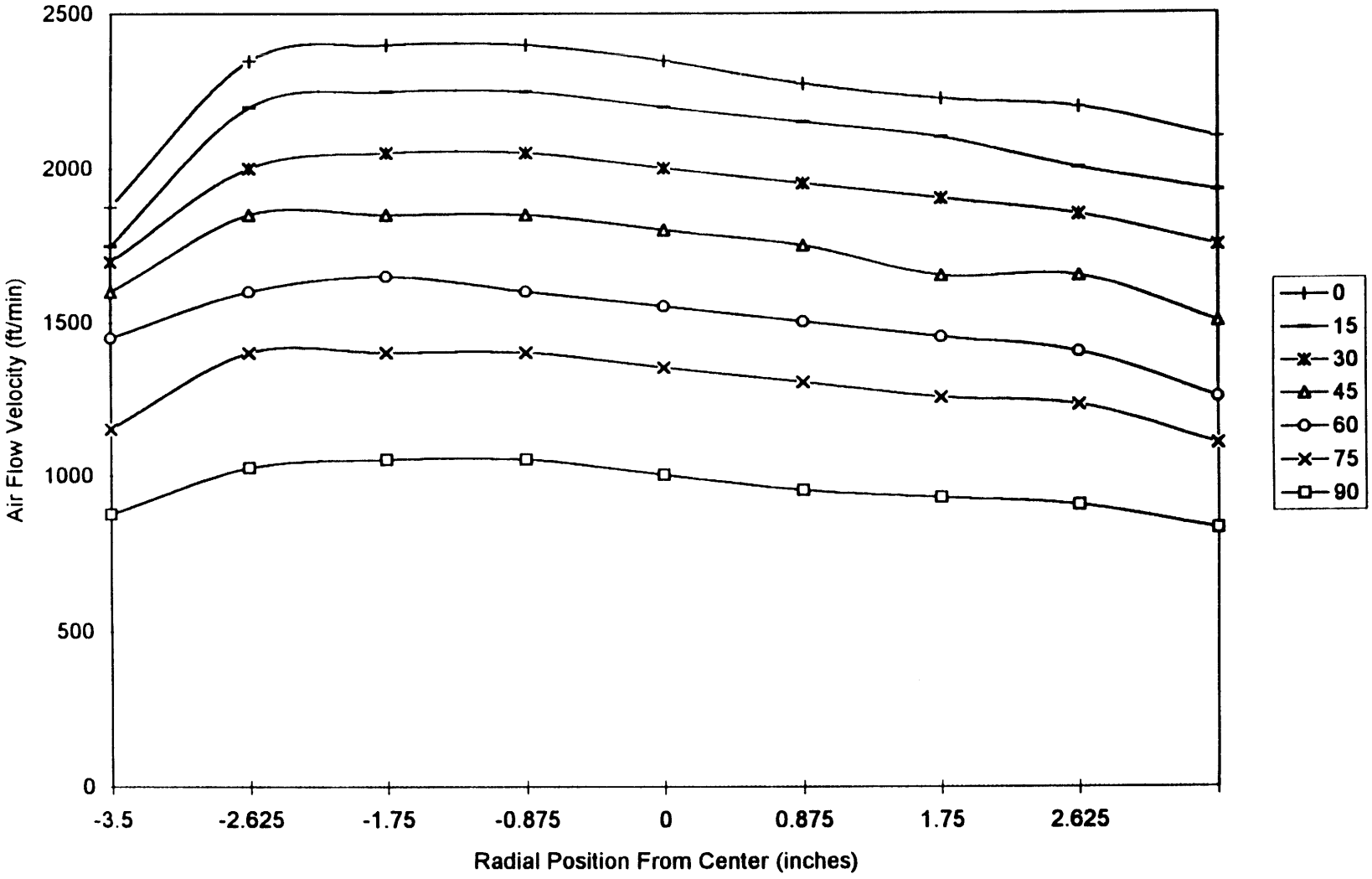

Figure 24, Calibration Curve for Nozzle

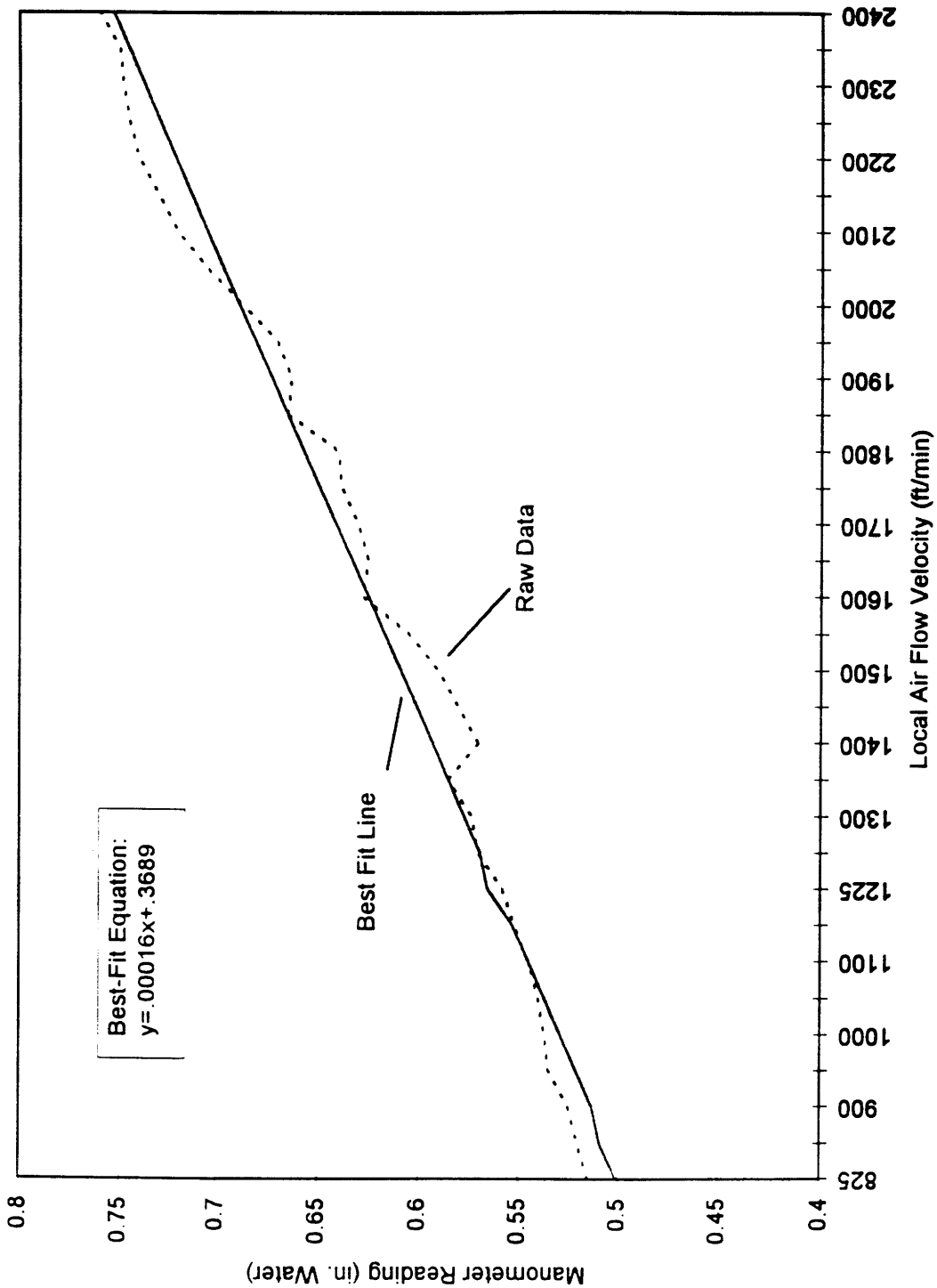

COULTER

LS Particle Size Analyzer

18 Apr 199

THE JET PULVERIZER CO.

| | | | |
|---|---|---|---|
| File name: | MIT.$09 | Group ID: | MIT |
| Sample ID: | SOIL | | |
| Operator: | GC | Run number: | 2 |
| Comments: | 8" TEST NO. 9 HAMMERED | | |
| Optical model: | Fraunhofer | | |
| LS 230 | Fluid Module | | |
| Start time: | 10:28 18 Apr 1996 | Run length: | 91 Seconds |
| Pump speed: | 48 | | |
| Obscuration: | 6% | | |
| PIDS Obscur: | 50% | | |
| Fluid: | Water | | |
| Software: | 2.05 | Firmware: | 2.02 2.02 |

Figure 25

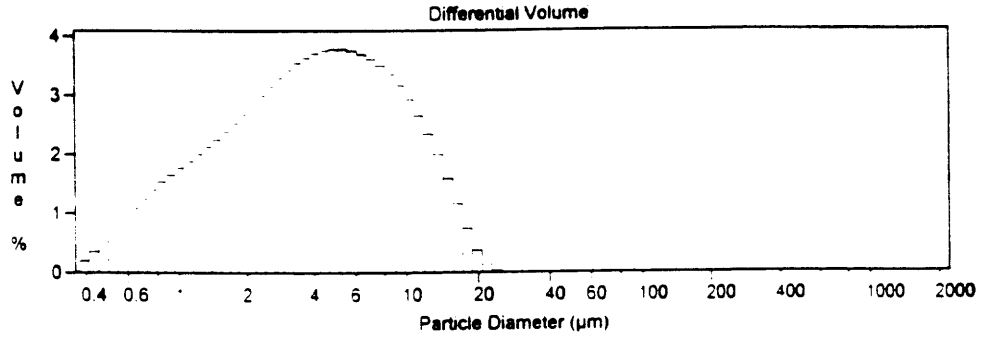


Volume Statistics (Arithmetic) mit.$09

Calculations from 0.375 µm to 2000 µm

| | | | |
|---|---|---|---|
| Volume | 100.0% | | |
| Mean: | 5.078 µm | 95% Conf. Limits: | 0-13.1 µm |
| Median: | 3.857 µm | S.D.: | 4.11 µm |
| Mean/Median Ratio: | 1.316 | Variance: | 16.9 $\mu m^2$ |
| Mode: | 4.878 µm | C.V.: | 80.9% |
| | | Skewness: | 1.22 Right skewed |
| | | Kurtosis: | 1.12 Leptokurtic |

| % > | 10 | 25 | 50 | 75 | 90 |
|---|---|---|---|---|---|
| Size µm | 11.17 | 7.221 | 3.857 | 1.862 | 0.974 |

# Figure 26, Development of Velocity Profile Along 0-Degree Plane

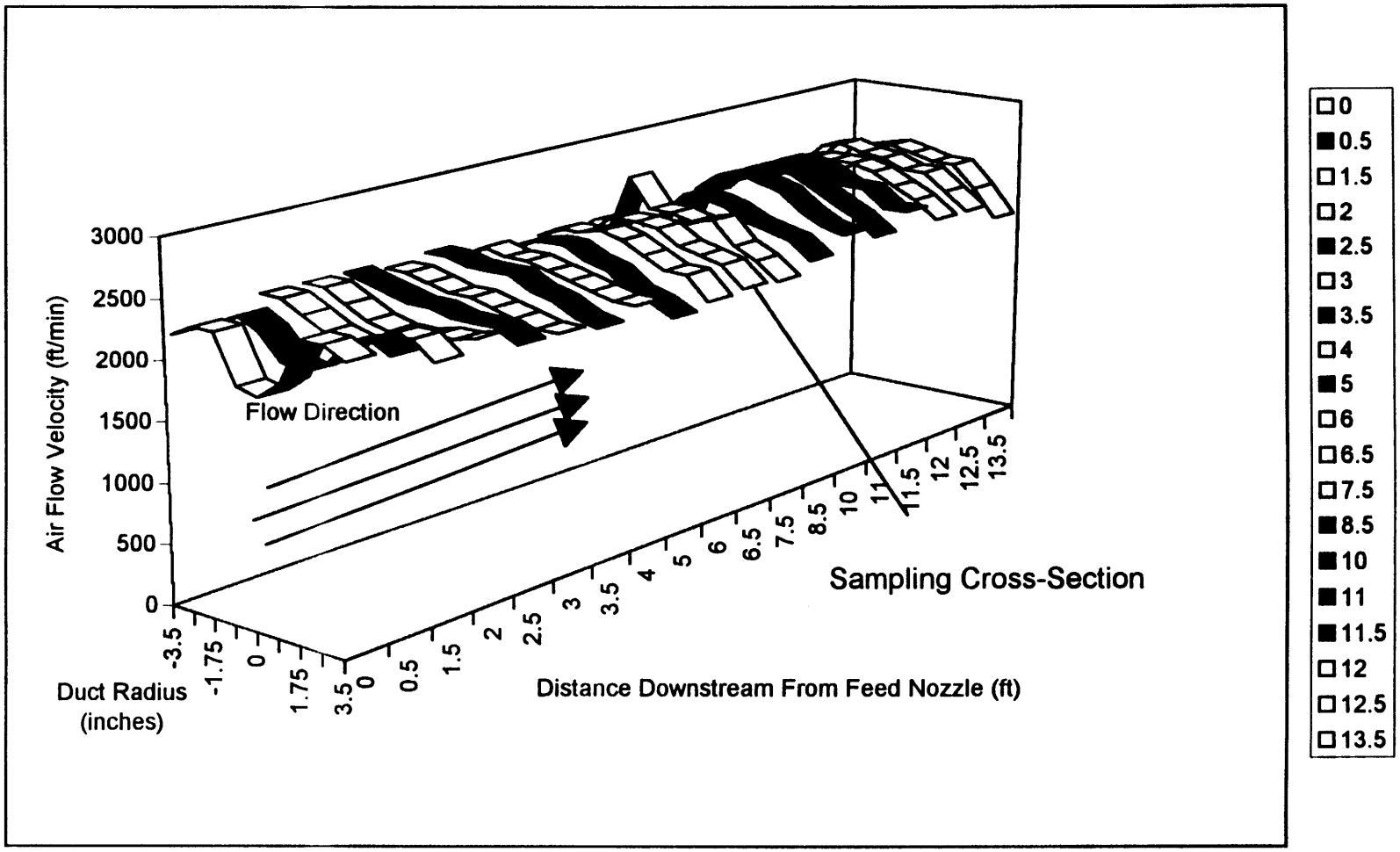

# Figure 27, Development of Velocity Profile Along 45-Degree Plane

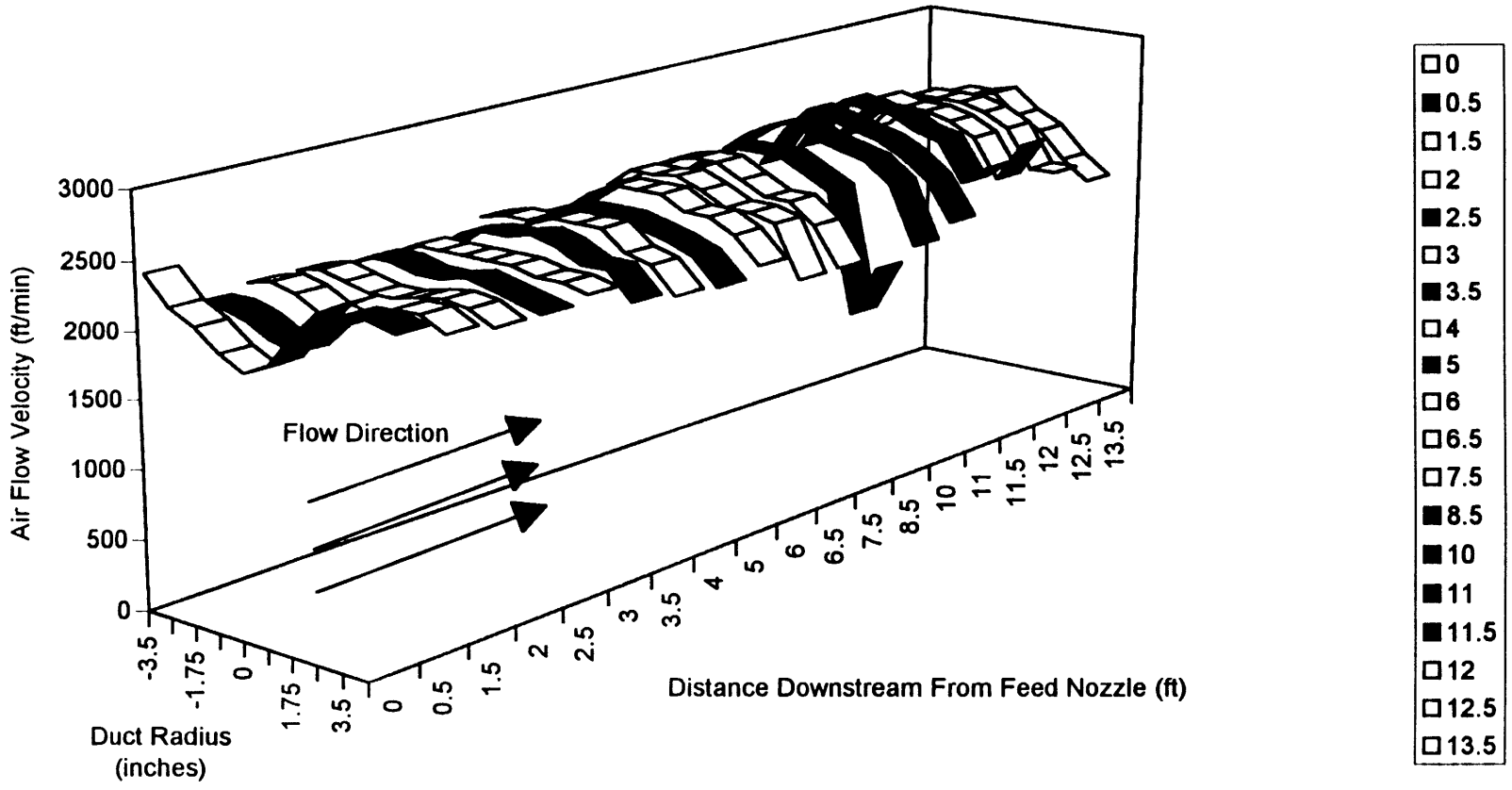

Figure 28, Development of Velocity Profile Along 90-Degree Plane

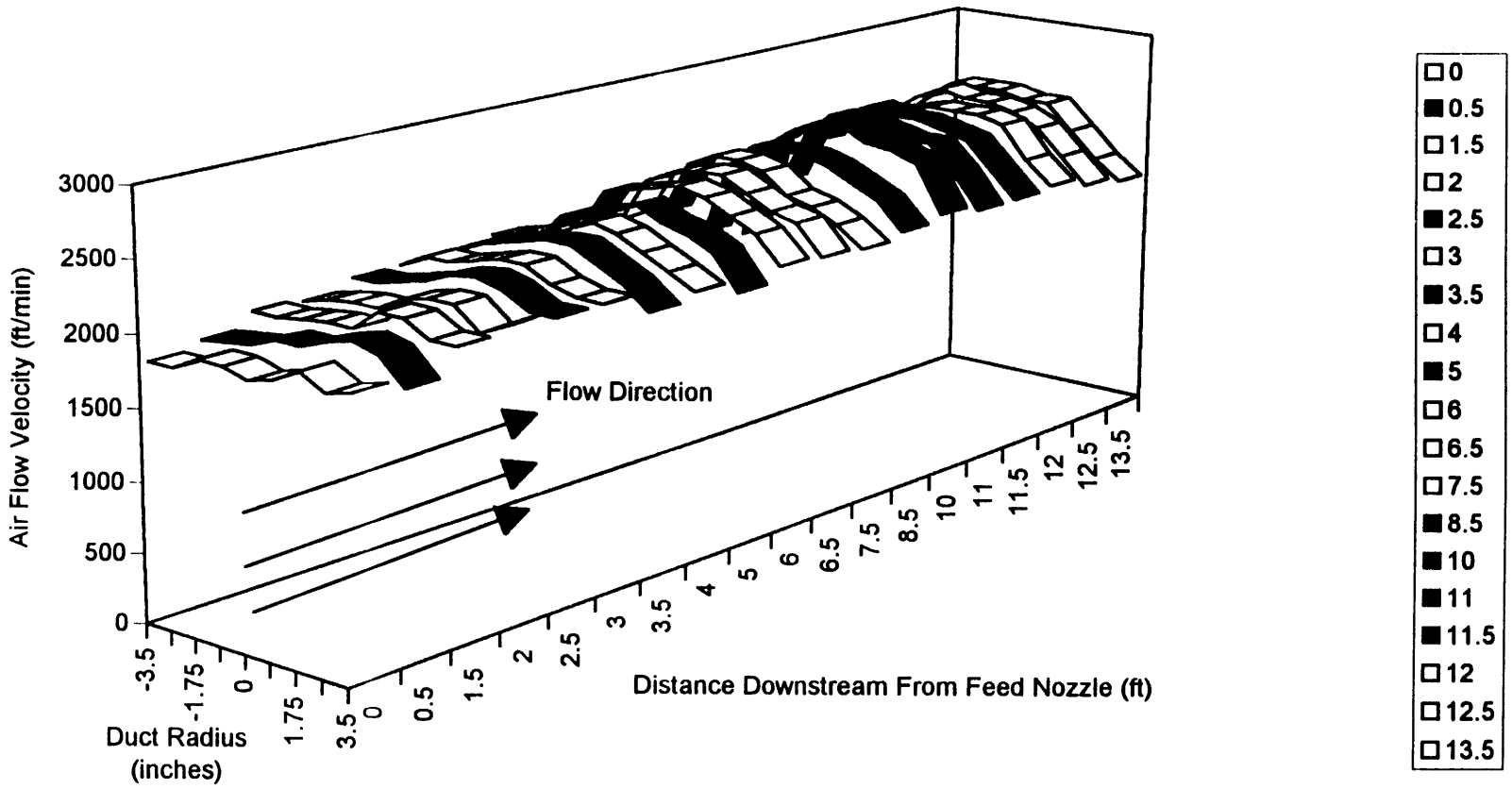

# Figure 29, Development of Velocity Profile Along 135-Degree Plane

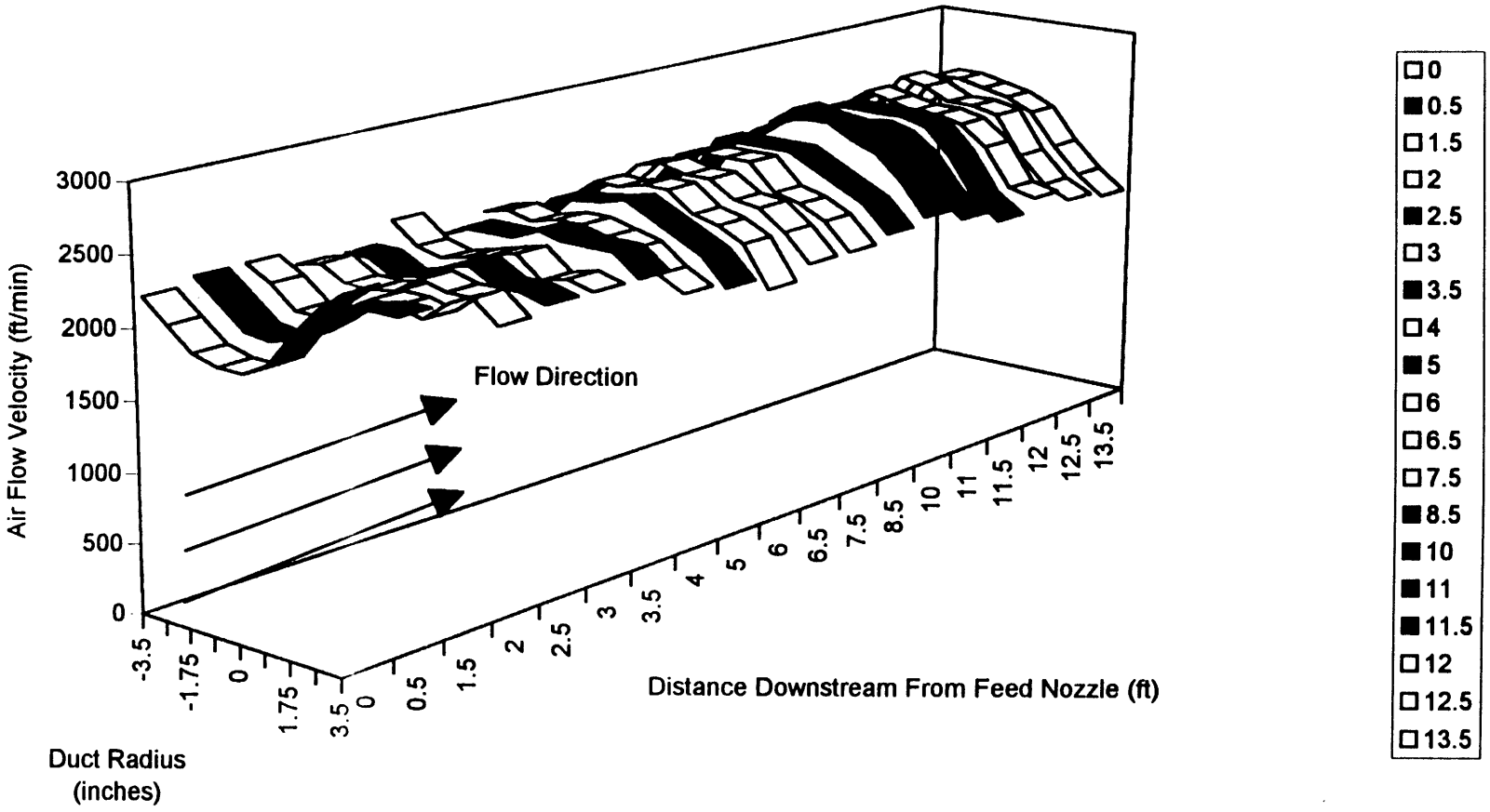

Figure 30, Duct Centerline Particulate Fluxes at Sampling Location

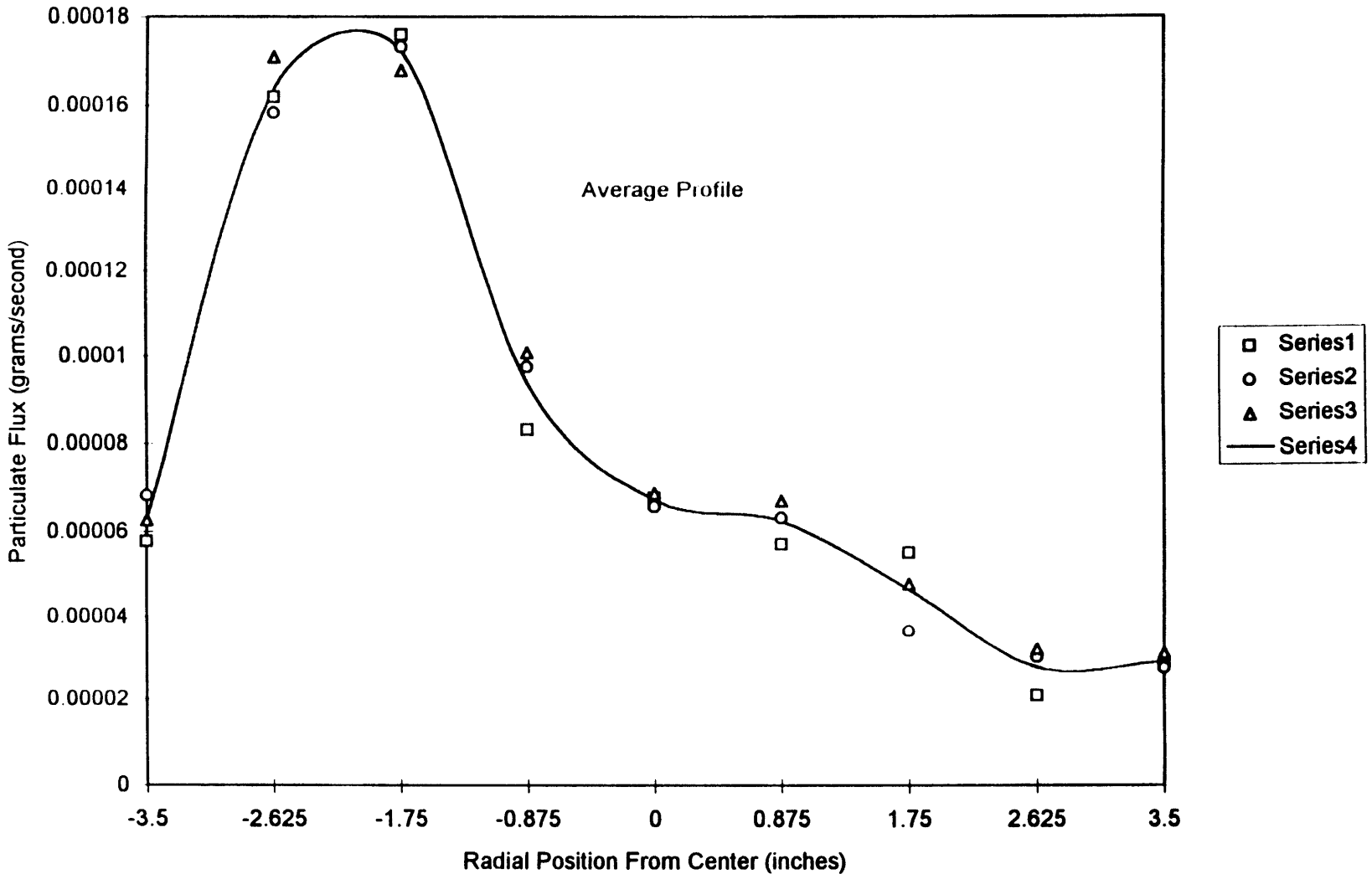

# Figure 31, Feeder Mechanism Performance vs. Time

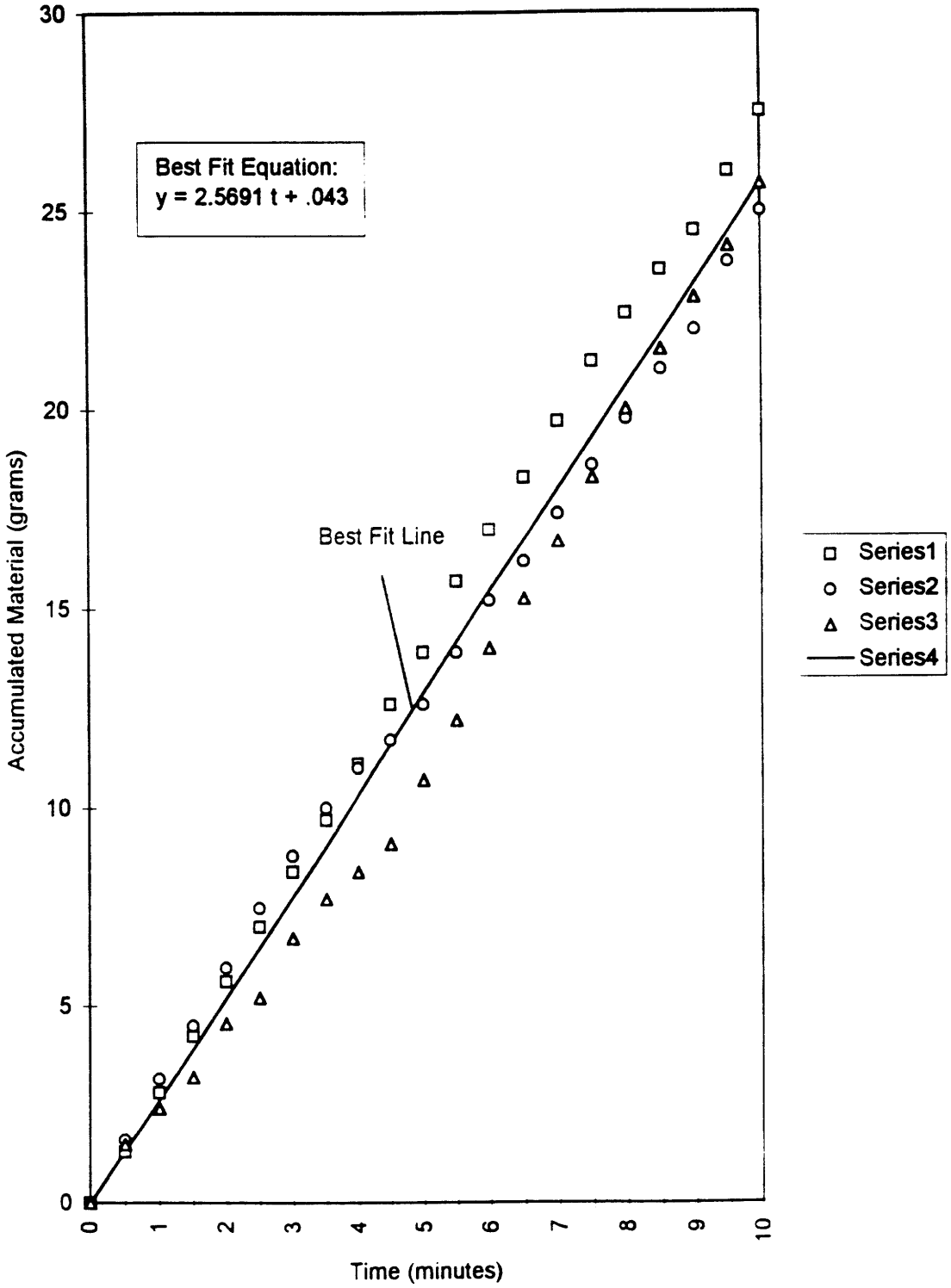

# Figure 32 Spectrum for Iron Calibration Test

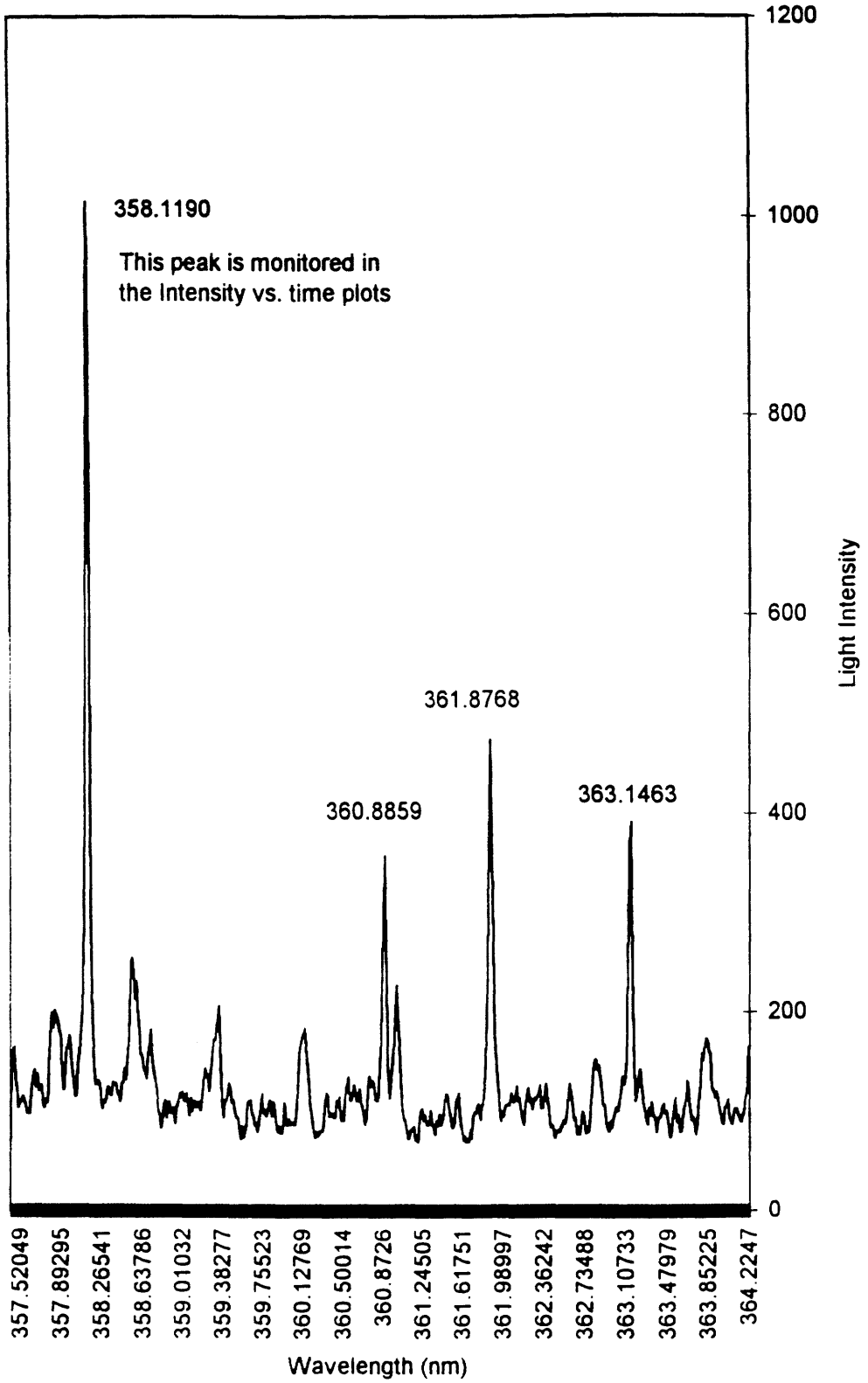

# Figure 33, Intensity vs. Time, Run 1

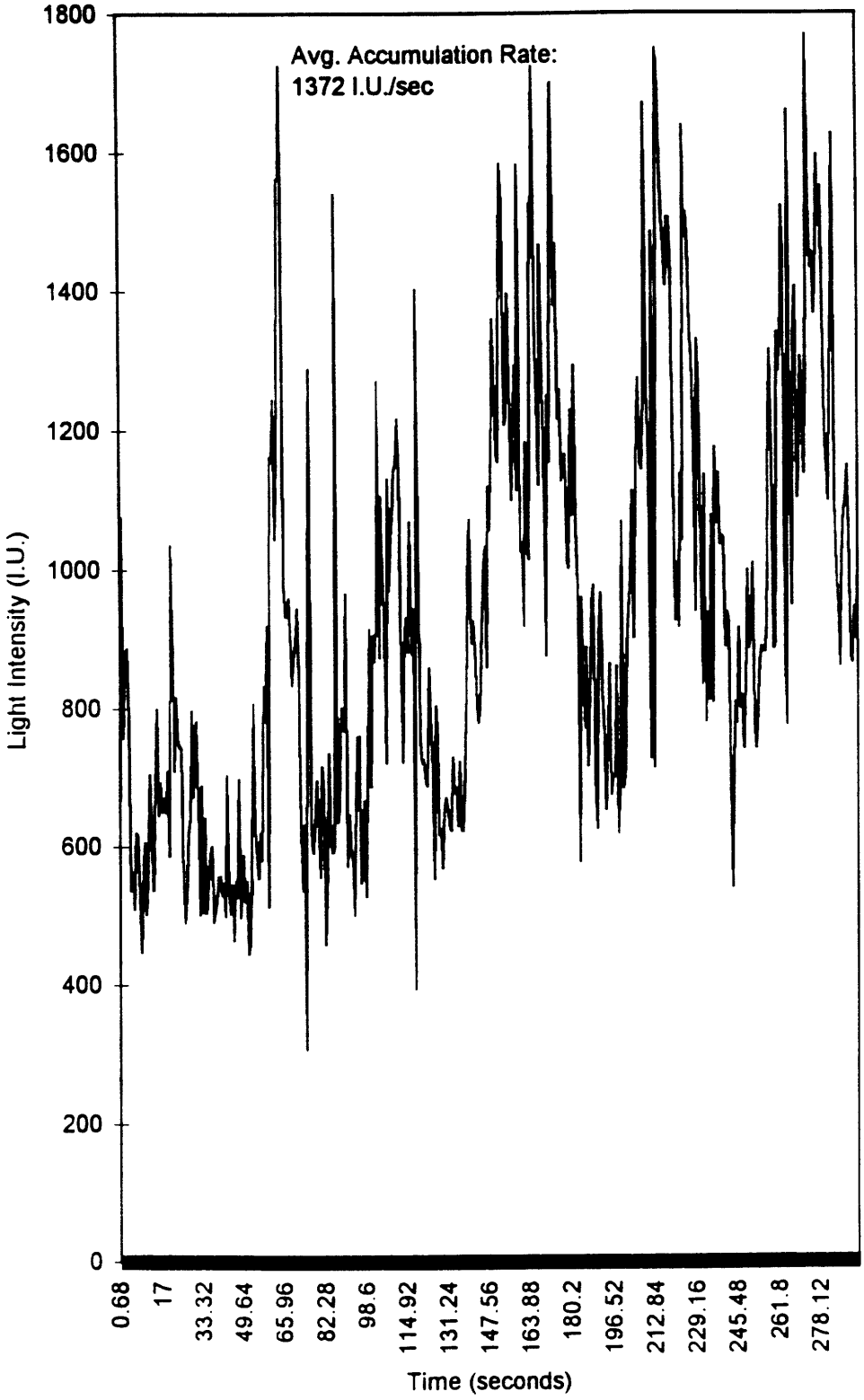

# Figure 34, Intensity vs. Time, Run 2

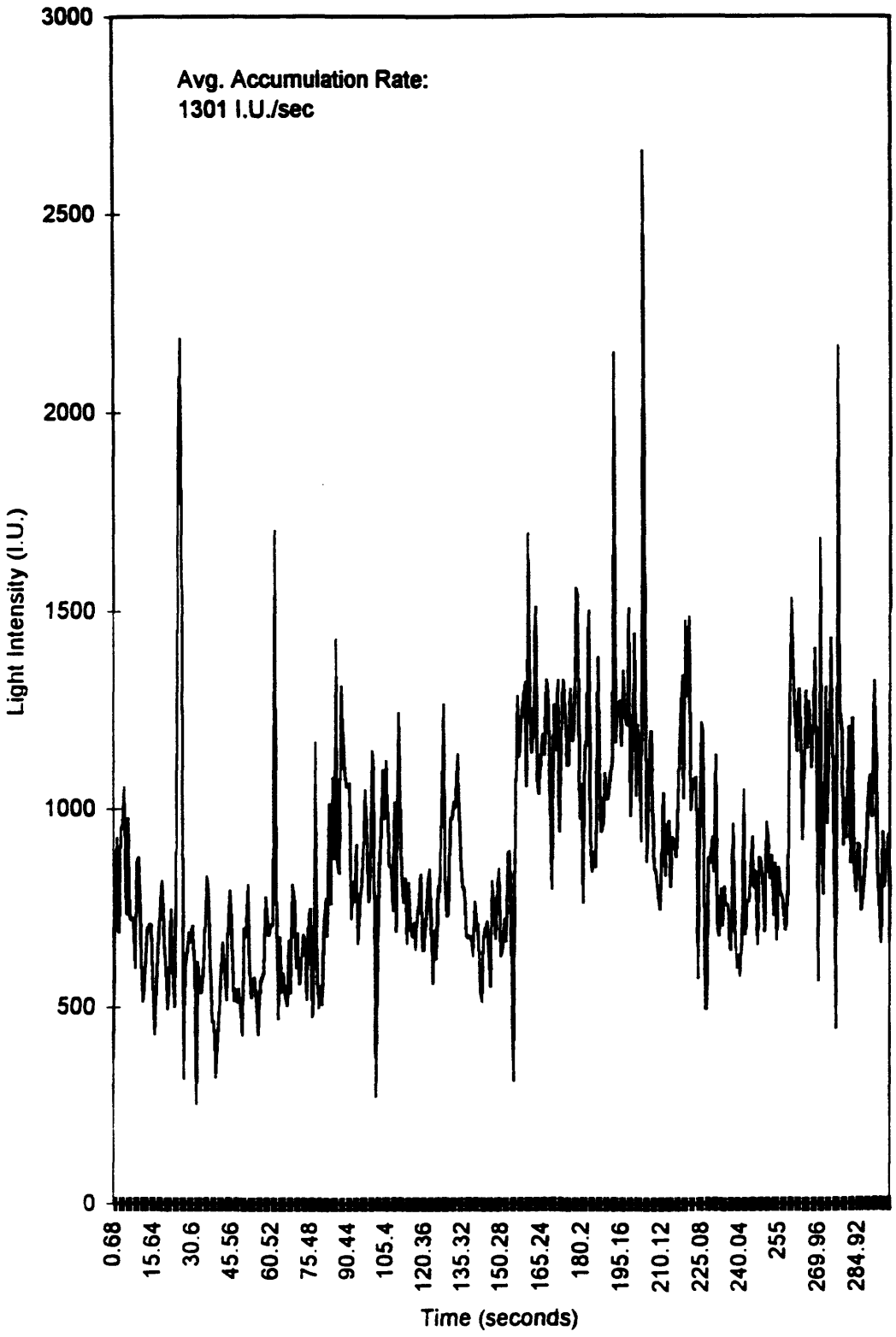

# Figure 35, Intensity vs. Time, Run 3

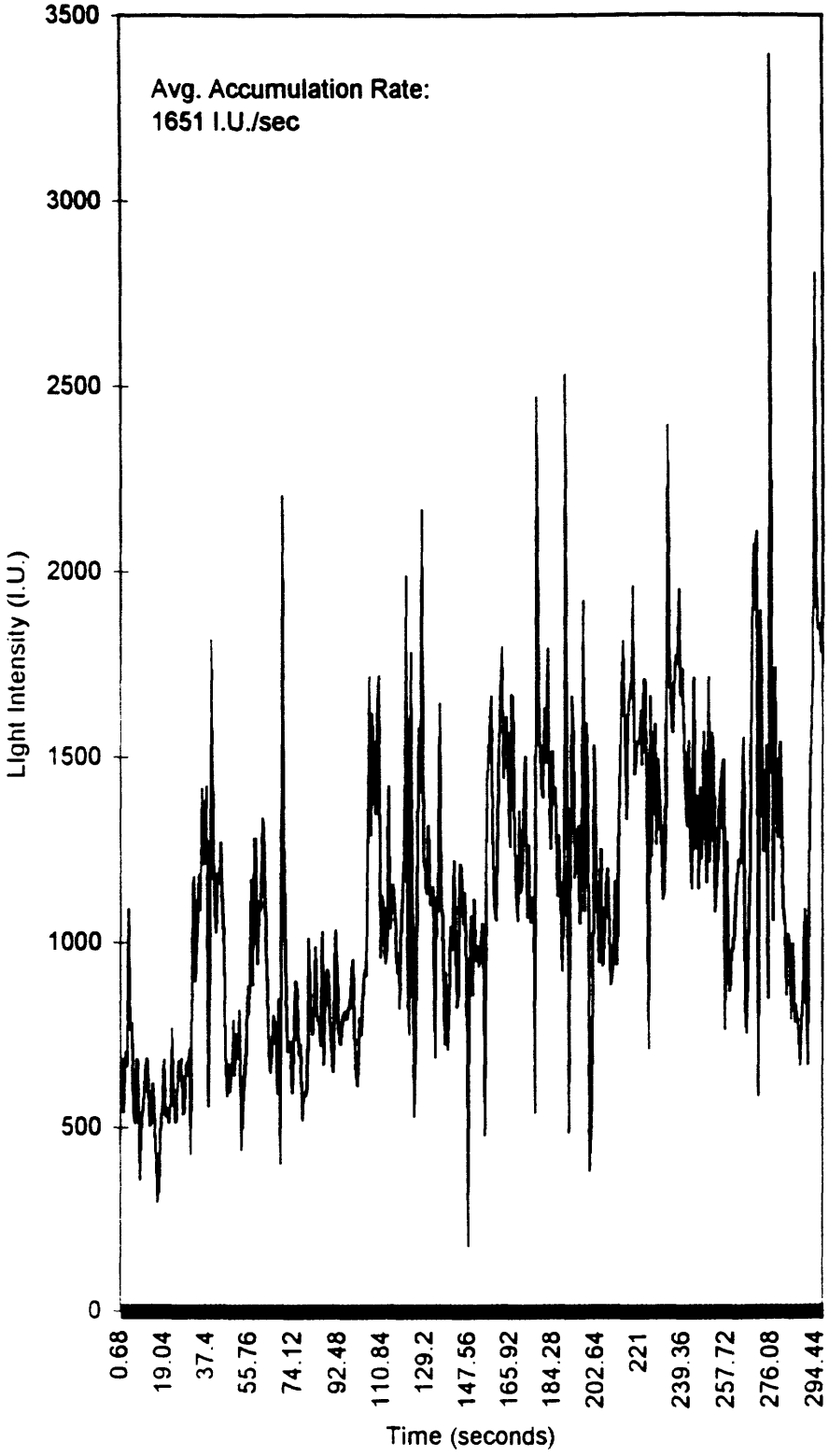

# Figure 36, Intensity vs. Time, Run 4

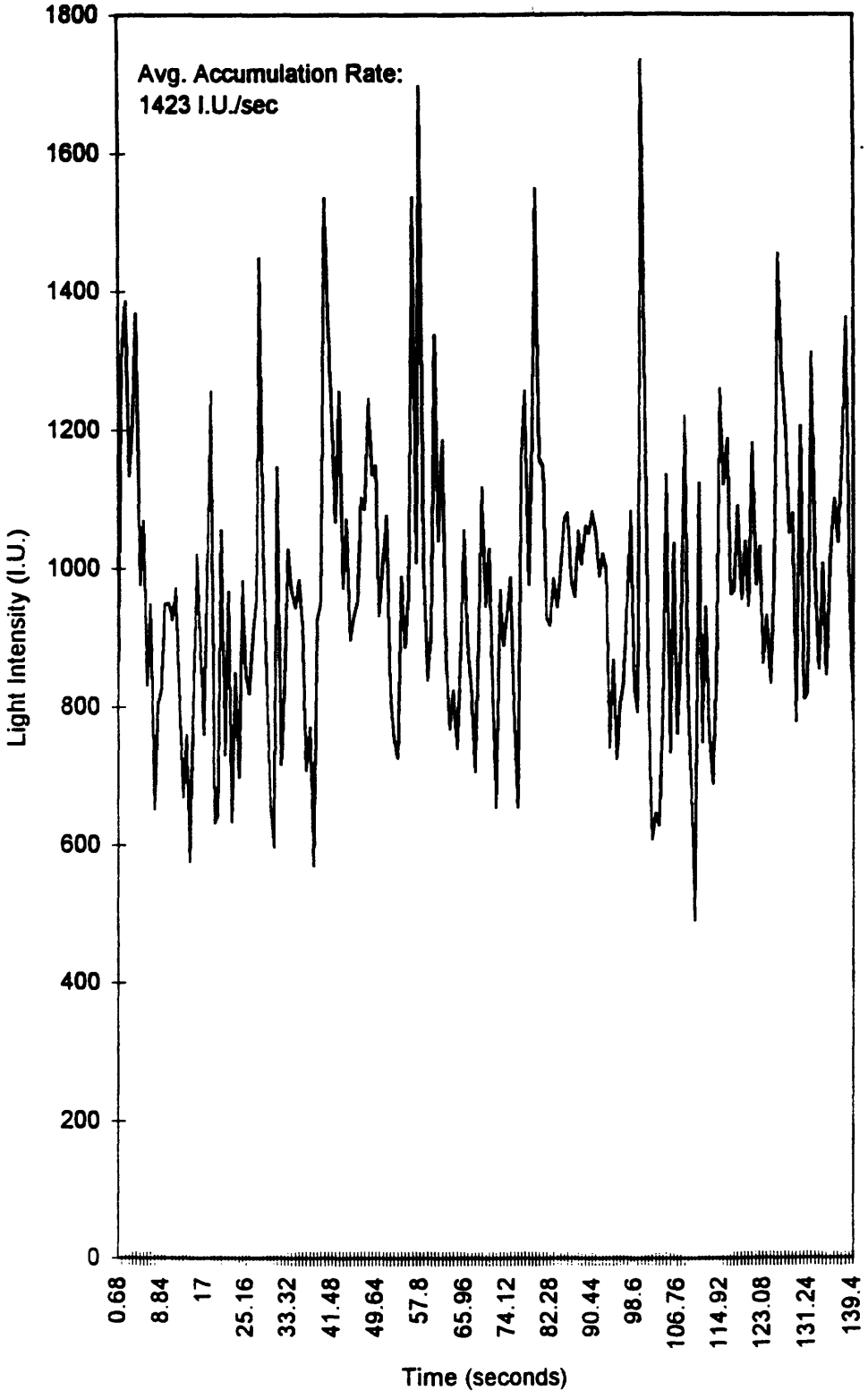

# Figure 37, Intensity vs. Time, Run 5